



UNIVERSITAT DE
BARCELONA

Pathogen-triggered programmed cell death in plants: Metacaspase 1-dependent pathways

Muerte celular programada desencadenada por patógenos en plantas: vías dependientes de Metacaspasa 1

Saúl Stalin Lema Asqui

ADVERTIMENT. La consulta d'aquesta tesi queda condicionada a l'acceptació de les següents condicions d'ús: La difusió d'aquesta tesi per mitjà del servei TDX (www.tdx.cat) i a través del Dipòsit Digital de la UB (diposit.ub.edu) ha estat autoritzada pels titulars dels drets de propietat intel·lectual únicament per a usos privats emmarcats en activitats d'investigació i docència. No s'autoritza la seva reproducció amb finalitats de lucre ni la seva difusió i posada a disposició des d'un lloc aliè al servei TDX ni al Dipòsit Digital de la UB. No s'autoritza la presentació del seu contingut en una finestra o marc aliè a TDX o al Dipòsit Digital de la UB (framing). Aquesta reserva de drets afecta tant al resum de presentació de la tesi com als seus continguts. En la utilització o cita de parts de la tesi és obligat indicar el nom de la persona autora.

ADVERTENCIA. La consulta de esta tesis queda condicionada a la aceptación de las siguientes condiciones de uso: La difusión de esta tesis por medio del servicio TDR (www.tdx.cat) y a través del Repositorio Digital de la UB (diposit.ub.edu) ha sido autorizada por los titulares de los derechos de propiedad intelectual únicamente para usos privados enmarcados en actividades de investigación y docencia. No se autoriza su reproducción con finalidades de lucro ni su difusión y puesta a disposición desde un sitio ajeno al servicio TDR o al Repositorio Digital de la UB. No se autoriza la presentación de su contenido en una ventana o marco ajeno a TDR o al Repositorio Digital de la UB (framing). Esta reserva de derechos afecta tanto al resumen de presentación de la tesis como a sus contenidos. En la utilización o cita de partes de la tesis es obligado indicar el nombre de la persona autora.

WARNING. On having consulted this thesis you're accepting the following use conditions: Spreading this thesis by the TDX (www.tdx.cat) service and by the UB Digital Repository (diposit.ub.edu) has been authorized by the titular of the intellectual property rights only for private uses placed in investigation and teaching activities. Reproduction with lucrative aims is not authorized nor its spreading and availability from a site foreign to the TDX service or to the UB Digital Repository. Introducing its content in a window or frame foreign to the TDX service or to the UB Digital Repository is not authorized (framing). Those rights affect to the presentation summary of the thesis as well as to its contents. In the using or citation of parts of the thesis it's obliged to indicate the name of the author.



UNIVERSITAT DE
BARCELONA



Facultat de Biologia

Departament de Genètica, microbiologia i estadística

Programa de doctorat: Genètica

**“Pathogen-triggered programmed cell death in plants:
Metacaspase 1-dependent pathways”**

(Muerte celular programada desencadenada por patógenos en
plantas: Vías dependientes de Metacaspasa 1.)

Memòria presentada per Saúl Stalin Lema Asqui per tal d'optar al títol de Doctor per la Universitat de Barcelona. Tesi doctoral realitzada sota la direcció de la Dra. Núria Sánchez Coll i del Dr. Marc Valls Matheu al Departament de Genètica, Microbiologia i Estadística de la Facultat de Biologia (UB) i al Centre de Recerca Agrigenòmica (Crag).

Signatura dels directors,

Signatura del tutor

Dra. Núria Sánchez Coll. Dr. Marc Valls i Matheu

Dr. Marc Valls i Matheu

Signatura del doctorand,

Saúl S. Lema Asqui

BARCELONA, JUNE 2018

ACKNOWLEDGMENTS

Más de una década me ha tomado llegar hasta este punto, y que por mucho que se me hubiese permitido soñar jamás me lo hubiese imaginado, aunque el camino ha sido largo y a veces lleno de peripecias, que sin el apoyo de cada una de las personas, que de una u otra forma han aportado con palabras, gestos, caricias y uno que otro golpe para guiarme; y ver realizado uno de los momentos mas esperados en mi vida. Nunca he sido un buen escritor y el escribir estas palabras ha resultado el momento mas duro de toda mi vida, porque quisiera transmitir con ellas toda la gratitud que tengo para con todos ustedes que me han acompañado a lo largo de esta aventura.

Primeramente, quiero agradecer de todo corazón a mi familia que han sabido entenderme y apoyarme a lo largo de todo este tiempo, a mi madre **Inés** que ha sido el pilar fundamental de mi carrera y fundamentalmente de mi vida; que sepas que siempre, aunque nunca lo parezca escucho tus consejos; a mi hermana **Karina** a la cual extraño demasiado y siento haberme perdido gran parte de tu vida ñaña, gracias por haberme apoyado siempre y nunca haber dudado que podría conseguir lo que me propusiese, a mi padre **Saúl** que siempre ha sabido encontrar las palabras adecuadas para reconfortarme en los momentos mas difíciles. A ti **Daniela** que has sido mi apoyo incondicional durante este tiempo, sin tu presencia, apoyo, comprensión y amor este logro no sería lo mismo, gracias por estar conmigo incluso en los momentos que te volvía loco; a toda mi familia en Ecuador a mis abuelitas, a mis tíos y primos que nunca dudaron que podría ser capaz de conseguir lo que me propusiera; volar como siempre me lo decían, millón de gracias por su apoyo a la distancia.

A la **Dra. Núria Sánchez**, no me alcanzan las palabras para agradecerte haber sido la guía sin descanso de este camino, te agradezco por todas tus enseñanzas, por haber creído en mí incluso cuando las situaciones apuntarán a todo lo contrario, eres una de las personas que mas admiro y siempre me sentiré orgulloso de haber podido compartir contigo esta experiencia eres uan de las personas mas geniales y unas de las mas grandes científicas.

Al **Dr. Marc Valls** por haber tenido toda esa tenacidad y ese positivismo para conmigo, tu apoyo, consejos y reglas me han llevado a culminar con éxito este viaje. Gracias por siempre haber tenido ese deseo altruista de guiarme por este camino, ayudarme no solo en las situaciones laborales sino también en las personales.

Muchísimas gracias a ustedes dos por todos los consejos, gracias por haber impulsado incluso en contra de mismo, viviré siempre agradecido por haber sido esa fuente de inspiración y motivación. Gracias por no dejarme decaer y siempre haberme hecho sentir parte de una gran familia desde el primer día.

To all my old and new lab mates, you were my family during these years I really will miss you all. Share with all of you this time was the most amazing adventure in my life. Thank you for all the support, for all advices and for all never-ending conversations. Thank you so much **Alex, Marc, Marina, Crina, Eugenia, Jose, Liang, Pau, Brian, Anurag**, you make my life really easy no matter how difficult where the times; your unconditional support, your eternal happiness sometimes too much, made this way unforgettable. I never will forget you.

Al Gobierno Ecuatoriano y en especial a la SENESCYT por haberme otorgado la beca para poder realizar mis estudios de Doctorado.

A todas las personas en el CRAG cuya ayuda y consejos fueron muy útiles durante esta etapa.

INDEX

TABLE OF CONTENTS

ACKNOWLEDGMENTS.....	I
INDEX.....	v
INTRODUCTION	1
Chapter1: Programmed Cell Death	3
Importance of programmed cell death in plant development and disease.	3
Chapter 2: Role of the Hypersensitive Response in plant immunity	4
Plant immunity: an evolutionary fight against pathogens.....	4
The <i>Arabidopsis thaliana</i> - <i>Pseudomonas syringae</i> interaction as genetic tool to understand Hypersensitive Response	6
Hypersensitive response: a programmed cell death strategy to restricted pathogen attacks.....	7
Metacaspases as main regulators of HR.....	9
OBJECTIVES	13
PUBLICATIONS	17
Informe del director de tesi del factor d'impacte dels articles publicats.....	19
Dying two deaths — programmed cell death regulation in development and disease	21
AtSERPIN1 is an inhibitor of the Metacaspase AtMC1-mediated cell death and autocatalytic processing <i>in planta</i>	31
Detection and Quantification of Protein Aggregates in Plants.....	57
DRAFT 1	67
AtHIR2, a new regulator of AtMC1-mediated cell death in plants.....	69
Abstract.....	69
Introduction	69

Material and Methods.....	74
Discussion.....	83
DISCUSSION.....	87
General discussion	89
A different mode of action to control and activate the hypersensitive response in plants via AtMC1.	89
Negative regulation as a fate-controller of AtMC1 determine its activation and degradation.	89
A conserved inhibitor function over proteases.....	91
A step towards the elucidation of the HR cell death pathway ignited upon NB-LRR activation by pathogen recognition	93
CONCLUSIONS	97
Conclusions.....	99
SUMMARY.....	101
Summary in English	103
Resumen en Español	105
BIBLIOGRAPHY.....	107
ANEXS.....	121

INTRODUCTION

Chapter1: Programmed Cell Death

Importance of programmed cell death in plant development and disease.

Although cell death was defined as the inevitable and passive ending of life, this concept changed in the early 60s, when it was discovered that specific cells and tissues are genetically controlling a sequence of events programmed to self-destruct (Lockshin & Williams, 1964, 1965). A tightly regulated balance in multicellular organisms is essential for maintenance of all functions during development and under environmental stress. Programmed cell death is an essential process which contributes to the preservation of this balance during development and in response to biotic and abiotic stress. In the last decades many are the studies that have contributed advancing the understanding of programmed cell death and its functions in a variety of processes including growth, and immune responses for homeostasis maintenance.

In both plants and animals programmed cell death plays a central role to control regular development and pathogen invasion and proliferation of diseases. Although some features are shared among plant and animal cell death including condensation, shrinkage and fragmentation of the cytoplasm and nucleus, nuclear DNA fragmentation and formation of apoptotic -like bodies (Coll, Epple, & Dangl, 2011) there are a number of key differences between how these organisms initiate and regulate cell death. This is not surprising given the intrinsic differences existing between two kingdoms: plants are sessile organisms that lack physical escape function, a circulatory system and adaptive immune system, and their cells have additional structures, including cell wall, chloroplasts and vacuole (Reape, Molony, & McCabe, 2008). Plant cells have the inherent ability to induce localized cell death in specific tissues, or organs during different developmental process: during the early stages of embryogenesis and root morphogenesis, during xylem formation, for floral development, in some cases of leaf morphogenesis and during organ senescence (Daneva, Gao, Van Durme, & Nowack, 2016). Besides developmental PCD, plant PCD occurs as response to pathogen invasion that include the hypersensitive response, cell death-inducing toxins and responses to necrotrophic pathogens, but also elicited in response to environmental stress (Kabbage, Kessens, Bartholomay, & Williams, 2017).

In the publication 1 developmental PCD and pathogen-triggered PCD are described and compared, highlighting the most recent advances in the field.

Chapter 2: Role of the Hypersensitive Response in plant immunity

Plant immunity: an evolutionary fight against pathogens.

Plants are higher organisms that in comparison to animals are constantly exposed to pathogen attacks due to their static nature. To overcome this challenge, plants have evolved refined mechanisms of protection against harmful attacks, improving their ability to sense invaders and respond appropriately to control the disease. Some of the mechanisms that plants use to fight pathogens share certain common features with animals (Dodds & Rathjen, 2010). One of these common features are pattern-recognition receptors (PRRs), a set of membrane proteins that pose the first layer of defense against pathogen attack. PRRs recognize conserved highly conserved features of pathogens, which have been termed PAMPs –for pathogen associated molecular patterns (Boller & He, 2009). The best characterized PRRs are receptor like kinases FLS2 (Gomez-Gomez & Boller, 2000) and EFR (Zipfel et al., 2006) which are activated by interaction of essential structures that are common in multiple microbes, pathogenic or not, due to the conserved nature of PAMPs (Zipfel, 2014). FLS2 recognizes flagellin, by binding directly to 22 amino acids conserved epitope of PAMP located at N-terminal domain, known as flagellin 22 (flg22) (Chinchilla, Bauer, Regenass, Boller, & Felix, 2006). Similarly, to what has been discovered for flagellin, plants can perceive elongation factor TU (EF-Tu) via directly binding of 18 amino acids conserved N-acetylated epitope defined as elf18 (Kunze et al., 2004; Zipfel et al., 2006).

The plant defense system is multilayered (Jones & Dangl, 2006). The first layer of defense is constituted by PRR perception of PAMPs (described above) and is known as PAMP-triggered immunity (PTI) (Ausubel, 2005; Jones & Dangl, 2006). PTI is often effective as a defense mechanism, activating the production of reactive oxygen species (ROS) such as peroxide and nitric oxide, MAP kinase signaling, calcium-dependent protein kinases (CDPKs), induced biosynthesis of phytoalexins, WRKY transcription factors and calcium influx (McDowell & Dangl, 2000; Meng & Zhang, 2013; Newman, Sundelin, Nielsen, & Erbs, 2013; Rasmussen, Roux, Petersen, & Mundy, 2012). However, pathogens have been evolved a sophisticated strategy to avoid defense responses suppressing PTI

(Ingle, Carstens, & Denby, 2006) by delivery of a variety of effector proteins through the type III secretion system (T3SS) into plant cells (Burkinshaw & Strynadka, 2014; Coburn, Sekirov, & Finlay, 2007). Type III effectors use a variety of mechanisms to suppress PTI (Block, Li, Fu, & Alfano, 2008; de Torres et al., 2006; Xiang et al., 2008).

In this constant evolutionary battle, plants have evolved a set of receptor proteins called resistance proteins able to recognize pathogen effectors, which was classically known as the gene-for-gene resistance or the Flor model (Flor, 1971) constitute a second layer of plant defense called effector-triggered immunity (ETI) (Block et al., 2008; Dodds & Rathjen, 2010; Jones & Dangl, 2006). The majority of the receptor proteins interacting with pathogen effectors belong to the nucleotide binding leucine rich repeat (NB-LRR) family. Based on the presence of an N-terminal coiled-coil (CC) or Toll/interleukin-1 receptor-like (TIR) motifs, NB-LRR proteins are categorized into CC-NB-LRR or TIR-NB-LRR subfamilies, respectively (Elmore, Lin, & Coaker, 2011). Some well-studied NB-LRR proteins in *Arabidopsis thaliana* are RPM1 (Bisgrove, Simonich, Smith, Sattler, & Innes, 1994; Grant et al., 1995) and RPS2 (Bent et al., 1994; Kunkel, Bent, Dahlbeck, Innes, & Staskawicz, 1993) that belong to CC-NB-LRR class of NB-LRR proteins that are characterized by coiled coil motif (CC) at N-terminal and a C-terminal tandem array of leucine-rich repeats (Dangl & Jones, 2001; DeYoung & Innes, 2006; Elmore et al., 2011).

NB-LRR proteins are thought to amplify PTI signaling, involving ROS production and ion fluxes, leading to enhanced defense gene expression (Nimchuk, Eulgem, Holt, & Dangl, 2003). This recognition by NB-LRR proteins triggers signaling events for ETI, which can take place either via straight detection of pathogen effectors, which directly interact with NB-LRR, or indirect recognition of pathogen effector that through a guard protein that detects post-transcriptional or physical modifications and also interacts with NB-LRR (guard model) (Dangl & Jones, 2001). NB-LRR can be localized in different cell compartments and organelles, activation of NB-LRR is followed by triggered response of Ca⁺⁺ dependent kinase (CPKs), MAPK cascade and production of ROS. These responses resemble those triggered during PTI, but ETI responses also involve the activation of certain phytohormones like salicylic acid (SA) and jasmonic acid (JA) (Cui, Tsuda, & Parker, 2015).

Generally, ETI causes strong immune responses, including a kind of plant programmed cell death characterized by fast and quick death of cells at

attempted infection sites, which is termed hypersensitive response (further referred as HR) (Coll et al., 2011; Mur, Kenton, Lloyd, Ougham, & Prats, 2008).

The *Arabidopsis thaliana*-*Pseudomonas syringae* interaction as genetic tool to understand Hypersensitive Response

The *Arabidopsis*-*P. syringae* pathosystem has added a value knowledge to the elucidation of mechanisms fundamental plant recognition of pathogens, signal transduction pathways controlling plant defense responses, host susceptibility, and pathogen virulence and avirulence factors (Katagiri, Thilmony, & He, 2002). The *Arabidopsis thaliana*-*Pseudomonas syringae* interaction has been used for a long time as a model pathosystem to study both ETI and PTI, contributing to a better understanding of these two layers of plant immunity. Interestingly, some of the NB-LRR proteins identified in *Arabidopsis* have homologous in crops as is the case for RPM1, present in pea, bean and soybean (Dangl et al., 1992), which may contribute to the elucidation of new strategies to improve crops.

Pseudomonas syringae is a Gram negative, rod shaped flagellated bacteria that can infect *Arabidopsis* and a wide variety of plants, like tomato, potato, soybean, bean among others. Although, a huge variety of pseudomonas strains have been reported in the field, the most common used in the lab conditions is *P. syringae pathovar tomato DC3000* which has been for a long time used to understand ETI regulation; introducing a single effector in a virulent strain, transforms the virulent strain in an avirulent one, allowing studies of gene-for-gene resistance (Katagiri et al., 2002). For example, receptors RPS2 and RPM1 confer resistance to strains of *Pseudomonas syringae* carrying the avirulence genes *avrRpt2* and *avrB* or *avrRpm1* respectively. These approaches have identified RPM1-interacting protein 4 (RIN4), a plasma membrane protein that upon infection with *P. syringae* expressing either *avrB* or *avrRpm1* becomes phosphorylated and interacts with RPM1 leading to ETI (Mackey, Holt, Wiig, & Dangl, 2002). RIN4 is also involved in the activation of RPS2-mediated resistance, with which associates in the plasma membrane after depletion (Axtell & Staskawicz, 2003). Thus, RIN4 is a so-called guard protein that activates both RPM1 and RPS2 upon pathogen challenge (Axtell & Staskawicz, 2003; Mackey, Belkhadir, Alonso, Ecker, & Dangl, 2003; Mackey et al., 2002).

Since it is impossible to study every plant pathogen interaction, plant pathologists have turned to model systems that have allowed profounder studies of a few interactions in high detail and even making the possible the studies of Hypersensitive Response.

Hypersensitive response: a programmed cell death strategy to restricted pathogen attacks

The hypersensitive response (HR) was first described more than 100 years ago in observations of wheat leaf rust reported by Ward, 1902 and wheat black stem rust reported by Stackman (Stackman, 1915). Despite many examples of plant HR in the literature, very little is known about the molecular mechanisms that control this process. HR is a plant-specific type of PCD associated with successful plant innate immune responses, where the plant sacrifices a few cells to prevent further tissue colonization of the invading pathogen Fig. 1 (Morel & Dangl, 1997). The HR has been studied from different points of view, analyzing its macroscopic and microscopic features, but it remains an ill-defined process at the molecular level (Mur et al., 2008).

It is usually speculated that HR is triggered when ETI surpasses a certain threshold of induction. However, it is still unclear whether HR is indispensable for resistance. There are examples reported of NB-LRR-mediated defense without HR (Bendahmane, Kanyuka, & Baulcombe, 1999; Hatsugai et al., 2017). Why has then been HR conserved through evolution? One hypothesis is that HR may control further pathogen growth in host plants by participating in the activation of systemic acquired resistance (SAR), a form of innate immune responses that occurs at distal regions of the plants through the phytohormone salicylic acid and characterized by the increase expression of pathogenesis-related genes (*PR* genes) (Durrant & Dong, 2004; Jones & Dangl, 2006).

HR signaling triggers a chain of events initiated by the activation of a set of hypersensitive response early markers, called *hsr* (hypersensitive response) (Lacomme & Roby, 1999) or *hir* (hypersensitive-induced reaction) genes (Nadimpalli, Yalpani, Johal, & Simmons, 2000; Rostoks, Schmierer, Kudrna, & Kleinhofs, 2003). Induction of these genes is followed by a rapid burst of reactive oxygen species (ROS), disruption of membranes and loss of cellular compartmentalization, cross linking of phenolics with cell wall components and reinforcement of the plant cell wall by an increase of callose and lignin, production of antimicrobial proteins (defensins) and antimicrobial secondary

metabolites (phytoalexins) and transcriptional reprogramming (Hofius, Tsitsigiannis, Jones, & Mundy, 2007).

HR is also accompanied by clear morphological changes of the plant cell. One of the early morphological characteristics of HR is cessation of cytoplasmic streaming, vacuolization of the cytosol (Morel & Dangl, 1997; Mur et al., 2008) and reorganization of the cytoskeleton (Smertenko & Franklin-Tong, 2011). Although plant HR shares common characteristics with animal apoptosis, the morphology of plant cells defines several considerable differences between plant PCD and animal apoptosis. In plants the presence of chloroplasts provides an additional ROS source and the presence of plant cell wall precludes phagocytosis, which is characteristic of apoptosis (Williams & Dickman, 2008)

Another important aspect of HR is the existence of regulatory mechanisms that help restricting the spread of cell death so that HR is a localized phenomenon. A tight negative regulation of HR must take place in adjacent tissues that prevent runaway cell death. However, very little is known about this anti-cell death signaling mechanisms taking place in the tissues surrounding HR.

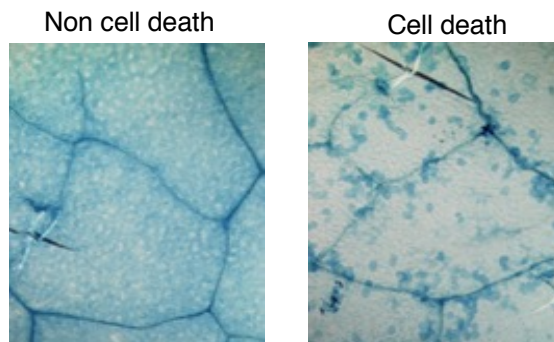


Figure 1. Cell death staining in Arabidopsis leaves.

Columbia-0 *Arabidopsis* plants were inoculated with mock (non-cell death) and *Pto* DC3000 (*avrRpt2*) (cell death) and stained using trypan blue.

Metacaspases as main regulators of HR

In animals, caspases are the main regulators and executioners of programmed cell death. One of the most intriguing differences between plant and animal HR is caused by the lack of caspase-like homologs in plants. Although no plant genes share high sequence similarity with caspases, in 2000 a family of proteins with high structural similarity to caspases using *in silico* analyses and were named metacaspases (Uren et al., 2000).

Like caspases, metacaspases are part of the CD clan of cysteine proteases found in plants, fungi, yeast and protozoa, which have been shown to control similar aspects of cell death (Carmona-Gutierrez, Frohlich, Kroemer, & Madeo, 2010; Minina, Coll, Tuominen, & Bozhkov, 2017; Tsiatsiani et al., 2011). Metacaspases can be subdivided in 3 groups (Figure 2) (Choi & Berges, 2013; Uren et al., 2000). Type I are found in yeast, plants and fungi and contain an N-terminal proline-rich domain and a Zn-finger motif, whereas type II metacaspases can exclusively be found in higher plants, they lack the N-terminal domain and their p20 and p10 domains are separated by a long linker region (Coll et al., 2011). The N-terminal prodomain of metacaspases contains a plant-specific LSD1-like zinc-finger domain followed by a proline-rich domain. Interestingly, both motifs usually participate in protein-protein interactions and could indicate that oligomerization is important for type I metacaspase functions, in analogy with initiator/inflammatory caspases (Coll et al., 2010; Lam & Zhang, 2012). Type III metacaspases are a new group recently identified exclusively *in algae* in which the p10 subunit precedes the p20 subunit and exhibit a calcium dependent activity (Choi & Berges, 2013; Klemencic & Funk, 2017).

Nine metacaspases are encoded in the Arabidopsis genome: AtMC1–AtMC3 (Type I) and AtMC4–AtMC9 (Type II). Two type I metacaspases have been shown to antagonistically regulate HR cell death in the context of *P. syringae avrRpm1* infection: AtMC1 is a positive regulator of HR-inducing cell death and AtMC2 negatively regulates cell death (Coll et al., 2010) Interestingly, Arabidopsis metacaspase AtMC1 acts synergistically with autophagy to promote HR-inducing cell death (Coll et al., 2014).

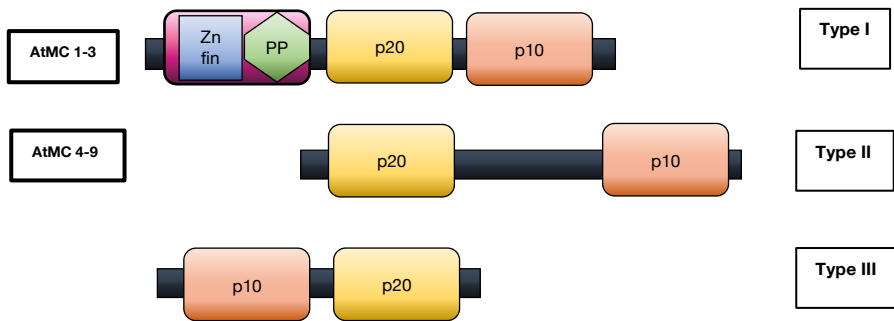


Figure 2. Schematic representation of three types of metacaspases.

As caspases, metacaspases enclose a conserved cysteine-histidine catalytic dyad in the p20 domain. As caspases, metacaspases seem to require autoprocessing for maturation, but whereas caspases cleave after an Asparagine residue, metacaspases cleave after Arginine or Lysine residues (Vercammen et al., 2004; Watanabe & Lam, 2005). Auto-processing activity of metacaspases tested (except for AtMC9) is highly dependent on Ca^{2+} , which indicates that their activity might be regulated by local changes in the concentration of Ca^{2+} ions (Y. Zhang & Lam, 2011). Metacaspase structure shows certain similarities with caspases, although, the existence of important architectural differences was reported in *Saccharomyces cerevisiae* (Wong, Yan, & Shi, 2012) and *Trypanosoma brucei* (McLuskey et al., 2012), which may explain some of the differences in the function, the crystal structure of Yeast Yca1 shows the existence of 2 extra β -sheets, which precludes the possibility of homodimerization. Similarly, it was reported in *Trypanosoma* TbMCA 2 the existence of an unusual N-terminal domain, which was hypothesized to form a lid structure to limit substrate access. Interestingly, although TbMCA2 was crystallized associated to an inhibitor, in Yca1 crystallization the inhibitor was absent, however, in both cases Ca-binding sites were clearly defined by the presence of four aspartic residues, since autocatalytic processing and proteolytic activity is clearly facilitated by the presence of Ca^{++} (McLuskey et al., 2012; Wong et al., 2012). All these, together with the evidence of LSD1 interaction with the prodomain of AtMC1 negatively regulating the activity of metacaspase (Coll et al., 2010), reinforces the idea of the prodomain region as a repressor of AtMC1 activity.

Besides metacaspases, proteases that exhibit a caspases-like activity associated with cell death in plants were identified; Vacuolar processing

enzymes, phytaspases and saspases. Vacuolar processing enzymes (VPEs) belong to the cysteine protease family showing substrate specificity in respect to the peptide bond on the carboxyl side of aspartic acid (Asp) and asparagine (Asn) residues (Hatsugai, Kuroyanagi, Nishimura, & Hara-Nishimura, 2006). Under *in vitro* conditions these enzymes hydrolyze peptide bonds on the carboxyl side of aspartic acid residue of the synthetic caspase-1 substrate YVAD, but do not hydrolyze this bond in the synthetic caspase-3 substrate, DEVD (Hatsugai et al., 2006). VPEs are localized in the vacuole and have an acid pH optimum (Hatsugai et al., 2006). VPEs activate in an autocatalytic process at an acidic pH (Hiraiwa, Nishimura, & Hara-Nishimura, 1999). The process of VPE activation is based on removal of the C-terminal pro-peptide, which masks the active center (Hatsugai et al., 2006). The *Arabidopsis thaliana* genome contains 4 VPE homologues: α VPE, β VPE, γ VPE and δ VPE, which may be classified into two subfamilies: one specific for seeds and the second one for vegetative organs, whereas in agreement with the classification of plant vacuoles (Kinoshita et al. 1999). VPEs participate in plant cell induced by toxins during pathogen challenged, as was shown in *Arabidopsis* where were silencing all four VEP genes and treated with the mycotoxin fumonisin B1(FB1) which is a strong inducer to trigger plant hypersensitive responses, the cell death did not occur at the contrary of the wild type (Kuroyanagi et al., 2005)

Phytaspases and saspases are serine proteases characterized by a catalytic triad of aspartate, histidine and serine (Dodson & Wlodawer, 1998), were identified in *Avena Sativa* when were infected with the necrotrophic fungus *Cochliobolus Victoria*, which induces cell death (Lorang et al., 2012). On the other hand, tobacco phytaspase cleaved the VirD2 protein from the *Agrobacterium tumefaciens* upon HR induction, *in vivo* and *in vitro* evidences suggest that a caspase-like protease is activated in tobacco plants during the N gene-mediated HR triggered by TMV infection (Chichkova et al., 2004).

Most of the CD clan protease family members are active enzymes with a wide-range of substrates, and many of them are constitutively expressed and thus require tight regulation of activity to prevent unwanted proteolysis (Verma, Dixit, & Pandey, 2016). Although CD proteases have extended range of target substrates, in the case of metacaspases only small set substrates could be defined so far, Tudor staphylococcal nuclease (TSN) is a substrate identified *in vivo* as a common substrate for both *Norway spruce* metacaspase mCII-Pa and human caspase-3, suggesting the existence of a certain degree of conservation in PCD processes between plants and animals (Sundstrom et al., 2009). Also, it

has reported in an *in vitro* assay that cysteine protease XCP2 was degraded in presence of recombinant AtMC9 protein (Bollhoner et al., 2013). Finally, Glyceraldehyde 3-phosphate dehydrogenase (GADPH) was discovered as specific substrate of Yca1 yeast metacaspase, which mediates H₂O₂-induced apoptosis cleaved of Yca1 in a dependent Nitric Oxide mediation (Silva et al., 2011), showing a conserved function in both animals and plants.

As mentioned in the previous section, equally important to the positive regulation of HR are its negative regulators to content the damage to the cells destined to die. In this context, conditional overexpression of AtMC1 resulted in ectopic cell death both in native and transiently expressed conditions, which indicated that a tight regulation of this protein must be in place in order to prevent uncontrolled cell death (Coll et al., 2010; Lema Asqui et al., 2017). So far, two negative regulators of AtMC1 have been identified: AtMC2 (Coll et al., 2010) and AtLSD1 (Dietrich et al., 1994). AtLSD1 interacts with AtMC1 through its prodomain. AtLSD1 is a scaffold protein that prevents runaway cell death by modulating ROS accumulation (Li, Chen, Mu, & Zuo, 2013). In contrast, AtMC2 negatively regulates AtMC1 without directly interacting with it. Interestingly, AtMC2 overexpression mimics the *atmc1* mutant phenotype showing reduced levels of cell death, whereas *atmc2* mutant shows increased cell death levels, even higher than in wild type line. Another interesting fact was that self-processing cleavage is not necessary for AtMC2 role. However, the precise role of the prodomain and details of its interplays remain to be clarified (Coll et al., 2010).

Although many aspects of the role of metacaspases and caspase-like proteases were disclosed in the last decade, the molecular mechanisms responsible for HR regulation and how the proteases are implicated in activation and control of cell death runaway are still largely unknown. The prerequisites for host proteases in plant-pathogen interactions are clearly enough, but the mechanism in which they action is frequently not. To provide new insights in mechanism regulation and on the role of signaling proteins, together with defining the protease pathways can provide a better understanding of immune response mechanisms.

OBJECTIVES

Aim of Study

The hypersensitive response is a paradigmatic type of programmed cell death, which plays an important role in certain plant-pathogen interactions. In our laboratory we have previously shown, that the Arabidopsis type I metacaspase AtMC1 is a positive regulator of pathogen-triggered PCD and that negative regulation of AtMC1 by AtLSD1 or AtMC2 can prevent runaway cell death. However, it remains unclear how the cell death signaling is activated after pathogen attack and whether additional HR negative regulators exist.

In our lab we set up an unbiased approach to identify new AtMC1 regulators based in an immunoaffinity purification of AtMC1-containing complexes coupled to mass spectrometry. The use of this approach has allowed us to identify new regulators of AtMC1 activity, in basal versus cell death inducing conditions.

This project started with a list of candidate partners identified under basal and cell death inducing conditions. The main goal of this thesis work was to characterize the functional role of the most prominent AtMC1 complex partners under a cell death-negative and cell death-positive contexts. Specifically, we established two major objectives:

Objective 1

To gather all the current knowledge in the field of programmed cell death and to elaborate a review article citing the relevant literature on programmed cell death in development and in response to pathogen challenge.

Objective 2

To define the functional role of Atserpin1, a negative regulator of protease activity that had been immunoaffinity purified with AtMC1 under basal conditions.

Objective 3

To define the functional role of AtHIR2, a hypersensitive induced reaction protein that had been immunoaffinity purified with AtMC1 under cell death conditions.

PUBLICATIONS

Informe del director de tesi del factor d'impacte dels articles publicats

La memòria de la tesi doctoral “Pathogen-triggered programmed cell death in plants: Metacaspase 1-dependent pathways” (Muerte celular programada desencadenada por patógenos en plantas: Vías dependientes de Metacaspasa 1.) presentada per Saúl Stalin Lema Asqui conté a la secció de publicacions 3 articles i 1 apartat en forma de manuscrit. La participació del doctorand en cadascun d'ells és la que es detalla a continuació:

Publicació 1

Títol: Dying two deaths — programmed cell death regulation in development and disease

Autors: Marlyes Huysmans, **Saúl Lema A**, Núria S. Coll y Moritz K Nowack.

Revista: Aquest article està publicat a la revista Current Opinion in Plant Biology (2017).

Índex d'impacte (2016): 7,357; Àrees: Ciències de plantes (Q1) Nombre de citacions: 10.

La participació del Saúl Lema ha consistit en la cerca exhaustiva i el buidatge de la bibliografia pertinent i -conjuntament amb N. S. Coll- la preparació i l'elaboració del manuscrit, sobretot de l'apartat de PCD a plantes .

Publicació 2

Títol: AtSERPIN1 is an inhibitor of the Metacaspase AtMC1-mediated cell death and autocatalytic processing *in planta*

Autors: **Saúl Lema A**, Dominique Vercammen, Irene Serrano, Marc Valls, Susana Rivas, Frank Van Breusegen, Frank L. Conlon, Jeffery L. Dangl y Núria S. Coll.

Revista: Aquest article està publicat a la revista New Phytologist (2017).

Índex d'impacte (2016): 7,330; Àrees: Ciències de plantes (Q1). Nombre de citacions: 5

El doctorand Saúl Lema Asqui és responsable de tota la part experimental d'aquest treball excepte les figures 1 i 4. També ha participat activament en la planificació del projecte, discussió dels resultats i elaboració del manuscrit i la resta d'autors externs han cedit dades.

Publicació 3

Títol: Detection and Quantification of Protein Aggregates in Plants

Autors: Marc Planas-Marqués, **Saúl Lema A** y Núria S. Coll

Revista: Aquest article està publicat a la revista Methods in Molecular Biology.

Índex d'impacte (2016): 0,510; Àrees: Biologia molecular(Q4); Nombre de citacions: 0

En aquest article, el doctorand Saúl Lema ha contribuït amb el disseny de la figura 1 i l'elaboració del manuscrit.

Manuscrit 1

Títol: AtHIR2, a new regulator of AtMC1-mediated cell death in plants.

Autors: **Saúl Lema A** y Núria S. Coll

El doctorand Saúl Lema ha dut a terme la totalitat del treball experimental, així com de la redacció d'aquest esborrany i de les figures presentades al manuscrit.

Els directors,

Núria Sánchez Coll
Barcelona, 12 d'Abril de 2018

Marc Valls Matheu

Dying two deaths – programmed cell death regulation in development and disease

Resumen de la publicación 1

Muriendo dos muertes: Regulación de la muerte celular programada en desarrollo y enfermedad.

La muerte celular programada (MCP) es un proceso celular fundamental que ha adoptado una plétora de funciones vitales en organismos multicelulares. En las plantas, los procesos de MCP tienen lugar como una parte inherente del desarrollo regular en tipos específicos de células o tejidos, pero también puede ser desencadenada por estreses bióticos o abióticos. A pesar de que en los últimos años hemos visto progresos en nuestro entendimiento de la regulación molecular de los diferentes procesos de MCP de las plantas, todavía no está claro si existe una maquinaria básica común que controla la muerte celular en el desarrollo y la enfermedad. En esta revisión, discutimos los avances recientes en el campo, comparando algunos aspectos de la regulación molecular que controlan el desarrollo y la muerte celular desencadenada por patógenos en las plantas.

Dying two deaths — programmed cell death regulation in development and disease

Marlies Huysmans^{1,2,4}, Saul Lema A^{3,4}, Nuria S Coll³ and Moritz K Nowack^{1,2}



Programmed cell death (PCD) is a fundamental cellular process that has adopted a plethora of vital functions in multicellular organisms. In plants, PCD processes are elicited as an inherent part of regular development in specific cell types or tissues, but can also be triggered by biotic and abiotic stresses. Although over the last years we have seen progress in our understanding of the molecular regulation of different plant PCD processes, it is still unclear whether a common core machinery exists that controls cell death in development and disease. In this review, we discuss recent advances in the field, comparing some aspects of the molecular regulation controlling developmental and pathogen-triggered PCD in plants.

Addresses

¹VIB Department of Plant Systems Biology, 9052 Gent, Belgium

²Department of Plant Biotechnology and Bioinformatics, Ghent University, 9052 Gent, Belgium

³Centre for Research in Agricultural Genomics (CSIC-IRTA-UAB-UB), Bellaterra-Cerdanyola del Valles 08193, Catalonia, Spain

Corresponding authors: Coll, Nuria S

(nuria.sanchez-coll@cragenomica.es) and

Nowack, Moritz K (moritz.nowack@vib.be)

⁴These authors contributed equally to the manuscript.

Current Opinion in Plant Biology 2017, **35**:37–44

This review comes from a themed issue on **Growth and development**

Edited by **Ji Hoon Ahn** and **Marcus Schmid**

For a complete overview see the [Issue](#) and the [Editorial](#)

Available online 16th November 2016

<http://dx.doi.org/10.1016/j.pbi.2016.11.005>

1369-5266/© 2016 The Authors. Published by Elsevier Ltd. This is an open access article under the CC BY-NC-ND license (<http://creativecommons.org/licenses/by-nc-nd/4.0/>).

Introduction

There is no life without death — in modern biology, this ancient axiom has proven to be of remarkable significance. In individual organisms, genetically encoded programs of ageing and death control the turnover of generations, which is the driver of adaptive evolution. Likewise, the genetically programmed death of cells (PCD) in multicellular organisms has acquired a multitude of crucial roles in development, homeostasis and immunity [1,2].

In plants, various forms of PCD have been described as an inherent part of development, as well as a response to

biotic and abiotic stresses. Developmentally controlled PCD (dPCD) occurs during vegetative and reproductive development, often as the final differentiation step of specific cell types; it ends the vital function of senescing or no longer required cells, or creates tissues composed of modified cell corpses that take over structural or storage functions [3]. On the other hand, pathogen-triggered PCD (pPCD) can be elicited in the host plant by invading agents. However, depending on the type of plant–pathogen interaction, pPCD will benefit either the plant or the pathogen [4]. Invasion of biotrophic or hemibiotrophic pathogens — those that feed exclusively or at early stages of their life cycle on live plant tissue — can be thwarted by pathogen detection, triggering hypersensitive response (HR) cell death at the site of attempted attack. In contrast, necrotrophic pathogens, which feed on dead plant tissue, have often developed strategies to silently invade the host plant and hijack its HR machinery, triggering unrestrained PCD at the site of infection and beyond.

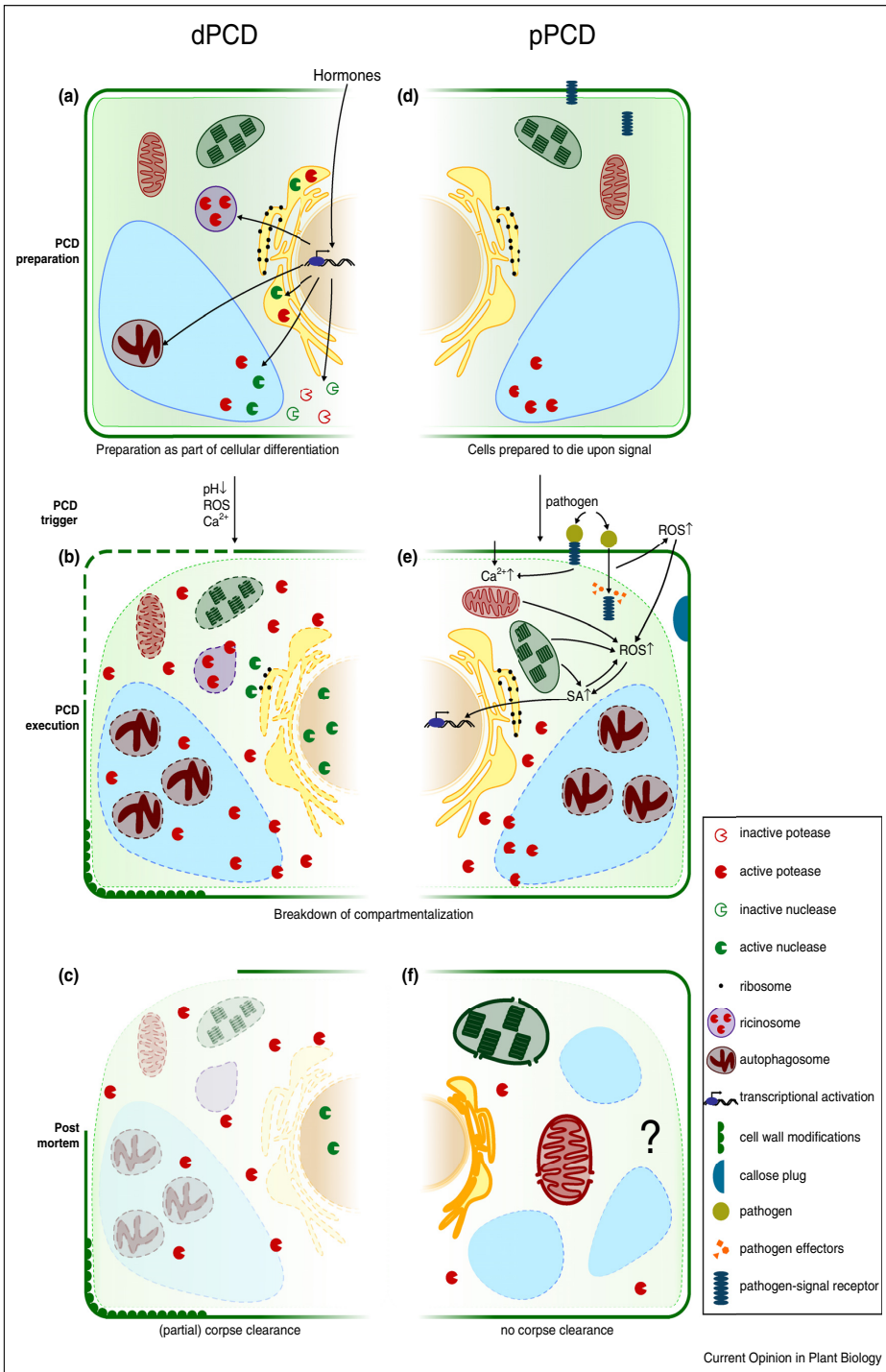
Morphologically, dPCD is associated with a vacuolar type of cell death, while pPCD shows features of both necrosis and vacuolar PCD [5]. However, the molecular regulation of PCD initiation and execution in development and disease remains largely unresolved. Especially the intriguing question of whether dPCD and pPCD are controlled by a common core machinery or by fundamentally different pathways is a matter of debate. In this review, we will highlight the recent advances in dPCD and pPCD research, focusing on comparing the molecular regulation of these different PCD types in plants.

The molecular regulation of dPCD

Hormonal signaling during dPCD

Different hormonal pathways are interconnected to fine-tune dPCD processes (Figure 1a). For instance jasmonic acid, ethylene, auxin and strigolactones have been implicated in dPCD signaling, although exact networks are often still unknown [6–8]. Among them, ethylene is the best-characterized dPCD hormone. In the lace plant (*Aponogetum madagascariensis*), increased ethylene levels, and decreased expression of repressive AmERS1 ethylene receptors is associated with PCD in specific leaf regions to create perforations [9]. After fertilization in *Arabidopsis* (*Arabidopsis thaliana*), ethylene signaling contributes to the elimination of the persistent synergid via cell fusion and nuclear degradation, terminating pollen tube attraction [10,11]. In xylogenic cell cultures of

Figure 1



Chronological overview of the different molecular steps during dPCD and pPCD. (a) to (c) show dPCD events. (a) dPCD preparation as a part of cellular differentiation is initiated by hormonal signaling. This leads to transcriptional activation of dPCD genes, like proteases and nucleases,

Zinnia elegans, chemical inhibition of ethylene signaling delays xylem differentiation, but also directly blocks PCD [12]. This finding indicates that hormones can control both upstream differentiation events as well as downstream dPCD execution.

Transcriptional preparation of dPCD

Plant hormones control many cellular processes via transcriptional regulation [13], including differentiation and dPCD (Figure 1a), although the connection between hormones and transcription factors (TFs) is often still missing. PCD as final differentiation step of certain cell types has to be tightly coordinated with earlier differentiation steps, as precocious or delayed PCD can severely interfere with cellular functions (see [3] for a recent review). NAC (NAM, ATAF and CUC) TFs are one of the most-studied TF families in this context. ORESARA1 (ANAC092) is a master regulator of leaf senescence downstream of ethylene, and upstream of genes that induce senescence and PCD, including BIFUNCTIONAL NUCLEASE 1 (BFN1) and other NAC TFs [14,15*]. Similarly, SOMBRERO (SMB/ANAC033) controls dPCD as a final step of lateral root cap (LRC) differentiation in Arabidopsis [16**]. In the *smb* mutant, LRC cells die in an aberrant, non-prepared fashion, and cell corpses remain non-degraded on the root surface. During xylem differentiation, VASCULAR-RELATED NAC DOMAIN 7 (ANAC030) is part of a complex transcriptional network that induces expression of downstream TFs and putative PCD executors [17].

Other TF families have also been implicated in dPCD control. In the receptive synergid of Arabidopsis, the two reproductive meristem TFs VERDANDI and VALKYRIE are directly activated by the MADS-box TF complex SEEDSTICK-SEPALLATA 3 to regulate synergid degeneration [18], a prerequisite for successful fertilization. After fertilization, the endosperm-expressed MADS-box TF AGAMOUS-LIKE 62 triggers PCD in the adjacent nucellus via an unknown signal that activates the PCD-promoting MADS-box TFs TRANSPARENT TESTA 16 and GORDITA [19*]. During mid-seed development, endosperm degeneration is initiated by a heterodimer of two endosperm-expressed bHLH TFs, ZHOUIPI (ZOU) and INDUCER OF CBP EXPRESSION 1 [20]. In the *zou* mutant, embryo growth is hampered by a persistent rigid endosperm, associated with reduced expression of cell wall modifying enzymes, indicating that cell wall

degradation might be a mechanical prerequisite for endosperm PCD [21].

Triggers of dPCD

The gradual buildup of dPCD competence in the course of cellular differentiation stands in contrast to the rapidly triggered execution of cell death. Several cellular signals, including calcium fluxes, accumulation of reactive oxygen species (ROS), and cytoplasmic acidification have been implicated in PCD triggering [22] (Figure 1b).

Calcium signaling is involved in many cellular processes [23], including PCD. During the self-incompatibility (SI) response in poppy (*Papaver rhoeas*), calcium influx triggers a signaling cascade that induces rapid PCD of the incompatible pollen tubes [24*]. In Arabidopsis ovules, fertilization requires coordinated disintegration of the pollen tube and the synergid cell. A calcium dialogue in both cells has been observed, and aberrant calcium signatures in the synergid obstruct pollen tube burst and synergid PCD [25**,26**].

ROS have been suggested to play a role in stress responses as well as dPCD. High levels of ROS can directly kill a cell by causing membrane leakage [27], whereas lower levels of ROS can have diverse signaling functions [22]. In the rice *dtc1* mutant, tapetum PCD is delayed due to a failure of ROS accumulation [28*]. Altering ROS production via manipulation of RESPIRATORY BURST OXIDASE HOMOLOG E disturbs timing of tapetal PCD in Arabidopsis [29]. In the poppy SI response, ROS accumulate in the pollen tube [30], possibly to control pollen tube burst by cell wall remodeling, and prior to sperm delivery in Arabidopsis, ROS induce pro-PCD protease activity [31].

Finally, cytoplasmic acidification has been implicated in dPCD processes. The SI response in poppy causes a dramatic pH drop that is necessary and sufficient to activate several proteases, and to induce PCD [24*]. Also during LRC PCD in Arabidopsis, acidification of the cytoplasm was observed prior to cell death, and manipulation of intracellular pH affected cell death rates [16**].

dPCD execution and corpse clearance

Upon triggering signals, PCD execution and *post mortem* corpse clearance are initiated (Figure 1c). A multitude of lytic enzymes is activated or released from safe storage

(Figure 1 Legend Continued) which are sequestered or kept inactive. Only upon a cell death trigger, like calcium, ROS or pH drop, PCD execution is initiated. (b) During dPCD execution, lytic enzymes are activated or released from safe storage and degrade the various cellular compartments, and in the xylem, cell walls are fortified. Upregulation of autophagy can occur. (c) At the end of dPCD, the cell corpse is completely degraded, or only the fortified cell wall remains. (d) to (f) show pPCD events. (d) pPCD is only triggered upon pathogen attack, mediated by receptors present on the membrane or in the cytoplasm of all cells of a plant. (e) When a pathogen invades a plant cell, the activated receptor increases calcium and ROS levels in the cell, leading to the production of salicylic acid (SA). SA, in turn, induces transcription of pPCD related genes, and amplifies the ROS burst in a positive feedback loop, creating a toxic environment. (f) The exact mechanisms of cellular degradation during pPCD are still largely unknown, but complete cell corpse clearance is absent. The cells undergo vacuolization and the organelles swell and burst.

compartments to degrade cellular components [22]. Dying Arabidopsis LRC cells for instance are completely degraded via a cell-autonomous program controlled by SMB [16**]. In xylem cells, however, only the protoplast is degraded, while a fortified cell wall remains, fulfilling essential *post mortem* tasks in water transport and wood formation [32].

During corpse clearance, nucleic acid species are degraded. Although nuclear degradation is frequently reported [28*,29,33*,34*] only few molecular players have been identified. In the LRC of Arabidopsis, BFN1 is responsible for DNA degradation, because the *bfn1* mutant exhibits non-degraded nuclear remnants at the root surface. To allow a safe BFN1 production in living cells, this protein is only released from the endoplasmic reticulum (ER) upon PCD initiation [16**].

Besides nucleases, proteases are also involved in PCD execution and corpse clearance [22]. In tomato endosperm and the Arabidopsis root cap, cysteine proteases are stored in ER-derived compartments [35,36], while in the Arabidopsis tapetum, they are transported to the vacuole [33*]. For several proteases, caspase-like activities were found, for instance vacuolar processing enzymes (VPEs) or certain subunits of the proteasome [37] (for a recent overview of caspase-like activities in dPCD, see [22]). Despite the detection of caspase-like activities, their precise functions remain largely mysterious. On the other hand, the distantly caspase-related metacaspases (MCs) do not possess a caspase-like activity, and some of them have been implicated in dPCD. For instance, MC9 in Arabidopsis has been implicated in corpse clearance during xylem PCD [38]. Interestingly, independent findings suggest a connection between MCs and autophagy. MC9 in the tracheary elements (TEs) might have an additional *pre mortem* function in reducing autophagy levels to protect the surrounding cells [39]. Contrarily, in the spruce suspensor, mcII-Pa promotes autophagy, which is necessary for a controlled PCD execution and prevents the switch to a necrotic form of cell death [40].

The molecular regulation of pPCD

Hormonal signaling during pPCD

Plant hormones are crucial for plant immune responses, controlling complex and pathosystem-specific networks determining the outcome of a particular plant–pathogen interaction. Among them, SA is the only phytohormone strictly required for the establishment of pPCD. SA promotes pPCD leading to immunity against biotrophs and susceptibility towards necrotrophs [41,42]. Tightly regulated positive feedback loops between SA and ROS are essential to ensure rapid amplification of defense responses [43] (Figure 1e).

Considering the importance of SA signaling, it is not surprising that biotrophic/hemibiotrophic pathogens have

evolved strategies to subvert the SA signaling pathway as a virulence strategy. Some pathogens deliver effector proteins that directly interfere with cellular SA biosynthesis or signaling [4]. Alternatively, some pathogens suppress SA-mediated defenses by producing phytotoxins that tamper with the crosstalk between SA and other hormones involved in immunity. This is the case for coronatine from *Pseudomonas syringae*, which mimics the SA antagonist jasmonic acid [44*,45,46]. Another example is PSE1 from *Phytophthora parasitica*, a toxin that promotes auxin accumulation at infection sites, resulting in inhibition of SA-mediated cell death and increased pathogen growth [47].

Triggers of pPCD

Cytoplasmic immune receptor-mediated recognition at the site of attack has been considered as the main pPCD trigger during plant-biotrophic/hemibiotrophic pathogen interactions [48] (Figure 1d). In fact, pPCD phenotypes can be triggered by autoactivation of many different cytoplasmic immune receptor proteins and can be suppressed by removal of SA or inhibition of SA signaling pathways [49,50]. Membrane-associated immune receptor-like kinases (RLKs) can also regulate cell death. This is the case of BIR1, a suppressor of plant defense whose inactivation triggers pPCD mediated by association of two additional immune RLKs: SOBIR and BAK1 [51**]. In fact, the importance of the apoplast in pPCD has just started to emerge, as is the source of many potential pPCD triggers like RLK ligands, ROS, nitric oxide (NO) and proteases.

It is well established that pathogen perception triggers calcium influxes, as well as accumulation of SA, ROS and NO. SA signaling is preceded by oxidative bursts originating in different cellular compartments, but ROS acts also downstream of SA [52]. This positive SA–ROS feedback loop can be considered as a pPCD trigger, although the molecular details of this activation remain to be elucidated (Figure 1e).

The pPCD machinery has been conveniently hijacked by plant necrotrophic pathogens, some of which are able to secrete pPCD triggering toxins. A good example is the fungus *Cochliobolus victoriae*, which secretes victorin into host cells. This results in the activation of the cytoplasmic immune receptor LOV1, which causes pPCD and susceptibility to *C. victoriae* [53]. Another toxin with PCD-triggering activity is oxalic acid from the necrotrophic fungus *Sclerotinia sclerotiorum*. Oxalic acid deficiency renders *S. sclerotiorum* non-pathogenic, inducing autophagy-mediated cell death and various defense responses in the host [54,55].

Regulation, execution and confinement of pPCD

Transcriptional regulation during dPCD and pPCD are markedly different. A transcriptomic meta-analysis

revealed several clusters of genes providing unique transcriptional signatures for different plant PCD types. However, in the case of pPCD, the cluster identified includes a set of genes most of which are involved in defense, rather than specifically in pPCD [34*]. Nevertheless, TFs play essential roles in the establishment of immune responses in plants [56]. The best understood TF promoting pPCD and defense responses is undoubtedly Arabidopsis MYB30. MYB30 is involved in the SA amplification loop that controls pPCD. It also regulates the biosynthesis of very long chain fatty acids, precursors of lipid derivatives with roles in cell death signaling and basal defense [57].

Calcium has been proposed as a master regulator that contributes to triggering pPCD and ensures its timely and controlled execution [58]. Blocking calcium transport by LaCl₃ or ruthenium red inhibits pPCD [59]. The calcium-dependent protein kinases CPK1 and 2 have been shown to specifically regulate the onset of pPCD together with CPK5 and 6, which phosphorylate and activate various WRKY TFs [59]. Calcium also acts as a negative regulator of SA signaling presumably to shut down defenses when they are no longer needed [60]. In addition, a calcium-binding protein and a calcium-regulated ATPase have been identified as part of the meta-transcriptomic pPCD cluster [34*].

Autophagy can act as a positive or negative regulator of pPCD depending on the pathosystem [55,61**,62]. The Arabidopsis metacaspase AtMC1 acts synergistically with autophagy to promote pPCD [63**]. Similarly, retromer-mediated vacuolar trafficking has been shown to be required for defense and pPCD [64*]. Wheat metacaspase 4 (*TaMCA4*) overexpression enhances pPCD caused by effector-mediated recognition of the hemibiotrophic fungus *Puccinia striiformis* and contributes to disease resistance, whereas its silencing causes the opposite effect [65]. Several additional regulators have recently emerged as key for a proper establishment of pPCD. VPEs, phytase and saspase have been shown to be the most important sources of caspase-like activities involved in pPCD [66], although their individual contribution may vary depending on the specific pathosystem.

Equally important as positive regulation for pPCD establishment are negative regulators to confine the damage to the cells destined to die. Autophagy has been shown to prevent runaway pPCD [67]. AtMC1-mediated pPCD is negatively regulated by AtMC2 and AtLSD1 [68]. AtLSD1 function is partly mediated by its SA-dependent interaction with catalases, which have been proposed to prevent runaway cell death by modulating ROS accumulation [69]. Unfortunately, most studies carried out to date lack the spatio-temporal dimension of the interaction. It has been long assumed that positive regulators act at the HR site and negative regulators in the surrounding areas, but the

molecular evidence for this premise is mostly lacking and the functional zonation of pPCD remains to be clarified.

Conclusions

Among the various types of plant PCD, several distinct forms of dPCD and pPCD have been studied over the last years. Despite recent progress in identifying PCD regulators and in understanding their molecular mode of action, it remains hard to fathom whether dPCD and pPCD share canonical, evolutionary conserved core PCD regulators, or whether similarities are merely mechanistic parallels that have been independently adopted to fulfill analogous roles in the different contexts.

Undoubtedly, there are numerous similarities that can be observed in dPCD and pPCD. ROS and calcium have been implicated in signaling events leading to cell death in both contexts. Metacaspases have been assigned different roles in dPCD and pPCD, from upstream regulation to downstream *post mortem* cell clearance. Other proteases, for instance the VPEs with caspase-like activity, are involved in dPCD and pPCD processes as well [37]. Likewise, modulation of autophagy has been functionally implicated in both forms of PCD; as an effector of pPCD and as a corpse clearance mechanism during dPCD [70].

There is also common evidence of transcriptional regulation, though within different contexts. In many dPCD forms, cells need to gradually acquire a competence to execute cell death upon specific developmental signals. In contrast, cells always need to be ready to initiate immune responses upon pathogen attack independent of their cellular identity (Figure 1a,d). In order to be of selective advantage, transcriptional responses have to be rapid and direct to counteract pathogen attack, with death being sometimes unavoidable, but beneficial for the whole organism, as it has been conserved through evolution.

In a way, forms of pPCD can be regarded as a facultative outcome of signaling processes between different cells that come into contact (host and pathogen), and are in that way similar to some forms of dPCD that involve signaling between different cell types. For instance, poppy pollen dies only when contacting stigmatic papilla cells that express the cognate ('self') S-determinant [30]. Similarly, pollen and synergid cells only die in a controlled way after establishing an elaborate calcium dialogue [25**,26**]. Possibly these facultative non-cell autonomous forms of dPCD are more closely related to forms of pPCD than autonomous forms of differentiation-induced dPCD. Interestingly, the RLK FERONIA promotes both pollen tube reception as well as susceptibility to powdery mildew infection [71], corroborating the existence of molecular links between developmentally controlled and pathogen-related forms of PCD. More such regulators with dual roles in dPCD and pPCD may be expected to see the light in the near future of PCD research.

Acknowledgements

We are grateful for the critical and constructive comments on the present manuscript made by the reviewers and by members of the PCD lab at the VIB PSB department. We further acknowledge the help of Annick Bleys in preparing the manuscript, and the funding of M.K.N. by an ERC Starting Grant (PROCELLDEATH, EU project 639234). We apologize to those authors whose primary work could not be cited owing to space limitations.

References and recommended reading

Papers of particular interest, published within the period of review, have been highlighted as:

- of special interest
- of outstanding interest

1. Fuchs Y, Steller H: **Live to die another way: modes of programmed cell death and the signals emanating from dying cells.** *Nat Rev Mol Cell Biol* 2015, **16**:329-344.
 2. Van Hautegeem T, Waters AJ, Goodrich J, Nowack MK: **Only in dying, life: programmed cell death during plant development.** *Trends Plant Sci* 2015, **20**:102-113.
 3. Daneva A, Gao Z, Van Durme M, Nowack MK: **Functions and regulation of programmed cell death in plant development.** *Annu Rev Cell Dev Biol* 2016.
 4. Mukhtar MS, McCormack ME, Argueso CT, Pajeroska-Mukhtar KM: **Pathogen tactics to manipulate plant cell death.** *Curr Biol* 2016, **26**:R608-R619.
 5. van Doorn WG, Beers EP, Dangel JL, Franklin-Tong VE, Gallois P, Hara-Nishimura I, Jones AM, Kawai-Yamada M, Lam E, Mundy J *et al.*: **Morphological classification of plant cell deaths.** *Cell Death Differ* 2011, **18**:1241-1246.
 6. Qi T, Wang J, Huang H, Liu B, Gao H, Liu Y, Song S, Xie D: **Regulation of jasmonate-induced leaf senescence by antagonism between bHLH subgroup IIIe and III d factors in Arabidopsis.** *Plant Cell* 2015, **27**:1634-1649.
 7. Ueda H, Kusaba M: **Strigolactone regulates leaf senescence in concert with ethylene in Arabidopsis.** *Plant Physiol* 2015, **169**:138-147.
 8. Yin LL, Xue HW: **The MADS29 transcription factor regulates the degradation of the nucellus and the nucellar projection during rice seed development.** *Plant Cell* 2012, **24**:1049-1065.
 9. Rantong G, Evans R, Gunawardena AH: **Lace plant ethylene receptors, AmERS1a and AmERS1c, regulate ethylene-induced programmed cell death during leaf morphogenesis.** *Plant Mol Biol* 2015, **89**:215-227.
 10. Maruyama D, Volz R, Takeuchi H, Mori T, Igawa T, Kurihara D, Kawashima T, Ueda M, Ito M, Umeda M *et al.*: **Rapid elimination of the persistent synergid through a cell fusion mechanism.** *Cell* 2015, **161**:907-918.
- Live-cell imaging was used to show that the persistent synergid is eliminated during fertilization by fusing with the endosperm, thereby diluting pollen tube attractants and preventing polytuby. After cell fusion, the synergid nucleus gets degraded in the endosperm cytoplasm, which finalizes the disposal of the synergid cell.
11. Volz R, Heydlauff J, Ripper D, von Lyncker L, Gross-Hardt R: **Ethylene signaling is required for synergid degeneration and the establishment of a pollen tube block.** *Dev Cell* 2013, **25**:310-316.
 12. Pesquet E, Zhang B, Gorzsas A, Puhakainen T, Serk H, Escamez S, Barbier O, Gerber L, Courtois-Moreau C, Alatalo E *et al.*: **Non-cell-autonomous postmortem lignification of tracheary elements in *Zinnia elegans*.** *Plant Cell* 2013.
 13. Larrieu A, Vernoux T: **Comparison of plant hormone signalling systems.** *Essays Biochem* 2015, **58**:165-181.
 14. Kim HJ, Nam HG, Lim PO: **Regulatory network of NAC transcription factors in leaf senescence.** *Curr Opin Plant Biol* 2016, **33**:48-56.
 15. Kim HJ, Hong SH, Kim YW, Lee IH, Jun JH, Phee BK, Rupak T, Jeong H, Lee Y, Hong BS *et al.*: **Gene regulatory cascade of**

senescence-associated NAC transcription factors activated by ETHYLENE-INSENSITIVE2-mediated leaf senescence signalling in Arabidopsis. *J Exp Bot* 2014, **65**:4023-4036.

The authors identified new players in the gene regulatory network controlling senescence in Arabidopsis leaves. EIN2 directly or indirectly activates several senescence associated NAC TFs, which coordinate cellular catabolism and PCD processes.

16. Fendrych M, Van Hautegeem T, Van Durme M, Olvera-Carrillo Y, Huysmans M, Karimi M, Lippens S, Guerin CJ, Krebs M, Schumacher K *et al.*: **Programmed cell death controlled by ANAC033/SOMBRERO determines root cap organ size in Arabidopsis.** *Curr Biol* 2014.

The authors show that PCD is employed to achieve cell number homeostasis in the root cap of Arabidopsis. Root cap PCD is linked with root cap differentiation by the NAC transcription factor SMB, and is necessary for regular root growth. Downstream of SMB, the nuclease BFN1 is necessary for efficient nuclear degradation *post mortem*.

17. Endo H, Yamaguchi M, Tamura T, Nakano Y, Nishikubo N, Yoneda A, Kato K, Kubo M, Kajita S, Katayama Y *et al.*: **Multiple classes of transcription factors regulate the expression of VASCULAR-RELATED NAC-DOMAIN7, a master switch of xylem vessel differentiation.** *Plant Cell Physiol* 2015, **56**:242-254.
18. Mendes MA, Guerra RF, Castelnuovo B, Velazquez YS, Morandini P, Manrique S, Baumann N, Gross-Hardt R, Dickinson H, Colombo L: **Live and let die: a REM complex promotes fertilization through synergid cell death in Arabidopsis.** *Development* 2016.
19. Xu W, Fiume E, Coen O, Pechoux C, Lepiniec L, Magnani E: **Endosperm and nucellus develop antagonistically in Arabidopsis seeds.** *Plant Cell* 2016.

The authors show that Polycomb-group (PcG) proteins repress nucellus degeneration in the unfertilized ovule. Upon fertilization the endospermic MADS-box transcription factor AGL62 induces a hypothetical signal that releases PcG repression of the transcription factor TT16, which promotes nucellus degradation.

20. Denay G, Creff A, Moussu S, Wagnon P, Thevenin J, Gerentes MF, Chambrier P, Dubreucq B, Ingram G: **Endosperm breakdown in Arabidopsis requires heterodimers of the basic helix-loop-helix proteins ZHOUP1 and INDUCER OF CBP EXPRESSION 1.** *Development* 2014, **141**:1222-1227.
21. Fourquin C, Beauzamy L, Chamot S, Creff A, Goodrich J, Boudaoud A, Ingram G: **Mechanical stress mediated by both endosperm softening and embryo growth underlies endosperm elimination in Arabidopsis seeds.** *Development* 2016.
22. Van Durme M, Nowack MK: **Mechanisms of developmentally controlled cell death in plants.** *Curr Opin Plant Biol* 2016, **29**:29-37.
23. Uslu VV, Grossmann G: **The biosensor toolbox for plant developmental biology.** *Curr Opin Plant Biol* 2016, **29**:138-147.
24. Wilkins KA, Bosch M, Haque T, Teng N, Poulter NS, Franklin-Tong VE: **Self-incompatibility-induced programmed cell death in field poppy pollen involves dramatic acidification of the incompatible pollen tube cytosol.** *Plant Physiol* 2015, **167**:766-779.

A thorough analysis of pH dynamics in pollen tubes during the self-incompatibility (SI) response in poppy revealed that cytoplasmic acidification occurring prior to vacuolar rupture is both necessary and sufficient for SI-PCD. Acidification creates the optimal conditions for several hydrolase activities, and plays a role in the formation of actin foci.

25. Ngo QA, Vogler H, Lituiev DS, Nestorova A, Grossniklaus U: **A calcium dialog mediated by the FERONIA signal transduction pathway controls plant sperm delivery.** *Dev Cell* 2014, **29**:491-500.

Using different genetically encoded calcium sensors, this paper uncovered that proper sperm cell delivery in Arabidopsis requires tightly coordinated calcium oscillations in both the pollen tube and the receptive synergid. Ngo *et al.* showed that this calcium dialog relies on the FERONIA signaling pathway.

26. Denninger P, Bleckmann A, Lausser A, Vogler F, Ott T, Ehrhardt DW, Frommer WB, Sprunck S, Dresselhaus T, Grossmann G: **Male-female communication triggers calcium signatures during fertilization in Arabidopsis.** *Nat Commun* 2014, **5**:4645.

See annotation to [25**].

27. Van Aken O, Van Breusegem F: **Licensed to kill: mitochondria, chloroplasts, and cell death.** *Trends Plant Sci* 2015, **20**:754-766.
28. Yi J, Moon S, Lee YS, Zhu L, Liang W, Zhang D, Jung KH, An G: **Defective tapetum cell death 1 (DTC1) regulates ROS levels by binding to metallothionein during tapetum degeneration.** *Plant Physiol* 2016, **170**:1611-1623.
- The tapetum of the rice *dtc1* mutant fails to accumulate ROS, and shows delayed tapetum PCD resulting in male sterile plants. Possibly, DCT1 increases ROS levels by inhibiting the ROS scavenger OsMT2b prior to tapetum PCD.
29. Xie HT, Wan ZY, Li S, Zhang Y: **Spatiotemporal production of reactive oxygen species by NADPH oxidase is critical for tapetal programmed cell death and pollen development in Arabidopsis.** *Plant Cell* 2014, **26**:2007-2023.
30. Wilkins KA, Poulter NS, Franklin-Tong VE: **Taking one for the team: self-recognition and cell suicide in pollen.** *J Exp Bot* 2014, **65**:1331-1342.
31. Duan Q, Kita D, Johnson EA, Aggarwal M, Gates L, Wu HM, Cheung AY: **Reactive oxygen species mediate pollen tube rupture to release sperm for fertilization in Arabidopsis.** *Nat Commun* 2014, **5**:3129.
32. Escamez S, Tuominen H: **Programmes of cell death and autolysis in tracheary elements: when a suicidal cell arranges its own corpse removal.** *J Exp Bot* 2014, **65**:1313-1321.
33. Zhang D, Liu D, Lv X, Wang Y, Xun Z, Liu Z, Li F, Lu H: **The cysteine protease CEP1, a key executor involved in tapetal programmed cell death, regulates pollen development in Arabidopsis.** *Plant Cell* 2014, **26**:2939-2961.
- Using transcriptome profiling and mutant analyses, a function of the protease CEP1 in PCD of the tapetum is revealed. In the *cep1* mutant, tapetal cell death is delayed, leading to decreased transport of cell wall material to the pollen exine, and resulting in pollen aggregation and infertility.
34. Olvera-Carrillo Y, Van Bel M, Van Hautegeem T, Fendrych M, Huysmans M, Simaskova M, van Durme M, Buscaill P, Rivas S, SC N *et al.*: **A conserved core of programmed cell death indicator genes discriminates developmentally and environmentally induced programmed cell death in plants.** *Plant Physiol* 2015, **169**:2684-2699.
- An extensive meta-analysis of publically available transcriptome data shows that developmentally and environmentally induced PCD are regulated by largely distinct sets of genes. The authors identified a core of conserved indicator genes associated with developmental PCD.
35. Trobacher CP, Senatore A, Holley C, Greenwood JS: **Induction of a ricinosomal-protease and programmed cell death in tomato endosperm by gibberellic acid.** *Planta* 2013, **237**:665-679.
36. Hierl G, Howing T, Isono E, Lottspeich F, Gietl C: **Ex vivo processing for maturation of Arabidopsis KDEL-tailed cysteine endopeptidase 2 (AtCEP2) pro-enzyme and its storage in endoplasmic reticulum derived organelles.** *Plant Mol Biol* 2014, **84**:605-620.
37. Hatsugai N, Yamada K, Goto-Yamada S, Hara-Nishimura I: **Vacuolar processing enzyme in plant programmed cell death.** *Front Plant Sci* 2015, **6**:234.
38. Bollhoner B, Zhang B, Stael S, Denance N, Overmyer K, Goffner D, Van Breusegem F, Tuominen H: **Post mortem function of AtMC9 in xylem vessel elements.** *New Phytol* 2013.
39. Escamez S, Andre D, Zhang B, Bollhoner B, Pesquet E, Tuominen H: **METACASPASE9 modulates autophagy to confine cell death to the target cells during Arabidopsis vascular xylem differentiation.** *Biol Open* 2016, **5**:122-129.
40. Minina EA, Filonova LH, Fukada K, Savenkov EI, Gogvadze V, Clapham D, Sanchez-Vera V, Suarez MF, Zhivotovsky B, Daniel G *et al.*: **Autophagy and metacaspase determine the mode of cell death in plants.** *J Cell Biol* 2013, **203**:917-927.
41. Birkenbihl RP, Somssich IE: **Transcriptional plant responses critical for resistance towards necrotrophic pathogens.** *Front Plant Sci* 2011, **2**:76.
42. Pieterse CM, Leon-Reyes A, Van der Ent S, Van Wees SC: **Networking by small-molecule hormones in plant immunity.** *Nat Chem Biol* 2009, **5**:308-316.
43. Shirasu K, Nakajima H, Rajasekhar VK, Dixon RA, Lamb C: **Salicylic acid potentiates an agonist-dependent gain control that amplifies pathogen signals in the activation of defense mechanisms.** *Plant Cell* 1997, **9**:261-270.
44. Gimenez-Ibanez S, Boter M, Fernandez-Barbero G, Chini A, Rathjen JP, Solano R: **The bacterial effector HopX1 targets JAZ transcriptional repressors to activate jasmonate signaling and promote infection in Arabidopsis.** *PLoS Biol* 2014, **12**:e1001792.
- In this study the authors found that in a *Pseudomonas syringae* strain that does not produce the jasmonic acid mimic coronatine, the effector HopX1 promotes degradation of JAZ proteins, a family of JA repressors. This results in susceptibility by activation of jasmonic acid-induced defenses and repression of salicylic acid-dependent responses.
45. Jiang S, Yao J, Ma KW, Zhou H, Song J, He SY, Ma W: **Bacterial effector activates jasmonate signaling by directly targeting JAZ transcriptional repressors.** *PLoS Pathog* 2013, **9**:e1003715.
46. Katsir L, Schillmiller AL, Staswick PE, He SY, Howe GA: **COI1 is a critical component of a receptor for jasmonate and the bacterial virulence factor coronatine.** *Proc Natl Acad Sci U S A* 2008, **105**:7100-7105.
47. Kazan K, Lyons R: **Intervention of phytohormone pathways by pathogen effectors.** *Plant Cell* 2014, **26**:2285-2309.
48. Coll NS, Epple P, Dangl JL: **Programmed cell death in the plant immune system.** *Cell Death Differ* 2011, **18**:1247-1256.
49. Rodriguez E, El Ghoul H, Mundy J, Petersen M: **Making sense of plant autoimmunity and 'negative regulators'.** *FEBS J* 2016, **283**:1385-1391.
50. Bruggeman Q, Raynaud C, Benhamed M, Delarue M: **To die or not to die? Lessons from lesion mimic mutants.** *Front Plant Sci* 2015, **6**:24.
51. Liu Y, Huang X, Li M, He P, Zhang Y: **Loss-of-function of Arabidopsis receptor-like kinase BIR1 activates cell death and defense responses mediated by BAK1 and SOBIR1.** *New Phytol* 2016.
- This study highlights the importance of membrane-associated receptor-like kinases (RLKs) in pPCD triggering. Constitutive activation of cell death and defense responses in the receptor-like kinase (RLK) BIR1 are mediated by two additional RLKs BAK1 and SOBIR1.
52. Herrera-Vasquez A, Salinas P, Holuigue L: **Salicylic acid and reactive oxygen species interplay in the transcriptional control of defense genes expression.** *Front Plant Sci* 2015, **6**:171.
53. Lorang J, Kidarsa T, Bradford CS, Gilbert B, Curtis M, Tzeng SC, Maier CS, Wolpert TJ: **Tricking the guard: exploiting plant defense for disease susceptibility.** *Science* 2012, **338**:659-662.
54. Kim KS, Min JY, Dickman MB: **Oxalic acid is an elicitor of plant programmed cell death during *Sclerotinia sclerotiorum* disease development.** *Mol Plant Microbe Interact* 2008, **21**:605-612.
55. Kabbage M, Williams B, Dickman MB: **Cell death control: the interplay of apoptosis and autophagy in the pathogenicity of *Sclerotinia sclerotiorum*.** *PLoS Pathog* 2013, **9**:e1003287.
56. Buscaill P, Rivas S: **Transcriptional control of plant defence responses.** *Curr Opin Plant Biol* 2014, **20**:35-46.
57. Raffaele S, Vaillieu F, Leger A, Joubes J, Miersch O, Huard C, Blee E, Mongrand S, Domergue F, Roby D: **A MYB transcription factor regulates very-long-chain fatty acid biosynthesis for activation of the hypersensitive cell death response in Arabidopsis.** *Plant Cell* 2008, **20**:752-767.
58. Stael S, Kmiecik P, Willems P, Van Der Kelen K, Coll NS, Teige M, Van Breusegem F: **Plant innate immunity – sunny side up?** *Trends Plant Sci* 2015, **20**:3-11.
59. Gao X, Chen X, Lin W, Chen S, Lu D, Niu Y, Li L, Cheng C, McCormack M, Sheen J *et al.*: **Bifurcation of Arabidopsis NLR immune signaling via Ca(2+)-dependent protein kinases.** *PLoS Pathog* 2013, **9**:e1003127.
60. Du L, Ali GS, Simons KA, Hou J, Yang T, Reddy AS, Poovaiah BW: **Ca(2+)/calmodulin regulates salicylic-acid-mediated plant immunity.** *Nature* 2009, **457**:1154-1158.

61. Li Y, Kabbage M, Liu W, Dickman MB: **Aspartyl protease-mediated cleavage of BAG6 is necessary for autophagy and fungal resistance in plants.** *Plant Cell* 2016, **28**:233-247.

The authors show that the co-chaperone BAG6, required for basal defense against fungi in plants, is cleaved in a caspase-1-like dependent manner *in vivo*, which triggers autophagy in the host. Autophagy induction results in disease resistance, coupling fungal recognition with the defense induction.

62. Teh OK, Hofius D: **Membrane trafficking and autophagy in pathogen-triggered cell death and immunity.** *J Exp Bot* 2014, **65**:1297-1312.

63. Coll NS, Smidler A, Puigvert M, Popa C, Valls M, Dangl JL: **The plant metacaspase AtMC1 in pathogen-triggered programmed cell death and aging: functional linkage with autophagy.** *Cell Death Differ* 2014, **21**:1399-1408.

This study demonstrates that the metacaspase AtMC1 plays developmentally regulated antagonistic as a cell death regulator. In young plants AtMC1 acts as a positive regulator of pPCD, whereas in older plants negatively regulates aging. Both AtMC1-mediated pathways occur additively to autophagy, indicating a high degree of complexity in the regulation of these essential pathways.

64. Munch D, Teh OK, Malinovsky FG, Liu Q, Vetukuri RR, El Kasmi F, Brodersen P, Hara-Nishimura I, Dangl JL, Petersen M *et al.*: **Retromer contributes to immunity-associated cell death in Arabidopsis.** *Plant Cell* 2015, **27**:463-479.

This study highlights the importance of membrane trafficking in pPCD regulation. The authors discover that the retromer complex, essential for

protein sorting and vacuolar trafficking, contributes to autoimmunity and is a positive regulator of pPCD.

65. Wang X, Wang X, Feng H, Tang C, Bai P, Wei G, Huang L, Kang Z: **TaMCA4, a novel wheat metacaspase gene functions in programmed cell death induced by the fungal pathogen *Puccinia striiformis* f. sp. tritici.** *Mol Plant Microbe Interact* 2012, **25**:755-764.

66. Salvesen GS, Hempel A, Coll NS: **Protease signaling in animal and plant-regulated cell death.** *FEBS J* 2016, **283**:2577-2598.

67. Liu Y, Schiff M, Czymmek K, Tallozy Z, Levine B, Dinesh-Kumar SP: **Autophagy regulates programmed cell death during the plant innate immune response.** *Cell* 2005, **121**:567-577.

68. Coll NS, Vercammen D, Smidler A, Clover C, Van Breusegem F, Dangl JL, Epple P: **Arabidopsis type I metacaspases control cell death.** *Science* 2010, **330**:1393-1397.

69. Li Y, Chen L, Mu J, Zuo J: **LESION SIMULATING DISEASE1 interacts with catalases to regulate hypersensitive cell death in Arabidopsis.** *Plant Physiol* 2013, **163**:1059-1070.

70. Minina EA, Bozhkov PV, Hofius D: **Autophagy as initiator or executioner of cell death.** *Trends Plant Sci* 2014, **19**:692-697.

71. Kessler SA, Shimosato-Asano H, Keinath NF, Wuest SE, Ingram G, Panstruga R, Grossniklaus U: **Conserved molecular components for pollen tube reception and fungal invasion.** *Science* 2010, **330**:968-971.

AtSERPIN1 is an inhibitor of the Metacaspase AtMC1-mediated cell death and autocatalytic processing *in planta*

Resumen de la publicación 2

AtSERPIN1 es un inhibidor de la muerte celular y procesamiento auto-catalítico mediados por la Metacaspasa AtMC1 *in planta*

- La respuesta hipersensible (RH) es un fenómeno localizado de muerte celular programada que se produce en respuesta al reconocimiento de patógenos en el lugar mismo de la invasión. A pesar de que más que un siglo de investigación en RH, poco se sabe sobre cómo está rigurosamente regulado y cómo puede ser confinado espacialmente a unas pocas células.
- AtMC1 es una Metacaspasa de *Arabidopsis Thaliana* que regula positivamente la RH. Aquí, hemos utilizado un enfoque imparcial para identificar nuevos reguladores de AtMC1. La purificación de inmunoafinidad en complejos que contenían AtMC1 nos llevó a la identificación del inhibidor de proteasa AtSerp1.
- Nuestros datos claramente mostraron que la co-immunoprecipitación entre AtMC1-AtSerp1 y la formación del complejo entre ellos se perdió por la mutación del sitio catalítico en AtMC1, además que el prodominio de AtMC1 no es requerido para la interacción. AtSerp1 bloquea el autoprocesamiento de AtMC1 e inhibe la muerte celular mediada por AtMC1. Nuestros resultados constituyen un ejemplo *in vivo* de una Serpina actuando como un inhibidor suicida en plantas, evocando la actividad de serpinas animales y virales sobre reguladores inmunes y de muerte celular, incluyendo la caspasa-1.
- Estos resultados indican una función conservada de un inhibidor de proteasa sobre reguladores de muerte celular de diferentes reinos con modos de acción no relacionados entre sí (es decir, caspasas vs metacaspasas).

AtSERPIN1 is an inhibitor of the metacaspase AtMC1-mediated cell death and autocatalytic processing *in planta*

Saul Lema Asqui¹, Dominique Vercammen^{2,3}, Irene Serrano⁴, Marc Valls⁵, Susana Rivas⁴, Frank Van Breusegem^{2,3,6,7}, Frank L. Conlon^{8,9,10,11}, Jeffery L. Dangl^{12,13,14,15,16} and Núria S. Coll¹

¹Centre for Research in Agricultural Genomics (CRAG), CSIC-IRTA-UAB-UB, Campus UAB, Bellaterra, Barcelona 08193, Spain; ²Department of Plant Systems Biology, VIB, Ghent 9052, Belgium; ³Department of Plant Biotechnology and Bioinformatics, Ghent University, Ghent 9052, Belgium; ⁴LIPM, Université de Toulouse, INRA, CNRS, Castanet-Tolosan, France; ⁵Department of Genetics, Universitat de Barcelona and Centre for Research in Agricultural Genomics (CSIC-IRTA-UAB-UB) Edifici CRAG, Campus UAB, Bellaterra, Catalonia 08193, Spain; ⁶Department of Medical Protein Research, VIB, Ghent 9000, Belgium; ⁷Department of Biochemistry, Ghent University, Ghent 9000, Belgium; ⁸Department of Biology, University of North Carolina, Chapel Hill, NC 27599, USA; ⁹Department of Genetics, University of North Carolina, Chapel Hill, NC 27599, USA; ¹⁰McAllister Heart Institute, University of North Carolina, Chapel Hill, NC 27599, USA; ¹¹Lineberger Cancer Center, University of North Carolina, Chapel Hill, NC 27599, USA; ¹²Department of Biology, University of North Carolina, Chapel Hill, NC 27599-3280, USA; ¹³Howard Hughes Medical Institute, University of North Carolina, Chapel Hill, NC 27599-3280, USA; ¹⁴Curriculum in Genetics and Molecular Biology, University of North Carolina, Chapel Hill, NC 27599-3280, USA; ¹⁵Carolina Center for Genome Sciences, University of North Carolina, Chapel Hill, NC 27599-3280, USA; ¹⁶Department of Microbiology and Immunology, University of North Carolina, Chapel Hill, NC 27599-3280, USA

Summary

Author for correspondence:

Núria S. Coll

Tel: +34 93 5606600

Email: nuria.sanchez-coll@cragenomica.es

Received: 20 June 2016

Accepted: 16 December 2016

New Phytologist (2017)

doi: 10.1111/nph.14446

Key words: hypersensitive response (HR), metacaspase, plant–pathogen interactions, programmed cell death, protease, serpin.

• The hypersensitive response (HR) is a localized programmed cell death phenomenon that occurs in response to pathogen recognition at the site of attempted invasion. Despite more than a century of research on HR, little is known about how it is so tightly regulated and how it can be contained spatially to a few cells.

• AtMC1 is an *Arabidopsis thaliana* plant metacaspase that positively regulates the HR. Here, we used an unbiased approach to identify new AtMC1 regulators. Immunoaffinity purification of AtMC1-containing complexes led us to the identification of the protease inhibitor AtSerpin1.

• Our data clearly showed that coimmunoprecipitation between AtMC1 and AtSerpin1 and formation of a complex between them was lost upon mutation of the AtMC1 catalytic site, and that the AtMC1 prodomain was not required for the interaction. AtSerpin1 blocked AtMC1 self-processing and inhibited AtMC1-mediated cell death. Our results constitute an *in vivo* example of a Serpin acting as a suicide inhibitor in plants, reminiscent of the activity of animal or viral serpins on immune/cell death regulators, including caspase-1.

• These results indicate a conserved function of a protease inhibitor on cell death regulators from different kingdoms with unrelated modes of action (i.e. caspases vs metacaspases).

Introduction

Metacaspases are a family of proteases present in plants, fungi and protozoa (Uren *et al.*, 2000). They are members of the clan CD of cysteine proteases, featuring a unique tertiary structure termed the caspase-hemoglobinase fold that encloses a conserved cysteine–histidine catalytic dyad (Aravind & Koonin, 2002). Members of this superfamily also include caspases, animal cysteine proteases with aspartate specificity that have essential roles in inflammation and cell death. Metacaspases have typically been compared with caspases, but research has shown that despite their overall active site configuration, their mode of action might be radically different. First, they have different substrate sequence cleavage requirements: lysine or arginine for metacaspases and aspartic acid for caspases; second, metacaspase activity is not blocked by caspase inhibitors; and third, according to their

structure, metacaspases cannot form dimers the way caspases do (Salvesen *et al.*, 2016). Regardless of these differences, metacaspases have been shown to act as cell death regulators (Coll *et al.*, 2010, 2014; Tsiatsiani *et al.*, 2011; Wrzaczek *et al.*, 2015), although it is not clear how they exert this function or how they are regulated.

Arabidopsis metacaspases are the best characterized among plants. The *Arabidopsis* genome encodes nine metacaspases, AtMC1–AtMC3 (type I) and AtMC4–AtMC9 (type II). The main difference between type I and type II metacaspases is the presence (type I)/absence (type II) of an N-terminal prodomain. According to the crystal structure of the *Trypanosoma* type I metacaspase (McLuskey *et al.*, 2012), the prodomain rests as a lid on top of the catalytic fold, presumably precluding substrate access until cleavage or a conformational change occurs. In agreement with that proposal, the prodomains of AtMC1 and AtMC2

were shown to negatively regulate their function (Coll *et al.*, 2010).

We previously demonstrated that AtMC1 is a positive regulator of pathogen-triggered hypersensitive response (HR) cell death (Coll *et al.*, 2010), a plant reaction that takes place locally at the site of attempted pathogen attack upon recognition of the invader. In this context, catalytic integrity was critical for AtMC1 cell death function. Conditional overexpression of AtMC1 resulted in ectopic cell death, which indicated that a tight regulation of this protein must be in place in order to prevent uncontrolled cell death. So far, two negative regulators of AtMC1 have been identified: AtMC2 and the negative regulator of plant defense and HR, LSD1 (Dietrich *et al.*, 1994). AtMC1 interacted with LSD1 through its prodomain, whereas AtMC1 and AtMC2 did not interact with each other and the details of their interplay remain to be clarified (Coll *et al.*, 2010).

Here, we used an unbiased approach to identify new regulators of AtMC1 activity. Immunoaffinity purification of AtMC1-containing complexes led us to the identification of the protease inhibitor AtSerpin1. Our data clearly showed that coimmunoprecipitation between AtMC1 and AtSerpin1 was dependent on an intact AtMC1 catalytic site and the prodomain was not required for the interaction. Furthermore, AtSerpin1 blocked AtMC1 self-processing and inhibited AtMC1-mediated cell death. Together, our findings uncover AtSerpin1 as a bona fide AtMC1 inhibitor *in planta*.

Materials and Methods

Plant material and growth conditions

All experiments were performed using *Arabidopsis thaliana* (L.) Heynh. accession Col-0. Mutant *atmc1* and the transgenic *atmc1 P_{AtMC1}::AtMC1-HA* and *lsd1 atmc1 P_{AtMC1}::AtMC1-HA* were previously described in Coll *et al.* (2010). Mutant *atscrpin1* and transgenic Col-0 *35S::AtSerpin1-HA* lines were described in Lampl *et al.* (2010). *Arabidopsis* was grown under short-day conditions (9 : 15 h, 22 : 20°C, light : dark).

Nicotiana benthamiana was grown under long-day conditions (16 : 8 h, 25 : 22°C, light : dark).

DNA constructs

To obtain the *P_{AtMC1}::HA-AtMC1* construct, the product of an overlapping PCR using *AtMC1* promoter and HA-AtMC1 was directionally cloned into pENTR/D/TOPO Gateway vector (Invitrogen) and recombined into the plant binary Gateway-compatible vector pGWB1 (Nakagawa *et al.*, 2007).

The AtSerpin1 full-length cDNA was directionally cloned into pENTR/D/TOPO Gateway vector (Invitrogen) and recombined into the plant binary Gateway-compatible vector pGWB641 to obtain *35S::AtSerpin1-YFP* or pGWB642 to obtain *35S::YFP-AtSerpin1* (Nakamura *et al.*, 2010).

For subcellular localization experiments, fusion of fluorescent proteins to AtMC1, AtMC1-ΔN, AtMC1-CA and AtSerpin1

was performed using a multisite GATEWAY cloning strategy (Invitrogen) described previously (Gu & Innes, 2011). Briefly, the full-length open reading frames of *AtMC1*, *AtMC1-ΔN*, *AtMC1-CA* and *AtSerpin1* were cloned into the donor vector pBSDONR P1-P4 (an ampicillin-resistant vector derived from pDONR221 P1-P4 from Invitrogen) (Gu & Innes, 2011) using the BP cloning Kit (Invitrogen). C-terminal eGFP (Cormack *et al.*, 1996) and C-terminal red fluorescent protein (RFP) (Campbell *et al.*, 2002) were cloned into the entry vector pBSDONR P4r-P2. To fuse AtMC1, AtMC1-ΔN, AtMC1-CA and AtSerpin1 with the epitope tags, the P1-P4 clones were recombined with corresponding P4r-P2 and the desired destination vectors using Gateway LR clonase II (Invitrogen). For AtMC1, AtMC1-ΔN, and AtMC1-CA, the earlier described pBSDONR constructs were recombined with the destination vector pEarleyGate100 (Earley *et al.*, 2006). For AtSerpin1, the corresponding pBSDONR constructs were recombined with the steroid-inducible destination vector pBAV154 (Vinatzer *et al.*, 2006).

Plasmids were transformed into *Agrobacterium tumefaciens* strain GV3101 (pMP90) by electroporation and plated into selective Luria-Bertani (LB) agar plates.

Stable transformation of *Arabidopsis thaliana*

atmc1 P_{AtMC1}::AtMC1-HA plants were transformed with *35S::AtSerpin1-YFP* using *Agrobacterium tumefaciens* (GV3101)-mediated floral dip as previously described (Clough & Bent, 1998). Homozygous double transgenic lines were selected on Murashige & Skoog (MS) media supplemented with 20 μg ml⁻¹ Basta (glufosinate-ammonium). *atmc1* plants were transformed with *P_{AtMC1}::HA-AtMC1* using *A. tumefaciens* (GV3101)-mediated floral dip as previously described (Clough & Bent, 1998). Homozygous transgenic lines were selected on MS media supplemented with 50 μg ml⁻¹ hygromycin.

Immunoisolation of protein complexes from *Arabidopsis*

Homozygous *atmc1* or *lsd1 atmc1 P_{AtMC1}::AtMC1-HA* were used for immunoaffinity purification 24 h after spraying them with 300 μM BTH as previously described (Coll *et al.*, 2010). All materials and reagents for immunoisolation were from Thermo Fisher Scientific (Waltham, MA, USA), unless otherwise stated. AtMC1-HA complexes were immunoisolated using magnetic beads (M-270 epoxy Dynabeads) conjugated to a monoclonal HA antibody (MMS-101P MONO HA.11; Covance, Princeton, NJ, USA). For conjugation, 100 μg of antibody were first washed and concentrated to the final volume of 100 μl by three rounds of adding 500 μl of phosphate-buffered saline and centrifugation at 9000 g for 15 min at 4°C using a centrifugal filter (Amicon; Merck Millipore, Billerica, MA, USA). One hundred micrograms (100 μl) of clean antibody were added to 18 mg of magnetic beads washed with 0.1 M sodium phosphate buffer (pH 7.4). Then, 120 μl of 3 M ammonium sulfate and 120 μl of 0.1 M sodium phosphate buffer (pH 7.4) were added. Beads were incubated overnight at 30°C on an orbital shaker. In parallel, 10 g of leaves

were snap-frozen in liquid nitrogen and cryogenically lysed using a Retsch MM 301 Mixer Mill (20 cycles of 180 s at 30 Hz) (Retsch, Newtown, PA, USA). The frozen powder was resuspended in cold lysis buffer (20 mM K-HEPES pH 7.4, 110 mM $\text{CH}_3\text{CO}_2\text{K}$, 2 mM MgCl_2 , 0.1% Tween-20, 1 μM ZnCl_2 , 1 μM CaCl_2), supplemented with protease inhibitor cocktail (Roche). Lysates were homogenized using a polytron (two cycles of 15 s). The cell lysate was centrifuged at 1000 g at 4°C for 10 min. The supernatant was collected and filtered through a syringe-driven 5 μm filter to remove any particles from lysate that did not pellet. The protein concentration of the lysate was measured, to adjust all samples to the same concentration. A fraction of the lysate was reserved to run on a sodium dodecyl sulfate–polyacrylamide gel electrophoresis (SDS-PAGE) (total protein).

Beads were equilibrated by washing three times with lysis buffer. After that, 1 ml of lysate was added to the beads. Beads were then incubated at 4°C on an orbital shaker. After 1 h, tubes were placed on a Dynal (Thermo Fisher Scientific, Waltham, MA, USA) magnetic rack, flowthrough was discarded and beads were washed five times with lysis buffer. Forty microliters of elution buffer (4 \times NuPAGE LDS Sample Buffer and 20 \times NuPAGE Sample Reducing Buffer; Thermo Fisher Scientific) supplemented with 2 μl of 1 M iodoacetamide were added per sample and incubated 1 h at room temperature. Subsequently, samples were transferred to 70°C to elute proteins off the beads. Eluted proteins were partially separated at 150 V on a NuPAGE 3–12% 1-mm-thick Bis-Tris protein gel using NuPAGE MOPS running buffer, supplemented with NuPAGE Antioxidant in the inner gel chamber. The gel was stained using Coomassie SimplyBlue SafeStain (Thermo Fisher Scientific). Each lane was excised and divided in eight fragments. Fragments were individually analyzed by mass spectrometry.

Protein characterization using mass spectrometry

Excised SDS-PAGE gel bands were in-gel-digested with trypsin. The extracted peptides were separated on a nanoAcquity HPLC system (Waters Corp., Milford, MA, USA) with a 360 μm OD \times 75 μm ID analytical column (14 cm of Magic 5 μm C18AQ resin; Michrom Biosciences, Bruker Corp., Billerica, MA, USA). The liquid chromatography (LC) system was directly connected through an electrospray ionization source interfaced to an LTQ Orbitrap Velos ion trap mass spectrometer (Thermo Fisher Scientific) controlled by XCALIBUR software (v.2.1.0.1140; Thermo Fisher Scientific) and operated in the data-dependent mode in which the initial MS scan recorded the mass to charge (m/z) ratios of ions over the range 400–2000. Raw files were searched using MASCOT (v.2.3.02; Matrix Science, Wyndham Place, UK). Search parameters included peptide mass tolerance of 10 ppm and fragment ion tolerance of 0.8 mass units.

Isolated protein complexes were analyzed by mass spectrometry as previously described (Kaltenbrun *et al.*, 2013). Briefly, tandem mass spectra were extracted by PROTEOME DISCOVERER (Thermo Fisher Scientific), and all MS/MS samples were analyzed with SEQUEST (v.1.2.0.208; Thermo Fisher Scientific), set up to search the Arabidopsis UniProt-SwissProt protein sequence database,

assuming digestion pattern with trypsin. SCAFFOLD (v. Scaffold_3_00_06; Proteome Software Inc., Portland, OR, USA) was used to validate MS/MS-based peptide and protein identifications. Peptide sequences were deemed a match if they could be established at >95.0% probability as specified by the PEPTIDEPHET algorithm (Keller *et al.*, 2002). In turn, protein identifications were deemed a match if they could be established at >99.0% probability by the PROTEINPHET algorithm and have at least one sequenced peptide.

The mass spectrometry proteomics data have been deposited to the ProteomeXchange Consortium via the PRIDE partner repository with the dataset identifier PXD005134 and 10.6019/PXD005134. The description of all files uploaded to ProteomeXchange can be found in Supporting Information Table S1.

Transient protein expression in *N. benthamiana*

Transient *A. tumefaciens*-mediated transformation of *N. benthamiana* leaves was performed as previously described (Coll *et al.*, 2010). Whole *N. benthamiana* leaves (*c.* 500 mg each) transiently expressing the constructs to test together with the anti-silencing vector p19 (Voinnet *et al.*, 2003) – Dex::AtMC1-HA + 35S::p19 (OD₆₀₀ 0.2 + 0.1), Dex::AtMC1-HA + 35S::AtSerpin1 + 35S::p19 (OD₆₀₀ 0.2 + 0.4 + 0.1), Dex::AtMC1- Δ N-HA + 35S::p19 (OD₆₀₀ 0.4 + 0.1), Dex::AtMC1- Δ N-HA + 35S::AtSerpin1 + 35S::p19 (OD₆₀₀ 0.4 + 0.4 + 0.1), Dex::AtMC1-CA-HA + 35S::p19 (OD₆₀₀ 0.2 + 0.1), Dex::AtMC1-CA-HA + 35S::AtSerpin1 + 35S::p19 (OD₆₀₀ 0.2 + 0.4 + 0.1), 35S::AtSerpin1 + 35S::p19 (OD₆₀₀ 0.4 + 0.1) – were frozen in liquid nitrogen before further processing for protein extraction.

Colocalization experiment

Agrobacterium tumefaciens cultures carrying the indicated constructs were grown and resuspended in water at OD₆₀₀ = 0.8 (Wroblewski *et al.*, 2005). For coexpression of multiple constructs, suspensions were mixed in equal ratios. Bacterial suspension mixtures were infiltrated using a needleless syringe. Samples were collected for microscopic imaging 40 h after infiltration.

Confocal laser scanning microscopy

Confocal laser scanning microscopy was performed on a Leica SP2 AOBS inverted confocal microscope (Leica Microsystems, Wetzlar, Germany) equipped with a \times 40, numerical aperture-1.2 water objective. eGFP fusion was excited with a 488 nm Argon laser and detected using a 505–530 bandpass emission filter. RFP fusions were excited using a 561 nm He-Ne laser and detected using a custom 595–620 nm bandpass emission filter.

Coimmunoprecipitation assays and protein analysis

Frozen samples were ground using a mortar and pestle on 3 ml of lysis buffer (200 mM K-HEPES pH 7.4, 1.1 M $\text{C}_2\text{H}_3\text{KO}$, 20 mM MgCl_2 , 1% Tween-20, 10 μM ZnCl_2 , 10 μM CaCl_2),

supplemented with 5 mM dithiothreitol (DTT), and protease inhibitor cocktail (Roche). Homogenized samples were filtered through miracloth (Millipore) and collected in 15 ml tubes. Samples were then centrifuged for 15 min at 4°C and 7000 g to separate the cell debris from the total protein extract.

For coimmunoprecipitation, total protein extracts were diluted to 2 mg ml⁻¹ and incubated with 50 µl of anti green fluorescent protein (GFP) magnetic beads (MACS; Miltenyi Biotec, Bergisch, Gladbach, Germany), for 2 h at 4°C under constant rotation. Bound proteins were eluted according to the manufacturer's instructions. Twenty-five micrograms of total protein (input), an equal volume of flowthrough (unbound) and 20 µl of eluate were loaded onto an SDS-PAGE gel. Immunoblots were performed using 1 : 5000 anti-GFP mouse monoclonal antibody (clone B-2; Santa Cruz Biotechnology, Dallas, TX, USA) or 1 : 5000 monoclonal anti-HA-HRP (clone 3F10; Roche).

To test binding between AtMC1 and AtSerpin1, we followed the protocol established by Roberts *et al.* (2011). In essence, protein extraction was performed using a Laemmli buffer (120 mM Tris-HCl pH 6.8, 4% SDS (w/v), 15% glycerol (v/v), 0.02% bromophenol (w/v)) with or without DTT (5 mM) as reducing agent. Proteins were then separated on 10% or 7.5% SDS-PAGE gels and probed with 1 : 5000 monoclonal anti-HA-HRP (clone 3F10; Roche) or 1 : 5000 anti-GFP mouse monoclonal antibody (clone B-2; Santa Cruz Biotechnology).

Chemical treatments

Dexamethasone was applied to *N. benthamiana* leaf surfaces using cottonballs to induce expression of *AtMC1* forms under the control of the dexamethasone promoter (Coll *et al.*, 2010) 48 h after agroinfiltration. Leaves were treated with 0.2 µM dexamethasone and samples were collected 24 h later.

Three-week-old *Arabidopsis* plants were sprayed with 150 µM benzol(1,2,3)thiadiazole-7-carbothioic acid S-methyl ester.

The proteasome inhibitor MG-132 (2 µM in 0.2% dimethyl sulfoxide; Sigma-Aldrich) was applied on *N. benthamiana* leaf surfaces 24 h after dexamethasone treatment and samples were collected 12 h later.

Cell death analyses

Ion leakage assays were carried out using 3-wk-old *N. benthamiana* plants transiently expressing different protein combinations (see the 'Transient protein expression in *N. benthamiana*' subsection earlier). At least four leaves per combination were used. Fifteen disks were extracted per leaf with a cork borer (7 mm diameter) and placed on a plate with distilled water during 1 h. After that, 10 disks were placed in a flask containing 10 ml of distilled water (six replicates per sample). Conductivity was measured over time using a hand electrical conductivitymeter (FG3-FIVEGO, Schwerzenbach, Switzerland).

Trypan blue staining of *N. benthamiana* leaves was performed by collecting whole leaves in 50 ml tubes (each leaf in a separate tube) 72 h after cell death induction and covered with a total of

35 ml of a 1 : 3 dilution of trypan blue stock solution (Keogh *et al.*, 1980). The tubes were incubated in previously boiled water for 15 min, and then cleared overnight with chloral hydrate on an orbital shaker. Pictures were taken 72 h after cell death induction. Pictures were also processed adding a binary mask using [IMAGEJ] (v.1.50i; National Institutes of Health, Bethesda, MD, USA).

Arabidopsis single cell death assay was performed according to Coll *et al.* (2010).

Results

Two forms of AtMC1 coexist in plants: full length and a prodomain-less

We previously showed that removal of AtMC1 prodomain enhances its pro-death activity in *Arabidopsis* (Coll *et al.*, 2010). To determine whether prodomain removal occurs in nature, we compared the processing pattern of N-terminally vs C-terminally tagged protein from transgenic plants expressing *HA-AtMC1* or *AtMC1-HA* under the control of AtMC1 promoter (*P_{AtMC1}::HA-AtMC1* or *P_{AtMC1}::AtMC1-HA*, respectively) (Fig. S1). Immunoblot using an anti-HA antibody clearly showed that AtMC1-HA is present in both its full-length form (41 kDa) and a fragment of *c.* 36 kDa, presumably corresponding to an auto-processed form (Fig. 1). By contrast, in plants expressing HA-AtMC1 only the full-length form of the protein could be detected by anti-HA immunoblot. This supports the idea that the spontaneously formed smaller AtMC1 fragment corresponds to the prodomain-less version of the protein, indicative of N-terminal processing.

Immunoaffinity isolation identified the protease inhibitor AtSerpin1 as part of AtMC1-containing protein complexes

In order to identify regulators of AtMC1 activity under native conditions, we performed immunoaffinity purification of AtMC1-containing complexes using rosette leaves from 4-wk-old *atmc1* plants expressing AtMC1 under the control of its own promoter (*atmc1 P_{AtMC1}::AtMC1-HA*, Fig. S1). Immunopurified proteins were partially resolved using SDS-PAGE (Fig. S2) and in-gel-digested with trypsin. Analysis was performed using nLC-

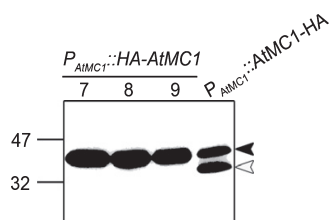


Fig. 1 The prodomain of the metacaspase *Arabidopsis thaliana* AtMC1 is cleaved in plants. Immunoblot using anti-HA antibodies of three independent *atmc1 P_{AtMC1}::HA-AtMC1* T₁ lines (7–9) compared with homozygous *atmc1 P_{AtMC1}::HA-AtMC1*. Black and white arrows indicate full-length and cleaved AtMC1, respectively.

tandem MS (MS/MS) on an LTQ Orbitrap Velos. Two independent biological replicates were performed. Raw MS/MS spectra were first analyzed by SEQUEST database searches (PROTEOME DISCOVERER) and loaded into SCAFFOLD for further analysis. Protein identifications from all replicates were filtered using stringent confidence parameters (see the Materials and Methods section). Through this analysis we detected 154–1300 proteins per condition, among which we identified the protease inhibitor AtSerpin1. AtSerpin1 was not identified in the experimental controls used (Table S2).

AtSerpin1 inhibits AtMC1 autoprocessing *in vivo*

Conditional overexpression of *AtMC1* in *N. benthamiana* leaves resulted in accumulation of both full-length and processed forms similar to when expressed in *Arabidopsis* under the control of its native promoter (Fig. S3). AtMC1 cleavage was inhibited by mutation of the predicted catalytic site (Fig. 2b, AtMC1-CA), indicative of autoprocessing. AtSerpin1 coexpression with AtMC1 also blocked autocatalytic processing of AtMC1 (Figs 2a, S3). Absence of processed AtMC1 is consistent with the idea that AtSerpin1 acts as an inhibitor of AtMC1 cleavage *in planta*.

Interestingly, AtSerpin1 caused a sharp decrease in the levels of AtMC1-CA (Fig. 2b). To explain this observation, we hypothesized that AtSerpin1 might bind and/or alter the structure of the AtMC1 catalytic mutant, ultimately leading to its proteasomal degradation. To test whether the reduction in AtMC1-CA protein levels caused by AtSerpin1 coexpression was proteasome-dependent, we treated agroinfiltrated *N. benthamiana* leaves with

the proteasome inhibitor MG-132 or left them untreated. As shown in Fig. 2(b) the severe reduction of AtMC1-CA levels caused by *AtSerpin1* coexpression could be totally reverted by proteasome inhibition. However, the AtSerpin1-dependent degradation of AtMC1-CA might partly occur during protein extraction as a result of the reducing conditions caused by DTT. The data also indicated that, when expressed alone, AtMC1-CA is also partly degraded by the proteasome, as the levels increase after MG-132 treatment when compared with untreated leaves. By contrast, the native full-length and processed forms of AtMC1 do not seem to be subjected to proteasome-mediated degradation (Fig. 2b).

AtMC9 was shown to cleave AtSerpin1 *in vitro* at the predicted cleavage site (R351, corresponding to the predicted reactive center loop of AtSerpin1) (Vercammen *et al.*, 2004). Similarly, we observed that AtSerpin1 was cleaved by AtMC1 (Fig. 3). This cleavage was partly dependent on an intact catalytic site, as the levels of the cleaved fragment were lower or not detectable when YFP-AtSerpin1 (Fig. S4b) or AtSerpin1-YFP (Figs 3, S4a) was coexpressed with AtMC1-CA. In this experimental system, endogenous *N. benthamiana* proteases, including metacaspases, may also have the capacity to cleave AtSerpin1 as indicated by the cleavage products that appear on the sample expressing AtSerpin1 alone (Fig. 3, lane 5).

AtSerpin1 colocalizes and coimmunoprecipitates with AtMC1

To assess whether AtSerpin1 and AtMC1 colocalize, we obtained fluorescently tagged versions of both proteins (AtSerpin1-GFP and AtMC1-RFP) and tested their subcellular localization under confocal laser scanning microscopy. As shown in Fig. 4, both proteins colocalize in the cytoplasm. In addition, AtSerpin1-GFP, but not AtMC1, is visualized in the nucleus of *N. benthamiana* cells when transiently overexpressed, probably as the result of GFP cleavage.

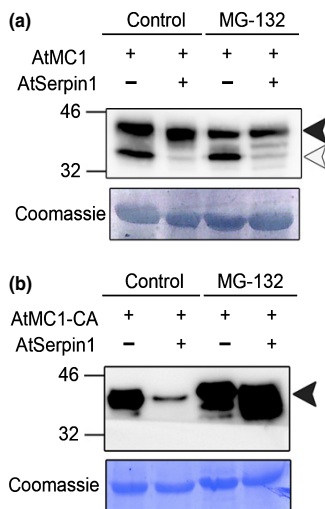


Fig. 2 AtSerpin1 inhibits AtMC1 autoprocessing and enhances proteasome-mediated degradation of the catalytic dead version of the protein (AtMC1-C220A). Wild-type and catalytic dead (CA) AtMC1-HA versions were transiently expressed in *Nicotiana benthamiana* leaves alone or in combination with *AtSerpin1-YFP*. Leaves were treated with 2 μ M MG-132 (+) or left untreated (-). Proteins were extracted 12 h later and either Coomassie-stained or immunoblotted using anti-HA antibodies to detect, respectively, AtMC1-HA (a) or AtMC1-CA-HA (b). Black and white arrows indicate full-length and cleaved AtMC1, respectively.

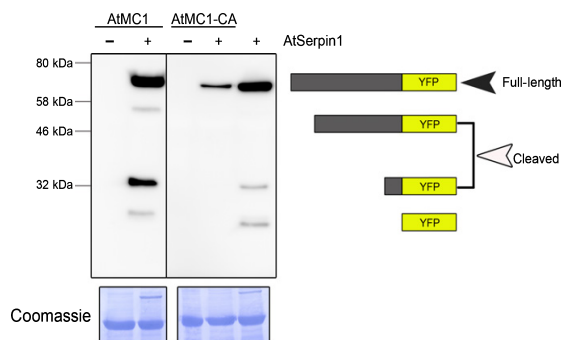


Fig. 3 AtSerpin1 is cleaved by AtMC1. *AtSerpin1-YFP* alone or in combination with *AtMC1-HA* or *AtMC1-CA-HA* was transiently expressed in *Nicotiana benthamiana* leaves. Total proteins were extracted and 50 μ g were either Coomassie-stained or immunoblotted using anti-GFP antibody. The black arrowhead indicates full-length AtSerpin1, whereas the white arrowhead points at the putative AtSerpin1 cleaved form. YFP, yellow fluorescent protein.

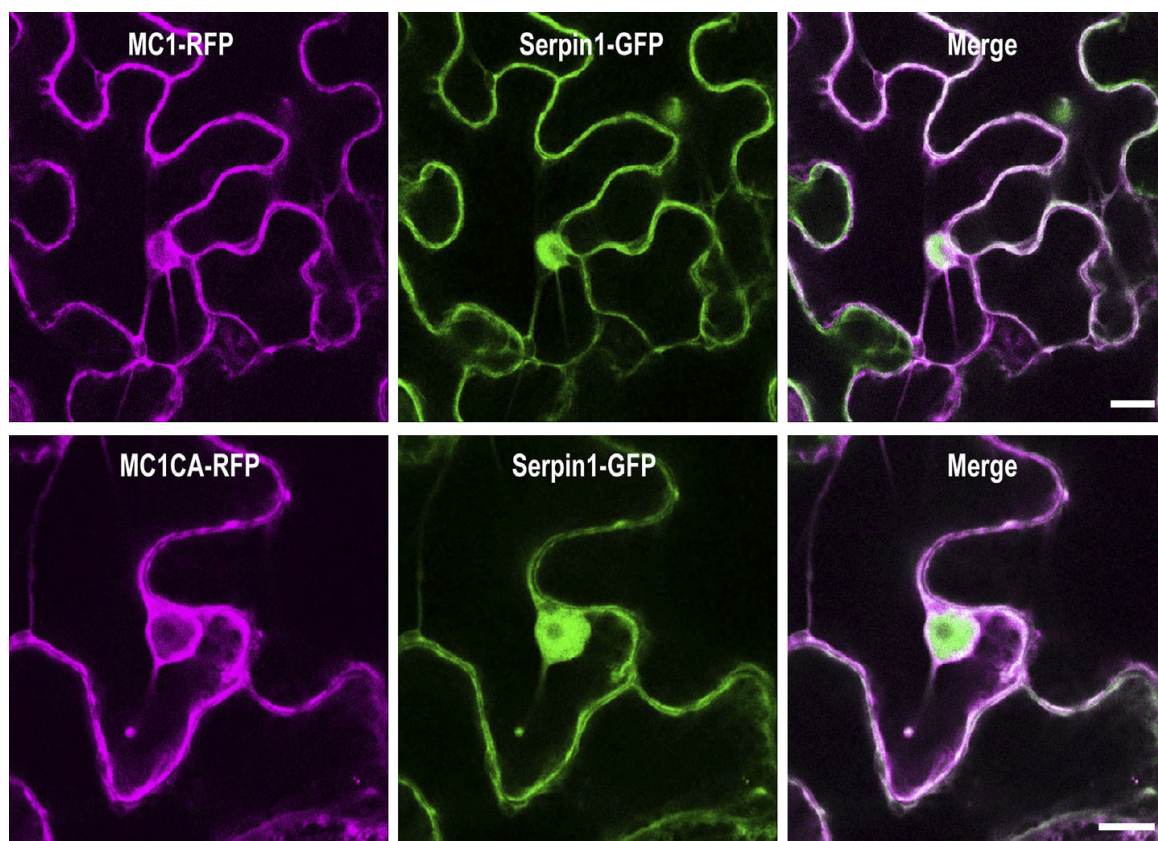


Fig. 4 Colocalization of AtSerpin1 and different forms of AtMC1. Confocal images of epidermal *Nicotiana benthamiana* cells 40 h after *Agrobacterium*-mediated transient expression of the indicated constructs. RFP, red fluorescent protein; GFP, green fluorescent protein. Bars, 15 μ m.

Next, we analyzed whether AtMC1 and AtSerpin1 were able to form covalent complexes. For this, we performed protein extraction under nonreducing conditions in *N. benthamiana* plants expressing AtMC1-HA (*c.* 40 kDa) alone or in combination with AtSerpin1-YFP (*c.* 72 kDa). The observed molecular weight of 100 kDa, detected by both GFP and HA antibody, is consistent with a noncanonical full-length serpin–protease complex (Figs 5, S5). This band is not present when using the reducing agent DTT in the extraction. The putative complex band also cannot be observed when, instead of wild-type AtMC1, the catalytic dead version of the protein AtMC1-CA is coexpressed together with AtSerpin1 in nonreducing conditions. This indicates that AtMC1–AtSerpin1 complex formation requires an AtMC1 intact catalytic site. Interestingly, the AtSerpin1-dependent degradation of AtMC1-CA seems to be lost under nonreducing conditions (Fig. 5). This could be a result of the stabilization of AtMC1 in an oxidizing environment.

To further specify the requirements of the AtMC1–AtSerpin1 noncanonical interplay, we performed coimmunoprecipitation experiments with AtSerpin1 and different AtMC1 forms. Total protein extracts from transiently expressed AtMC1-HA alone or together with AtSerpin1-YFP were incubated with magnetic beads coupled with anti-GFP antibody. Immunoblot of total protein

and the eluted fraction confirmed AtMC1 and AtSerpin1 coimmunoprecipitation (Fig. 6a). We obtained the same result when using Arabidopsis double transgenic plants coexpressing AtMC1 and AtSerpin1 (Fig. S6). As expected, the catalytic dead version of the protein (AtMC1-CA) did not coimmunoprecipitate with AtSerpin1 when transiently coexpressed in *N. benthamiana* (Fig. 6b). This corroborates the fact that an intact AtMC1 catalytic site is required for coimmunoprecipitation.

To determine whether AtSerpin1 interacts with AtMC1 through its prodomain, we performed coimmunoprecipitation using a prodomain-less version of AtMC1 (AtMC1- Δ N-HA) (Coll *et al.*, 2010). As shown in Fig. 6(c) this is not the case, as AtMC1- Δ N-HA still coimmunoprecipitated with AtSerpin1, albeit to a lesser extent than the full-length version.

AtSerpin1 inhibits AtMC1-dependent programmed cell death

To address whether AtSerpin1 had an effect on AtMC1-mediated cell death, we carried out ion leakage analysis on *N. benthamiana* plants transiently expressing the different forms of AtMC1 (AtMC1, AtMC1-CA and AtMC1- Δ N) alone or in combination with AtSerpin1 (Fig. 7a,b). As expected, AtMC1 expression

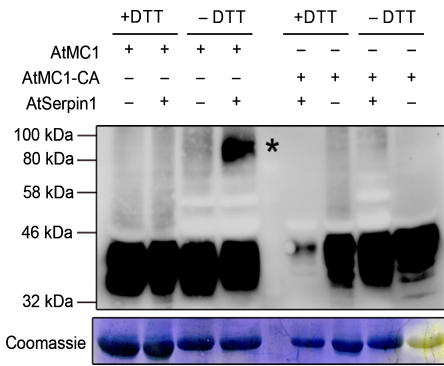


Fig. 5 Binding between AtMC1 and AtSerpin1 occurs only in presence of an intact catalytic site. Full-length *AtMC1-HA* and *AtMC1-CA-HA* were transiently expressed in *Nicotiana benthamiana* leaves alone or in combination with *AtSerpin1-YFP*. Total proteins were extracted under reducing (+DTT) or nonreducing (-DTT) conditions. Fifty micrograms of protein were separated on a sodium dodecyl sulfate–polyacrylamide gel electrophoresis and either Coomassie-stained or immunoblotted using anti-HA antibody. The asterisk indicates the putative *AtMC1-AtSerpin1* complex.

caused an increase in ectopic cell death over time. This cell death was also observed when expressing the ΔN form of the protein and was almost completely abolished in leaves expressing the catalytic dead version of *AtMC1* (*AtMC1-CA*). *AtSerpin1* clearly blocked *AtMC1*- and *AtMC1- ΔN* -dependent cell death, further supporting the idea that it acts as a bona fide inhibitor of *AtMC1* activity.

In order to genetically substantiate this claim, we monitored cell death on *atmc1*, *atserpin1* and *atmc1 atserpin1* mutant plants and plants overexpressing *AtSerpin1* (*AtSerpin1-HA*) compared with the wild-type. As a cell death trigger, we used *Pseudomonas syringae* pv tomato expressing the type III effector *avrRpm1* (*Pro DC3000(avrRpm1)*), which causes *AtMC1*-dependent HR cell death mediated by the RPM1 receptor (Coll *et al.*, 2010). Two-week-old plants were infected with *Pro DC3000(avrRpm1)* and cell death was quantified using a single cell death assay (Coll *et al.*, 2010, 2014). As previously observed, the lack of *atmc1* resulted in a sharp decrease in RPM1-mediated cell death (Fig. 7c). Double *atmc1 atserpin1* mutants showed reduced cell death levels, lower than the wild-type but higher than *atmc1* plants, whereas *atserpin1* mutants behaved similarly to the wild-type. Together, these data suggests that *AtSerpin1* acts as a negative regulator of cell death mediated by *AtMC1* via (an) additional protease(s) in Arabidopsis.

Discussion

AtMC1 is an autocatalytically active protease *in planta*

In the past we speculated that *AtMC1* and the animal inflammatory caspase-1, may share certain functional similarities (Coll *et al.*, 2010, 2014). This was based on the following facts: analogous catalytic domain structure; both are positive regulators of cell death induced upon immune receptor activation; presence of a prodomain that contains cell death-related motifs; and both

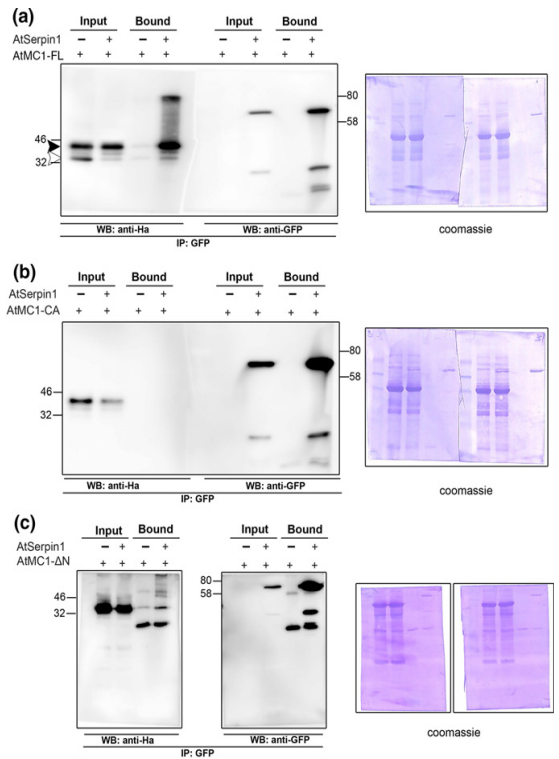


Fig. 6 *AtMC1-AtSerpin1* coimmunoprecipitation occurs independently of *AtMC1* prodomain but an intact catalytic center is required. Different *AtMC1-HA* forms (FL, full length; CA, catalytic dead; ΔN , prodomain-less) were transiently expressed in *Nicotiana benthamiana* leaves alone or in combination with *AtSerpin1-YFP*. Total proteins were extracted (input), incubated with magnetic beads coupled to green fluorescent protein (GFP) and, after stringent washes, proteins bound to the beads were eluted (bound). Input and bound fractions were either Coomassie-stained or probed against anti-GFP to detect *AtSerpin1* or against anti-HA to detect *AtMC1-FL* (a), *AtMC1-CA* (b) or *AtMC1- ΔN* (c). The black arrowhead indicates full-length *AtMC1*, whereas the white arrowhead points at the putative *AtMC1* cleaved form. WB, western blot; IP, immunoprecipitation. [Correction added after online publication 3 February 2017: the duplicated anti-GFP immunoblot in (a) has been replaced with the correct immunoblot and the Coomassie-stained panels in (a) and (b) have been switched to match their immunoblots. For clarity full images of all gels and Coomassies are now shown.]

are negatively regulated by an inactive member of their family (caspase-11 in the case of caspase-1 and *AtMC2* in the case of *AtMC1*).

In animals, the caspase-1-dependent response is very well characterized (Davis *et al.*, 2011). Upon immune receptor activation, supramolecular structures termed inflammasomes are assembled, recruiting multiple copies of full-length, inactive caspase-1. Within inflammasomes, many caspase-1 units are rapidly self-processed through induced proximity, releasing p10 and p20 subunits that then assemble into the active form, consisting of two p20–p10 heterodimers. Active caspase-1 can then carry out multiple processes in response to the initial inflammatory signal, generating a fast and efficient response.

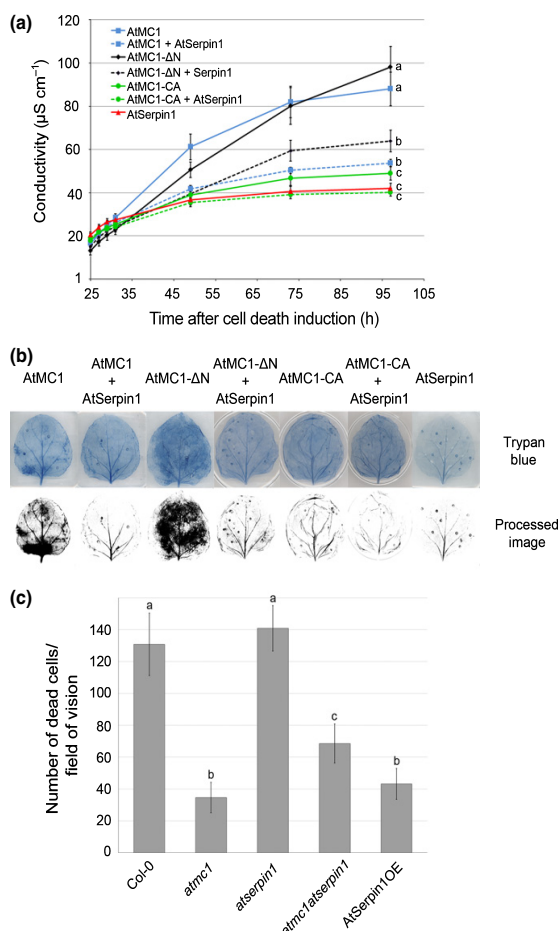


Fig. 7 AtSerpin1 inhibits AtMC1-mediated cell death. (a) Ion leakage assay using *Nicotiana benthamiana* leaves expressing the different forms of AtMC1-HA alone or in combination with AtSerpin1-YFP. Cell death was induced by dexamethasone treatment 48 h after agroinfiltration of the leaves (time 0). Each time point corresponds to the SE of six replicates containing 10 leaf disks each ($\pm 2 \times \text{SE}$). Letters indicate significant differences following post-ANOVA Tukey's honest significant difference test ($\alpha = 0.05$). This experiment was repeated five times with similar results. (b) Pictures of representative trypan blue-stained leaves expressing the different forms of AtMC1 alone or in combination with AtSerpin1 72 h after cell death induction (upper row) or the same images processed using Image J to highlight dead areas (lower row). (c) Single cell death assay of the indicated *Arabidopsis thaliana* lines. Dead cells (trypan blue-positive) were counted under an optical microscope 12 h after infection with 250 000 colony-forming units ml^{-1} *Pto* DC3000(*avrRpm1*). Values indicate the average of 50 samples per genotype $\pm 2 \times \text{SE}$. Letters indicate significant differences following post-ANOVA Tukey's honest significant difference test ($\alpha = 0.05$). The experiment is representative of five independent replicates.

Our data support the idea that AtMC1 is catalytically self-processed to release the prodomain and a fragment encompassing the p20 and p10 subunits. Several other type I metacaspases have been shown to self-cleave (Meslin *et al.*, 2007; Moss *et al.*, 2007; Zalila *et al.*, 2011; Li *et al.*, 2015). However, the link between cleavage and activation has not yet been established. In fact, for

the *Trypanosoma brucei* metacaspase TbMCA2, it was shown that cleavage is not critical for activation (Moss *et al.*, 2007). In *Arabidopsis*, AtMC1 appears to be maintained in an equipoise between the full-length and the processed form. Conditional overexpression of the processed form caused faster and more extensive cell death than the full-length version of AtMC1 (Coll *et al.*, 2010). This was in agreement with the idea that the prodomain is a negative regulator of type I metacaspase activity and might act as a physical barrier for substrate access (McLuskey *et al.*, 2012). However, we did not find any stress condition that increased the accumulation of the processed form (data not shown). This might imply that AtMC1 activation does not occur via enhanced processing but rather by relocalization of the prodomain-less form to a different subcellular compartment where relevant substrates are located or by post-translational modifications.

In fact, we still do not know whether AtMC1 or other type I metacaspases are recruited to death-induced supramolecular structures comparable to the inflammasome through their prodomain. Interestingly, the two metacaspase crystal structures resolved to date indicate that homodimerization through the equivalent interfaces as observed in caspases seem impossible (McLuskey *et al.*, 2012; Wong *et al.*, 2012). Thus, it remains an open question how AtMC1 and other metacaspases become active.

The interplay between AtSerpin1 and AtMC1 in plants

In the context of AtMC1 regulation, mechanisms to prevent its activation under homeostatic conditions must be in place to avoid unrestrained cell death propagation. Two negative regulators of AtMC1 function were identified earlier: AtMC2 and LSD1 (Coll *et al.*, 2010). Here, we have uncovered a novel negative regulator of AtMC1: the protease inhibitor AtSerpin1, which can block AtMC1 autocatalytic activity *in planta* and prevent AtMC1-mediated cell death.

Serpins are a superfamily of proteins, initially described as serine protease inhibitors, but now known to include cysteine protease inhibitors and even noninhibitory members (Gettins, 2002). Serpins are the most widespread and abundant peptidase inhibitors, being present in all domains of life and even in viruses (Rawlings *et al.*, 2004). In animals, serpins have been involved in cell survival, development and host defense against pathogens (Silverman *et al.*, 2010). Inhibitory serpins have been termed 'suicide inhibitors' or 'molecular mousetraps' because of their mode of action: cleavage by the target protease sets off a conformational change in the serpin whereby the protease is flipped and becomes trapped against the serpin protein body, with its catalytic core crushed and the consequent decrease in proteolytic activity (Huntington *et al.*, 2000).

The *Arabidopsis* genome encodes eight serpin genes (Fluhr *et al.*, 2012). Among them, the most abundant and best characterized is AtSerpin1. The *in vitro* proteolytic activities of two type II metacaspases, AtMC4 and AtMC9, were shown to be inhibited by AtSerpin1 (Vercammen *et al.*, 2004). In turn, AtMC9 was demonstrated to cleave AtSerpin1 *in vitro* at the predicted

cleavage site (reactive center loop) in a dose-dependent manner (Vercammen *et al.*, 2004). Our *in vivo* data indicate that AtMC1 might also be able to cleave AtSerpin1 through its reactive center loop, as the size of two fragments generated would be in agreement with the corresponding prediction.

Both AtMC4 and AtMC9 were shown to act as positive regulators of cell death in different contexts: AtMC4 was involved in pathogen-triggered cell death (Watanabe & Lam, 2011), whereas AtMC9 participates in developmental cell death, mediating cell clearance in late stages of xylem formation (Bollhoner *et al.*, 2013). In neither case has it been established that inhibition of AtMC activity by AtSerpin1 affects metacaspase function in these physiological contexts.

Here, we demonstrated inhibition of AtMC1 by AtSerpin1 *in vivo*. This inhibition was monitored as loss of self-processing of AtMC1 when coexpressed with AtSerpin1. Unfortunately, we have so far not been able to directly measure AtMC1 proteolytic activity, and thus we have not been able to assess the effect of AtSerpin1 on it. We also observed that AtMC1-CA was partly degraded by the proteasome and coexpression with AtSerpin1 dramatically exacerbated AtMC1-CA proteasomal degradation. AtMC1-CA is more prone to aggregation than its wild-type counterpart (Coll *et al.*, 2014) and cells have evolved different surveillance mechanisms to detect and eliminate potentially toxic protein aggregates. Thus, it is not surprising that at least part of the AtMC1-CA pool is delivered to the proteasome for degradation. The fact that AtSerpin1 coexpression enhances AtMC1-CA proteasome-mediated degradation could indicate that AtSerpin1 might interact and/or induce a conformational change in AtMC1-CA that further promotes its aggregation and, consequently, its elimination via the proteasome.

AtMC1 and AtSerpin1 colocalize and coimmunoprecipitate, indicating a possible interaction between the two proteins. In contrast to the previously shown AtMC1-LSD1 coimmunoprecipitation (Coll *et al.*, 2010), the prodomain was not required for the interaction between AtMC1 and AtSerpin. The interaction between AtMC1- Δ N and AtSerpin1 still took place, although it was weaker than with the full-length version of AtMC1, indicating a less stable interaction when the prodomain was missing. However, an intact AtMC1 catalytic center was required for the coimmunoprecipitation. This was presumably not the case for AtMC9-AtSerpin1 interaction, as a catalytic-dead version of AtMC9 was used as a bait for AtSerpin1 identification in the yeast two-hybrid assay (Vercammen *et al.*, 2006). The apparent discrepancy of the two observations might be explained by a weaker affinity between AtSerpin1 and catalytic-dead metacaspase mutants. These potentially weak interactions are probably eliminated by the stringent washes of a coimmunoprecipitation experiment, whereas they remain intact in yeast two-hybrid assays.

AtSerpin1 as an inhibitor of cell death proteases

In plants, AtSerpin1 might act as a pan-metacaspase inhibitor or even as a more general cell death protease inhibitor. AtSerpin1 was shown to covalently bind and to modulate the activity of the cell death protease RD21 (Lampl *et al.*, 2010, 2013). Our data

also indicate that AtSerpin1 forms a noncanonical complex with AtMC1, detected under nonreducing conditions. This discrepancy between the mode of interaction between different metacaspases and AtSerpin1 could be a result of the different mode of action of AtMC1 and 9, their localization (subcellular and tissular) and the processes in which they are involved.

Interestingly, the interplay between AtMC1 and AtSerpin1 seem to involve the full-length rather than the cleaved versions of the proteins. Although AtMC1 may be able to cleave AtSerpin1, the size of the complex detected, as well as the coimmunoprecipitated fragments indicate a noncanonical mode of action whereby AtSerpin1 would bind and inactivate AtMC1 but this interaction would not involve self-cleavage or direct AtSerpin1 cleavage by AtMC1. The fact that AtMC1 catalytic activity is required for the interaction with AtSerpin1 could suggest the involvement of a third partner that needs to be cleaved in order for the inhibition to take place or nondetectable modifications of AtMC1 and/or AtSerpin1.

Overexpression of *AtSerpin1* or a mutation in the protease RD21 led to reduced cell death after infection with the necrotrophic fungi *Botrytis cinerea* and *Sclerotinia sclerotiorum* but enhanced cell death in response to the hemibiotrophic fungus *Colletotrichum higginsianum* (Lampl *et al.*, 2013). In our conditions, infection with *Pto* DC3000(*avrRpm1*), a hemibiotrophic bacterium that causes HR in *A. thaliana* Col-0 background via the RPM1 receptor, resulted in decreased cell death in plants overexpressing *AtSerpin1*, comparable to *atmc1* mutants. Double *atmc1 atserpin1* mutants displayed an intermediate phenotype between wild-type and *atmc1* plants, which indicates that AtMC1 is negatively regulated by AtSerpin1 and also that *atserpin1* may control other proteases involved in this cell death process beyond *atmc1*. Whether AtSerpin1 inhibits AtMC1-regulated processes by directly interacting with AtMC1 or indirectly by modulating the activity of downstream proteases induced by AtMC1 remains an open question. Inhibition of AtMC1-mediated cell death by AtSerpin1 is also demonstrated by the dramatic effect of AtSerpin1 when transiently coexpressed with death-inducing forms of AtMC1 in *N. benthamiana* leaves. Discrepancy of results between *C. higginsianum* (Lampl *et al.*, 2013) and *Pto*, may be explained by the fact that, despite both being hemibiotrophs, their lifestyle, time and mode of infection are radically different and thus it is difficult to compare cell death outcomes at a given time point.

Inhibition of different cell death proteases by AtSerpin1 (Fig. S7) positions it as a conceivable guardian of cell homeostasis, preventing uncontrolled proteolysis of potentially dangerous proteins. The balance between the levels of AtSerpin1 and the levels of potentially active death proteases might be a powerful modulator of cell fate. Under normal conditions, molecule-by-molecule inactivation may serve as an effective surveillance mechanism that prevents uncontrolled cell death.

In animals, intracellular serpins have been shown to be major regulators of cell death and inflammation and this function partly occurs through direct inhibition of specific proteases, including caspases (Silverman *et al.*, 2010). Interestingly, this mechanism has been coopted by certain viruses, which are able to produce serpins in their hosts that block defenses (Gettins, 2002). For

example, the viral serpin CrmA efficiently inhibits caspase-1, escaping immune surveillance by the host (Ray *et al.*, 1992). In fact, in many species, lack of certain serpins results in severe phenotypes or cell death (Silverman *et al.*, 2010). The fact that *atserpin1* mutants have no dramatic phenotypes might be explained by the genetic redundancy within the serpin family in Arabidopsis, but more experimental evidence is needed to confirm this hypothesis.

The work presented here contributes to a better understanding of cell death control in plants. We have demonstrated that AtSerpin1 acts *in vivo* as an inhibitor of AtMC1-mediated cell death, emerging as a potential inhibitor of cell death proteases in plants. These results are of major evolutionary significance, as they indicate a conserved function of a protease inhibitor on cell death regulators from different kingdoms with unrelated mode of action (i.e. caspases vs metacaspases).

Acknowledgements

The authors would like to kindly thank Marc Planas, Simon Stael, Guy Salvesen, Vera Bonardi and Ignacio Rubio-Somoza for helpful comments. We thank David Smalley and Nedyalka Dicheva from the University of North Carolina Michael Hooker Proteomics Center for technical assistance with protein identification. Anouk Brackenier, Dominique Eeckhout and Geert De Jaeger from Ghent University and the Flanders Institute of Biotechnology (VIB) are thanked for sharing and helping to analyze the TAP results. Thanks to Robert Fluhr for sharing transgenic AtSerpin-HA seeds and anti-Serpin antibody, and to Roger Innes for kindly providing Gateway vectors for colocalization studies. This work was funded by projects AGL2013-46898-R (MINECO, Spain) to N.S.C. and M.V., EU-Marie Curie Actions (PCDMC-321738 and PIF-331392) and BP_B 00030 from the Catalan Government to N.S.C.; S.L.A. holds a fellowship Convocatoria Abierta 2013 Primera Fase (grant agreement no. AR2Q4017) from SENESCYT, Ecuador; J.L.D. is an Investigator of the Howard Hughes Medical Institute, supported by the HHMI and the Gordon and Betty Moore Foundation (GBMF3030); I.S. is supported by an AgreeSkills fellowship within the EU Marie-Curie FP7 COFUND People Programme (grant agreement no. 267196); S.R. is supported by the French Laboratory of Excellence project 'TULIP' (ANR-10-LABX-41; ANR-11-IDEX-0002-02). We acknowledge financial support from the Spanish Ministry of Economy and Competitiveness, through the 'Severo Ochoa Programme for Centres of Excellence in R&D 2016-2019 (SEV-2015-0533)'.

Author contributions

S.L.A. performed and designed experiments, analyzed data and wrote the manuscript. D.V. performed and designed experiments and analyzed data. I.S. performed experiments and analyzed data. M.V. designed experiments and analyzed data. S.R. designed experiments, analyzed data and wrote the manuscript. F.v.B. designed experiments, analyzed data and wrote the manuscript. F.L.C. designed experiments, analyzed data and wrote the

manuscript. J.L.D. designed experiments, analyzed data and wrote the manuscript. N.S.C. designed the research, performed experiments, analyzed data and wrote the manuscript. All authors reviewed the manuscript.

References

- Aravind L, Koonin EV. 2002. Classification of the caspase-hemoglobinase fold: detection of new families and implications for the origin of the eukaryotic serpins. *Proteins* 46: 355–367.
- Bollhoner B, Zhang B, Stael S, Denance N, Overmyer K, Goffner D, Van Breusegem F, Tuominen H. 2013. Post mortem function of AtMC9 in xylem vessel elements. *New Phytologist* 200: 498–510.
- Campbell RE, Tour O, Palmer AE, Steinbach PA, Baird GS, Zacharias DA, Tsien RY. 2002. A monomeric red fluorescent protein. *Proceedings of the National Academy of Sciences, USA* 99: 7877–7882.
- Clough SJ, Bent AF. 1998. Floral dip: a simplified method for Agrobacterium-mediated transformation of *Arabidopsis thaliana*. *Plant Journal* 16: 735–743.
- Coll NS, Smidler A, Puigvert M, Popa C, Valls M, Dangl JL. 2014. The plant metacaspase AtMC1 in pathogen-triggered programmed cell death and aging: functional linkage with autophagy. *Cell Death and Differentiation* 21: 1399–1408.
- Coll NS, Vercammen D, Smidler A, Clover C, Van Breusegem F, Dangl JL, Epple P. 2010. Arabidopsis type I metacaspases control cell death. *Science* 330: 1393–1397.
- Cormack BP, Valdivia RH, Falkow S. 1996. FACS-optimized mutants of the green fluorescent protein (GFP). *Gene* 173: 33–38.
- Davis BK, Wen H, Ting JP. 2011. The inflammasome NLRs in immunity, inflammation, and associated diseases. *Annual Review of Immunology* 29: 707–735.
- Dietrich RA, Delaney TP, Uknes SJ, Ward ER, Ryals JA, Dangl JL. 1994. Arabidopsis mutants simulating disease resistance response. *Cell* 77: 565–577.
- Earley KW, Haag JR, Pontes O, Opper K, Juehne T, Song K, Pikaard CS. 2006. Gateway-compatible vectors for plant functional genomics and proteomics. *Plant Journal* 45: 616–629.
- Fluhr R, Lampl N, Roberts TH. 2012. Serpin protease inhibitors in plant biology. *Physiologia Plantarum* 145: 95–102.
- Gettins PG. 2002. Serpin structure, mechanism, and function. *Chemical Reviews* 102: 4751–4804.
- Gu Y, Innes RW. 2011. The KEEP ON GOING protein of Arabidopsis recruits the ENHANCED DISEASE RESISTANCE1 protein to trans-Golgi network/early endosome vesicles. *Plant Physiology* 155: 1827–1838.
- Huntington JA, Read RJ, Carrell RW. 2000. Structure of a serpin–protease complex shows inhibition by deformation. *Nature* 407: 923–926.
- Kaltenbrun E, Greco TM, Slagle CE, Kennedy LM, Li T, Cristea IM, Conlon FL. 2013. A Gro/TLE–NuRD corepressor complex facilitates Tbx20-dependent transcriptional repression. *Journal of Proteome Research* 12: 5395–5409.
- Keller A, Nesvizhskii AI, Kolker E, Aebersold R. 2002. Empirical statistical model to estimate the accuracy of peptide identifications made by MS/MS and database search. *Analytical Chemistry* 74: 5383–5392.
- Keogh RC, Deverall BJ, McLeod S. 1980. Comparison of histological and physiological responses to *Phakopsora pachyrhizi* in resistant and susceptible soybean. *Transactions of the British Mycological Society* 74: 329–333.
- Lampl N, Alkan N, Davydov O, Fluhr R. 2013. Set-point control of RD21 protease activity by AtSerpin1 controls cell death in Arabidopsis. *Plant Journal* 74: 498–510.
- Lampl N, Budai-Hadrian O, Davydov O, Joss TV, Harrop SJ, Curmi PM, Roberts TH, Fluhr R. 2010. Arabidopsis AtSerpin1, crystal structure and *in vivo* interaction with its target protease RESPONSIVE TO DESICCATION-21 (RD21). *Journal of Biological Chemistry* 285: 13550–13560.
- Li M, Wang H, Liu J, Hao P, Ma L, Liu Q. 2015. The apoptotic role of metacaspase in *Toxoplasma gondii*. *Frontiers in Microbiology* 6: 1560.
- McLuskey K, Rudolf J, Proto WR, Isaacs NW, Coombs GH, Moss CX, Mottram JC. 2012. Crystal structure of a *Trypanosoma brucei* metacaspase. *Proceedings of the National Academy of Sciences, USA* 109: 7469–7474.

- Meslin B, Barnadas C, Boni V, Latour C, De Monbrison F, Kaiser K, Picot S. 2007. Features of apoptosis in *Plasmodium falciparum* erythrocytic stage through a putative role of PFMCA1 metacaspase-like protein. *Journal of Infectious Diseases* 195: 1852–1859.
- Moss CX, Westrop GD, Juliano L, Coombs GH, Mottram JC. 2007. Metacaspase 2 of *Trypanosoma brucei* is a calcium-dependent cysteine peptidase active without processing. *FEBS Letters* 581: 5635–5639.
- Nakagawa T, Kurose T, Hino T, Tanaka K, Kawamukai M, Niwa Y, Toyooka K, Matsuoka K, Jinbo T, Kimura T. 2007. Development of series of gateway binary vectors, pGWBs, for realizing efficient construction of fusion genes for plant transformation. *Journal of Bioscience and Bioengineering* 104: 34–41.
- Nakamura S, Mano S, Tanaka Y, Ohnishi M, Nakamori C, Araki M, Niwa T, Nishimura M, Kaminaka H, Nakagawa T *et al.* 2010. Gateway binary vectors with the bialaphos resistance gene, bar, as a selection marker for plant transformation. *Bioscience, Biotechnology, and Biochemistry* 74: 1315–1319.
- Rawlings ND, Tolle DP, Barrett AJ. 2004. Evolutionary families of peptidase inhibitors. *Biochemical Journal* 378: 705–716.
- Ray CA, Black RA, Kronheim SR, Greenstreet TA, Sleath PR, Salvesen GS, Pickup DJ. 1992. Viral inhibition of inflammation: cowpox virus encodes an inhibitor of the interleukin-1 β converting enzyme. *Cell* 69: 597–604.
- Roberts TH, Ahn JW, Lampl N, Fluhr R. 2011. Plants and the study of serpin biology. *Methods in Enzymology* 499: 347–366.
- Salvesen GS, Hempel A, Coll NS. 2016. Protease signaling in animal and plant-regulated cell death. *FEBS Journal* 283: 2577–2598.
- Silverman GA, Whisstock JC, Bottomley SP, Huntington JA, Kaiserman D, Luke CJ, Pak SC, Reichhart JM, Bird PI. 2010. Serpins flex their muscle: I. Putting the clamps on proteolysis in diverse biological systems. *Journal of Biological Chemistry* 285: 24299–24305.
- Tsatsiani L, Van Breusegem F, Gallois P, Zavalov A, Lam E, Bozhkov PV. 2011. Metacaspases. *Cell Death and Differentiation* 18: 1279–1288.
- Uren AG, O'Rourke K, Aravind LA, Pisabarro MT, Seshagiri S, Koonin EV, Dixit VM. 2000. Identification of paracaspases and metacaspases: two ancient families of caspase-like proteins, one of which plays a key role in MALT lymphoma. *Molecular Cell* 6: 961–967.
- Vercammen D, Belenghi B, van de Cotte B, Beunens T, Gavigan JA, De Rycke R, Brackenier A, Inze D, Harris JL, Van Breusegem F. 2006. Serpin1 of *Arabidopsis thaliana* is a suicide inhibitor for metacaspase 9. *Journal of Molecular Biology* 364: 625–636.
- Vercammen D, van de Cotte B, De Jaeger G, Eeckhout D, Casteels P, Vandepoel K, Vandenberghe I, Van Beeumen J, Inze D, Van Breusegem F. 2004. Type II metacaspases Atmc4 and Atmc9 of *Arabidopsis thaliana* cleave substrates after arginine and lysine. *Journal of Biological Chemistry* 279: 45329–45336.
- Vinatzer BA, Teitzel GM, Lee MW, Jelenska J, Horton S, Fairfax K, Jenrette J, Greenberg JT. 2006. The type III effector repertoire of *Pseudomonas syringae* pv. *syringae* B728a and its role in survival and disease on host and non-host plants. *Molecular Microbiology* 62: 26–44.
- Voinnet O, Rivas S, Mestre P, Baulcombe D. 2003. An enhanced transient expression system in plants based on suppression of gene silencing by the p19 protein of tomato bushy stunt virus. *Plant Journal* 33: 949–956.
- Watanabe N, Lam E. 2011. Arabidopsis metacaspase 2d is a positive mediator of cell death induced during biotic and abiotic stresses. *Plant Journal* 66: 969–982.
- Wong AH, Yan C, Shi Y. 2012. Crystal structure of the yeast metacaspase Yca1. *Journal of Biological Chemistry* 287: 29251–29259.
- Wroblewski T, Tomczak A, Michelmore R. 2005. Optimization of Agrobacterium-mediated transient assays of gene expression in lettuce, tomato and Arabidopsis. *Plant Biotechnology Journal* 3: 259–273.
- Wrzaczek M, Vainonen JP, Stael S, Tsatsiani L, Help-Rinta-Rahko H, Gauthier A, Kaufholdt D, Bollhoner B, Lamminmaki A, Staes A *et al.* 2015. GRIM REAPER peptide binds to receptor kinase PRK5 to trigger cell death in Arabidopsis. *EMBO Journal* 34: 55–66.
- Zalila H, Gonzalez IJ, El-Fadili AK, Delgado MB, Desponds C, Schaff C, Fasel N. 2011. Processing of metacaspase into a cytoplasmic catalytic domain mediating cell death in *Leishmania major*. *Molecular Microbiology* 79: 222–239.

Supporting Information

Additional Supporting Information may be found online in the Supporting Information tab for this article:

Fig. S1 Schematic representation of all constructs used in this study.

Fig. S2 Immunoprecipitation of AtMC1 native form in *Arabidopsis thaliana*.

Fig. S3 Comparison of AtMC1 expression levels when expressed under native vs dexamethasone-inducible promoter.

Fig. S4 Binding between AtMC1 and AtSerpin1.

Fig. S5 AtMC1 and AtSerpin1 co-immunoprecipitate in *Arabidopsis thaliana*.

Fig. S6 AtSerpin1 is cleaved by AtMC1.

Fig. S7 AtSerpin1, an inhibitor of cell death proteases in plants.

Table S1 Identification of AtMC1 and AtSerpin1 by LC-MS/MS after HA immunoaffinity purification

Table S2 Identification of AtMC1 and AtSerpin1 by LC-MS/MS after TAP purification

Please note: Wiley Blackwell are not responsible for the content or functionality of any Supporting Information supplied by the authors. Any queries (other than missing material) should be directed to the *New Phytologist* Central Office.

Supplementary Data

AtSERPIN1 is an inhibitor of the metacaspase AtMC1-mediated cell death and autocatalytic processing *in planta*

Running title: AtSERPIN1 is an AtMC1 inhibitor in plants

Saul Lema Asqui, Dominique Vercammen, Marc Valls, Frank van Breusegem, Frank L. Conlon, Jeff L. Dangl and Núria S. Coll

Table S1: Experimental design including all files uploaded to ProteomeXchange

(a) mzid files from the samples analyzed

mzid file name	Sample
Mudpit_2012_01_12_Coll_Conlon.mzid	<i>atmc1</i> (1st replicate)
Mudpit_2012_02_29_Coll_Conlon.mzid	<i>atmc1 P_{atmCI}:AMCI-HA</i> (1st replicate)
Mudpit_2012_03_30_Coll_Conlon.mzid	<i>atmc1</i> (2nd replicate)
Mudpit_2012_04_20_Coll_Conlon.mzid	<i>atmc1 P_{atmCI}:AMCI-HA</i> (2nd replicate)
Mudpit_2012_05_09_Coll_Conlon.mzid	<i>atmc1</i> (3rd replicate)
Mudpit_2012_06_18_Coll_Conlon.mzid	<i>lsd1 atmc1 P_{atmCI}:AMCI-HA</i> (1st replicate)
Mudpit_2012_07_27_Coll_Conlon.mzid	<i>atmc1</i> (4th replicate)
Mudpit_2012_08_26_Coll_Conlon.mzid	<i>atmc1 P_{atmCI}:AMCI-HA</i> (1st replicate)
Mudpit_2012_09_25_Coll_Conlon.mzid	<i>atmc1</i> (5th replicate)
Mudpit_2012_10_24_Coll_Conlon.mzid	<i>lsd1 atmc1 P_{atmCI}:AMCI-HA</i> (2nd replicate)

(b) Detailed raw files from the samples analyzed

Mudpit_2012_01_12_Coll_Conlon.mzid	Cut band (kDa)	Sample
2012_01_16B_Dangl_C1_R1	>75	<i>atmc1</i> (1st replicate)
2012_01_16C_Dangl_C2_R1	50-75	
2012_01_13C_Dangl_C3_R1	35-50	
2012_01_12D_Dangl_C4_R1	24-35	
2012_01_12C_Dangl_C5_R1	18-24	
2012_01_13E_Dangl_C6_R1	15-18	
2012_01_17E_Dangl_C7_R1	10-15	
2012_01_15E_Dangl_C8_R1	<15	
2012_01_17C_Dangl_C1_R2	>75	
2012_01_17B_Dangl_C2_R2	50-75	
2012_01_15B_C3_R2	35-50	<i>atmc1 P_{atmCI}:AMCI-HA</i> (1st replicate)
2012_01_13D_Dangl_C4_R2	24-35	
2012_01_13B_Dangl_C5_R2	18-24	
2012_01_14D_C6_R2	15-18	
2012_01_18C_Dangl_C7_R2	10-15	
2012_01_16D_Dangl_C8_R2	<15	

Mudpit_2012_02_29_Coll_Conlon.mzid	Cut band (kDa)	Sample
2012_02_09A_Dangl_Set3_3_1	>75	<i>atmc1</i> (2nd replicate)
2012_02_29C_Dangl_Set3_3_2	50-75	
2012_02_29B_Dangl_Set3_3_3	35-50	
2012_02_22B_Dangl_Set3_3_4	24-35	
2012_02_09C_Dangl_Set3_3_5	18-24	
2012_02_08E_Dangl_Set3_3_6	15-18	
2012_02_08F_Dangl_Set3_3_7	10-15	
2012_02_08G_Dangl_Set3_3_8	<15	
2012_02_22C_Dangl_Set3_3_1	>75	
2012_02_29E_Dangl_Set3_3_2_R2	50-75	
2012_02_29E_Dangl_Set3_3_3_R2	35-50	<i>atmc1 P_{atmCI}:AMCI-HA</i> (2nd replicate)
2012_02_22D_Dangl_Set3_3_4	24-35	
2012_02_09D_Dangl_Set3_3_5	18-24	
2012_02_09E_Dangl_Set3_3_6	15-18	
2012_02_09E_Dangl_Set3_3_7	10-15	
2012_02_09F_Dangl_Set3_3_8	<15	

Mudpit_2012_03_30_Coll_Conflom.mzid	Cut band (kDa)	Sample
2012_03_31C_Dangl_4_1_R1	>75	<i>atmc1</i> (3rd replicate)
2012_03_30D_Dangl_4_2_R1	50-75	
2012_03_30E_Dangl_4_3_R1	35-50	
2012_03_30F_Dangl_4_4_R1	24-35	
2012_03_31A_Dangl_4_5_R1	18-24	
2012_03_31B_Dangl_4_6_R1	15-18	
2012_03_31D_Dangl_4_7_R1	10-15	
2012_03_02A_Dangl_4_1_R2	>75	
2012_03_01A_Dangl_4_2_R2	50-75	
2012_03_01B_Dangl_4_3_R2	35-50	
2012_03_01C_Dangl_4_4_R2	24-35	
2012_03_01E_Dangl_4_5_R2	18-24	
2012_03_01D_Dangl_4_6_R2	15-18	
2012_03_01F_Dangl_4_7_R2	10-15	

Mudpit_2012_05_07_Coll_Conflom.mzid	Cut band (kDa)	Sample
2012_05_27C_Dangl_C1_R1	>75	<i>atmc1</i> (4th replicate)
2012_05_27E_Dangl_C1_R1	50-75	
2012_05_27F_Dangl_C1_R1	35-50	
2012_05_27G_Dangl_C1_R1	24-35	
2012_05_28A_Dangl_C1_R1	18-24	
2012_05_28B_Dangl_C1_R1	15-18	
2012_05_28C_Dangl_C1_R1	10-15	
2012_05_28D_Dangl_C1_R1	<15	
2012_05_28E_Dangl_C1_R2	>75	
2012_05_28F_Dangl_C1_R2	50-75	
2012_05_28G_Dangl_C1_R2	35-50	
2012_05_29A_Dangl_C1_R2	24-35	
2012_05_29B_Dangl_C1_R2	18-24	
2012_05_29C_Dangl_C1_R2	15-18	
2012_05_29D_Dangl_C1_R2	10-15	
2012_05_29E_Dangl_C1_R2	<15	

lsd1 atmc1 P_{AtMCI} :AtMCI-HA (1st replicate)

lsd1 atmc1 P_{AtMCI} :AtMCI-HA (2nd replicate)

Table S2: Identification of AtMC1 and AtSerp1 by LC-MS/MS after HA immunoaffinity purification

Background: *atmc1 P_{AtMC1}:AtMC1-HA*

Bait: AtMC1-HA	Experiment 1		Experiment 2	
	AtSerp1	AtMC1	AtSerp1	AtMC1
Spectral counts	6	34	2	2
Peptide count	2	3	2	1
Protein coverage (%)	6.6	15	11	4.1

Background: *lsd1 atmc1 P_{AtMC1}:AtMC1-HA*

Bait: AtMC1-HA	Experiment 1		Experiment 2	
	AtSerp1	AtMC1	AtSerp1	AtMC1
Spectral counts	-	4	-	12
Peptide count	-	1	-	2
Protein coverage (%)	-	4.1	-	4.1

Background: *atmc1*

Bait: -	Experiment 1		Experiment 2	
	AtSerp1	AtMC1	AtSerp1	AtMC1
Spectral counts	-	-	-	-
Peptide count	-	-	-	-
Protein coverage (%)	-	-	-	-

14 **Table S1: Experimental design including all files uploaded to**
15 **ProteomeXchange.** (a) mzid files from the samples analyzed. (b) Detailed raw
16 files from the samples analyzed.

17

18 **Table S2: Identification of AtMC1 and AtSerp1 by LC-MS/MS after HA**
19 **immunoaffinity purification.** The table indicates: Peptide count, number of
20 peptides with unique sequences matching the selected protein; Spectral count,
21 number of spectra identified for all peptides identified; Protein coverage %,
22 percentage of protein sequence covered by assigned peptide matches. The
23 following lines were used: *atmc1* complemented with $P_{AtMC1}::AtMC1-HA$, where
24 no cell death occurs and both AtMC1 and AtSerp1 were detected; the cell death-
25 induced *lsd1 atmc1 P_{AtMC1}::AtMC1-HA*, in which AtMC1 but not AtSerp1 were
26 detected; the *atmc1* mutant, in which neither AtMC1 nor AtSerp1 were detected
27 due to the absence of the AtMC1 transgene.

28

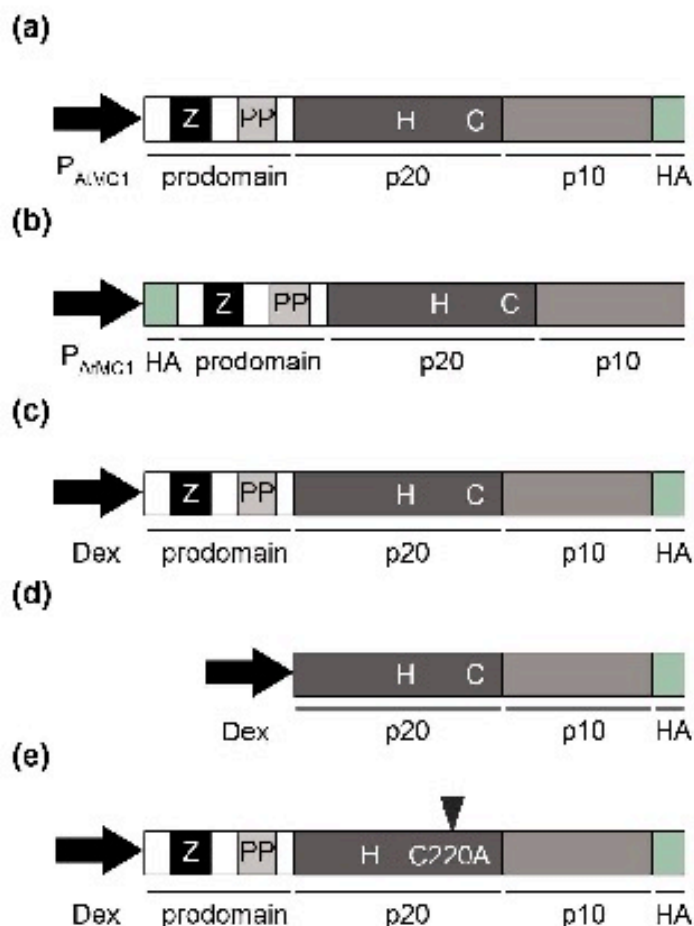


Figure S1: Schematic representation of the most relevant AtMC1 constructs used in this study: (a) *PAtMC1::AtMC1-HA*. (b) *PAtMC1::HA-AtMC1*, (c) *Dex::AtMC1-HA*, (d) *Dex::AtMC1-ΔN-HA* and (e) *Dex::AtMC1-CA-HA*. Promoters are displayed as arrows, P_{AtMC1} , or Dex; prodomain, containing an LSD1-like zinc finger (Z) and a prolin-rich domain (PP); p20 subunit containing the catalytic histidine (H) and cysteine (C); p10 subunit; HA tag.

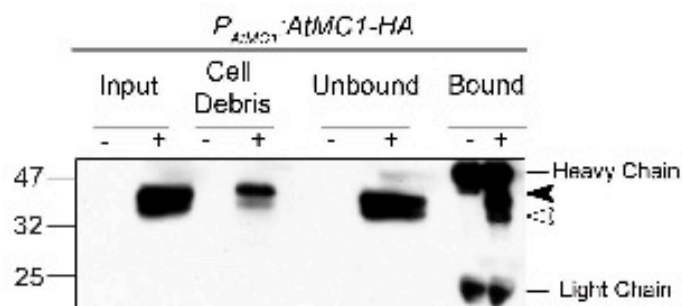


Figure S2: Immunoprecipitation of AtMC1 native form in *Arabidopsis thaliana*. Immunoblot using anti-HA displaying all fractions obtained in a representative immunoprecipitation experiment using *atmc1* (-) or *atmc1 P_{AtMC1}::AtMC1-HA* (+) plants: total protein extract (Input), cell debris discarded in the first centrifugation (Cell Debris), protein not bound to the HA beads (Unbound), elution at 70°C (Bound). Black and white arrows indicate full-length and cleaved AtMC1, respectively. Bands corresponding to the heavy and light antibody chains are also displayed.

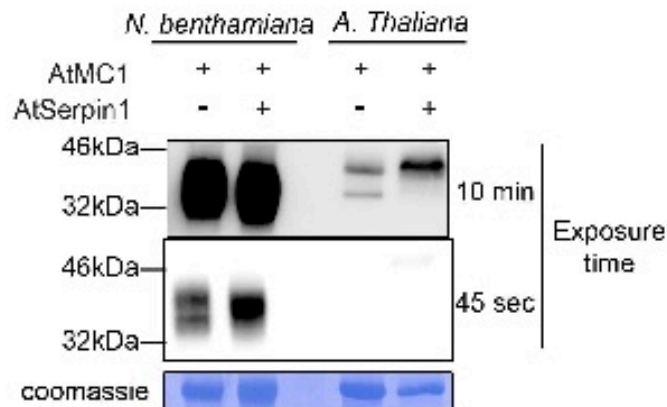
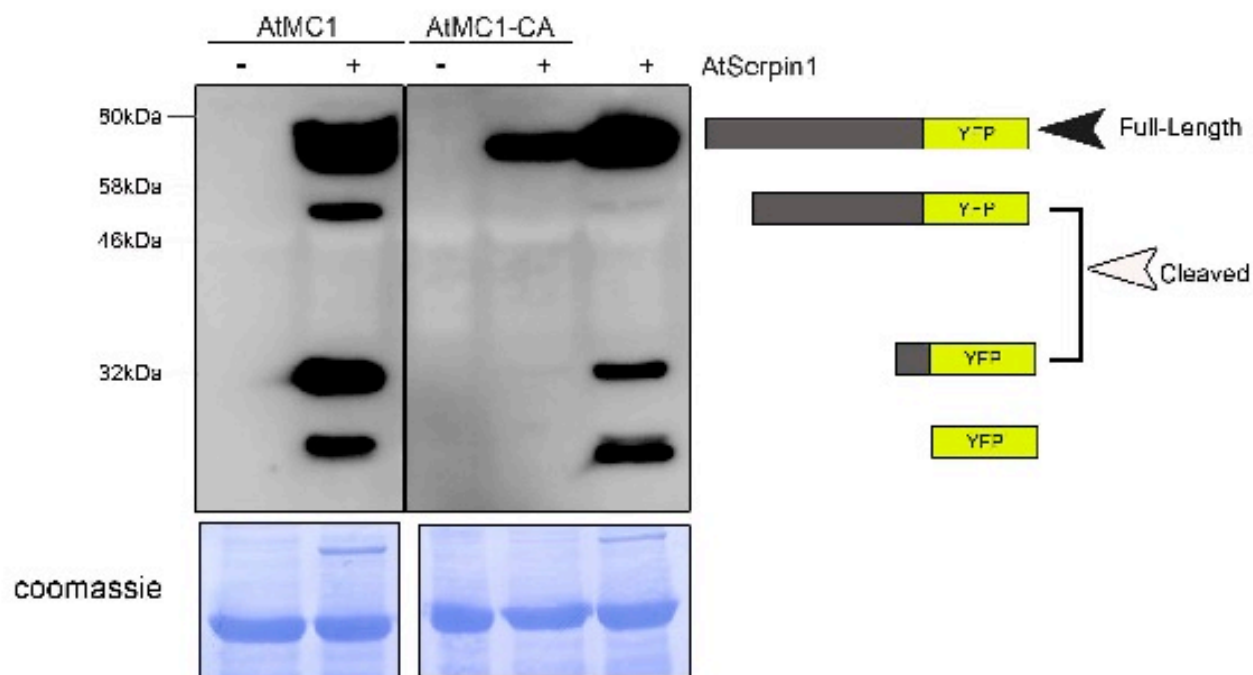


Figure S3: Comparison of AtMC1 protein levels in the different plant systems used. Immunoblot using anti-HA of *N. benthamiana* leaves transiently co-expressing *Dex::AtMC1-HA* alone or in combination with and *35S::AtSerp1-YFP* compared to Arabidopsis homozygous transgenic plants stably expressing $P_{AtMC1}::HA-AtMC1$ alone or in combination with *35S::AtSerp1-YFP*. Two different exposure times are displayed (10 min and 45 seconds). Proteins were coomassie stained to indicate protein levels.

(a)



(b)

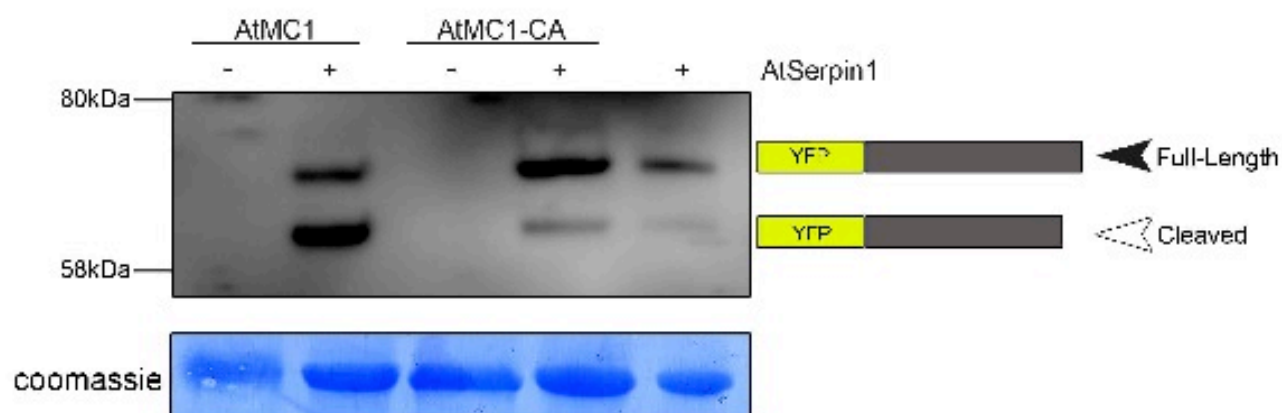
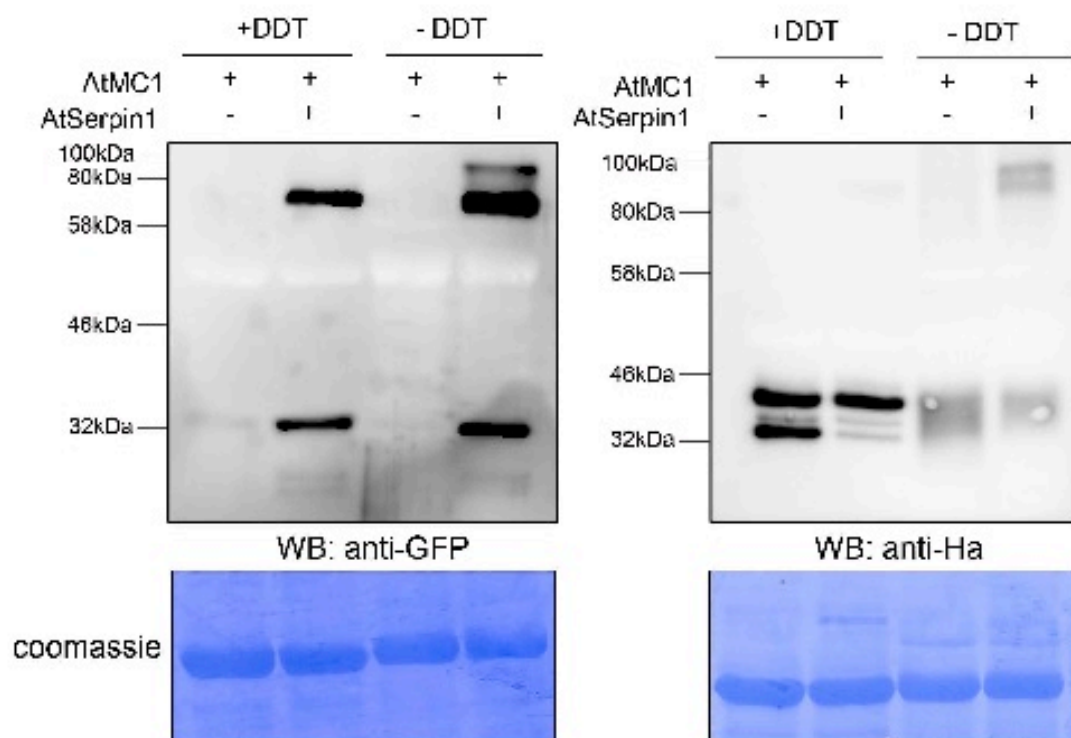


Figure S4: AtSerpin1 is cleaved by AtMC1. (a) *AtSerpin1*-YFP alone or in combination with *AtMC1*-HA or *AtMC1*-CA-HA and (b) YFP-*AtSerpin1* alone or in combination with *AtMC1*-HA or *AtMC1*-CA-HA were transiently expressed in *N. benthamiana* leaves. Total proteins were extracted and 50 μ g were either coomassie-stained or immunoblotted using anti-GFP antibody. The black arrowhead indicates full-length *AtSerpin1*, whereas the white arrowhead points at the putative *AtSerpin1* cleaved forms.

(a)



(b)

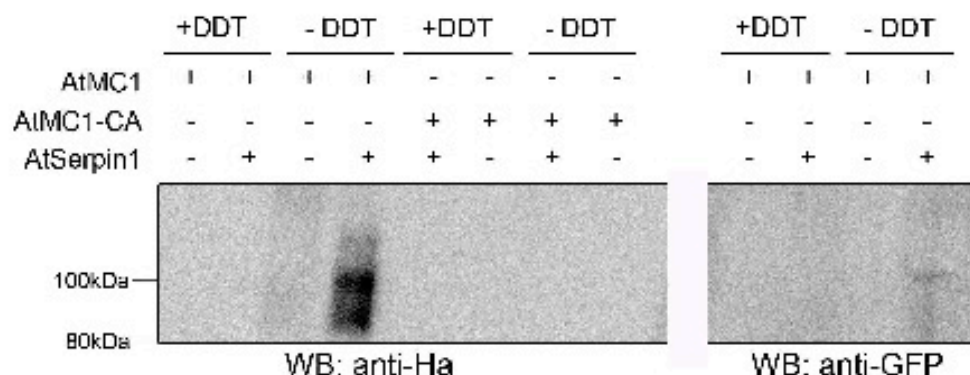


Figure S5: Binding between AtMC1-AtSerpin1. (a) Full-length *AtMC1-HA* was transiently expressed in *N. benthamiana* leaves alone or in combination with *AtSerpin1-YFP*. Total proteins were extracted under reducing (+DDT) or non-reducing (-DDT) conditions. 50 µg protein were separated on a 10% SDS-PAGE gel and either coomassie-stained or immunoblotted using anti-HA and anti-GFP antibodies. (b) Full-length *AtMC1-HA* and *AtMC1-CA-HA* were transiently expressed in *N. benthamiana* leaves alone or in combination with *AtSerpin1-YFP*. Total proteins were extracted under reducing (+DDT) or non-reducing (-DDT) conditions. 50 µg protein were separated on a 7.5% SDS-PAGE gel and either coomassie-stained or immunoblotted using anti-HA and anti-GFP antibodies.

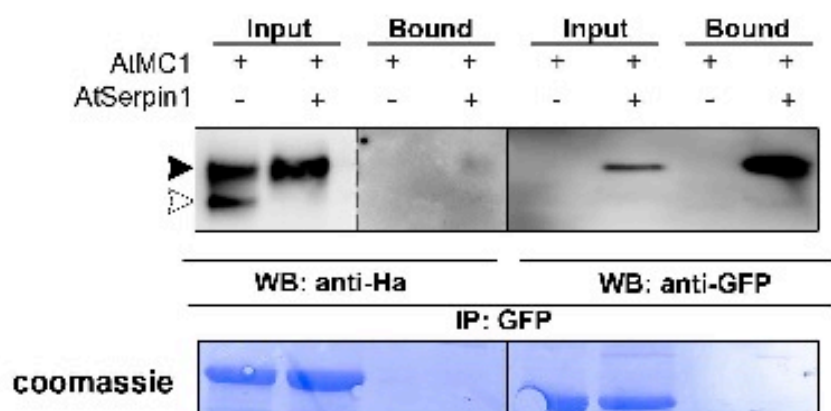


Figure S6: AtMC1 co-immunoprecipitates with AtSerpin1 in Arabidopsis. Co-immunoprecipitation experiments were performed on total proteins (input) extracted from rosette leaves of homozygous double transgenic plants co-expressing $P_{AtMC1}::AtMC1-HA$ and $35S::AtSerpin1-YFP$ or $P_{AtMC1}::AtMC1-HA$ as a control (both in an *atmc1* mutant background). Protein extracts were incubated with magnetic GFP beads and bound proteins were eluted off the beads (bound). Input and bound fractions were either coomassie-stained or immunoblotted using anti-HA to detect AtMC1 and anti-GFP to detect AtSerpin1. Black and white arrows indicate full-length and cleaved AtMC1, respectively.

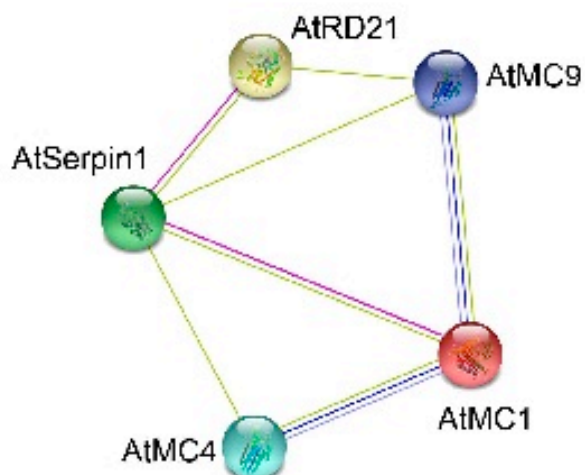


Figure S7: AtSerpin1, an inhibitor of cell death proteases in plants. AtSerpin1 interactome built in silico with the help of STRING, Search Tool for the Retrieval of Interacting Genes/Proteins, version 10. Edges represent the predicted functional links between proteins based on the following evidence: pink, experimental evidence; green, text mining; blue, co-occurrence; purple, homology.

Detection and Quantification of Protein Aggregates in Plants

Resumen publicación 3

Detección y Cuantificación de los agregados proteicos en plantas.

Las plantas están constantemente expuestas a un entorno complejo y cambiante que desafía su homeostasis celular. Las respuestas de estrés desencadenadas como consecuencia de condiciones desfavorables resultan en una mayor formación de agregados proteicos a nivel celular. Cuando la formación de proteínas mal plegadas sobrepasa la capacidad de la célula para eliminarlas, se acumulan agregados proteicos insolubles. En el campo de los animales, se está realizando un enorme esfuerzo para descubrir los mecanismos que regulan la formación de agregados debido a sus implicaciones en muchas e importantes enfermedades humanas. Debido a su importancia para la funcionalidad celular y la aptitud biológica, es igualmente trascendental ampliar la investigación de plantas en este campo. Aquí describimos un método basado en el fraccionamiento celular para obtener fracciones de agregados proteicos insolubles muy puras que posteriormente pueden ser semi-cuantificadas mediante el análisis de imágenes. Este método se puede utilizar como primer paso para evaluar si una afección particular resulta en una alteración de los niveles de formación de agregados proteicos.

Detection and Quantification of Protein Aggregates in Plants

Marc Planas-Marquès, Saul Lema A., and Núria S. Coll

Abstract

Plants are constantly exposed to a complex and changing environment that challenges their cellular homeostasis. Stress responses triggered as a consequence of unfavorable conditions result in increased protein aggregate formation at the cellular level. When the formation of misfolded proteins surpasses the capacity of the cell to remove them, insoluble protein aggregates accumulate. In the animal field, an enormous effort is being placed to uncover the mechanisms regulating aggregate formation because of its implications in many important human diseases. Because of its importance for cellular functionality and fitness, it is equally important to expand plant research in this field. Here, we describe a cell fractionation-based method to obtain very pure insoluble protein aggregate fractions that can be subsequently semi-quantified using image analysis. This method can be used as a first step to evaluate whether a particular condition results in an alteration of protein aggregate formation levels.

Key words Protein fractionation, Protein aggregates, Immunoblot, Silver stain, Proteostasis, Plants, Protocols

1 Introduction

Protein aggregation occurs as a result of protein misfolding. Cells are equipped with protein quality control systems that help refolding misfolded proteins or dispose of them when their repair is not possible to prevent the formation of protein aggregates [1]. Insoluble protein aggregates have to be eliminated to prevent sustained damage that can lead to defects in growth, a decrease in yield, accelerated aging, and even death.

In the animal field, the study of the processes leading to aggregation of misfolded proteins is the focus of extensive research as it is associated with various important human diseases such as Alzheimer's, Huntington's, and Parkinson's, among others [2, 3]. Previously thought as an uncontrolled and unspecific process, protein aggregation and disaggregation is emerging as a very complex, tightly regulated process conserved across all kingdoms [1].

In plants, the study of protein aggregate formation has mostly focused on chloroplastic processes [4–6]. In contrast, the cytoplasmic regulation of protein aggregation remains poorly understood. Recent work from our laboratory has shown that autophagic components and the death protease metacaspase 1 (AtMC1) are required for clearance of protein aggregates [7]. Autophagy and AtMC1 are emerging as central players in the proteostasis network, conserved across kingdoms [8–10]. We present here protocols developed in our laboratory to isolate and quantify protein aggregates. We use these to analyze differences in the formation of protein aggregates between different plant lines and physiological conditions.

2 Materials

2.1 Plant Growth

1. *Arabidopsis thaliana* seeds Col-0 ecotype.
2. Soil mix: 4.5 parts peat + 2 parts sand + 1 part vermiculite.
3. Controlled growth chamber: Aralab chamber D1200PLH with controlled temperature, humidity, and photoperiod (Aralab, Albarraque, Portugal).

2.2 Protein Extraction and Aggregate Isolation

1. Fractionation buffer: 20 mM Tris–HCl (pH 8), 1 mM EDTA (pH 8), and 0.33 M sucrose. Prepare the buffer from autoclaved 1 M stock solutions (*see Note 1*) and store it at 4 °C.
2. Fractionation buffer 0.3% Triton X-100: same buffer composition as in Fractionation buffer but adding Triton X-100 to reach a final concentration of 0.3%. Triton X-100 is added from a 10% stock solution.
3. Prior to the use of fractionation buffers, add 1 tablet of COMPLETE protease inhibitor (Roche, Basel, Switzerland) cocktail for every 10 ml of buffer and keep them on ice.
4. Protein Assay (Bio-Rad, Hercules, CA, USA).
5. SDS-loading buffer (5×): 250 mM Tris–HCl (pH 6.8), 50% glycerol, 0.5% bromophenol blue (BPB), 10% SDS, and 500 mM DTT (*see Note 2*).
6. Miracloth (Millipore, Billerica, MA, USA).
7. Beckman Coulter Optima™ L-100 XP Ultracentrifuge, SW60Ti rotor and 4 ml ultracentrifuge tubes.
8. Bioruptor® (Diagenode, Denville, NJ, USA).

2.3 Immunoblot

1. Anti-HA monoclonal antibody (3F10, Roche, Basel, Switzerland) at 1:5000 dilution.
2. Anti-cAPX antibody (Agrisera, Vännäs, Sweden) at 1:10,000 dilution.
3. Anti-PM ATPase antibody (Agrisera, Vännäs, Sweden) at 1:10,000 dilution.

2.4 Silver Stain

Prepare all solutions fresh with ultrapure water under a fume hood and keep at room temperature (*see Note 3*).

1. Fixing solution: 50% methanol, 37% formaldehyde, and 12% acetic acid. To prepare 100 ml, mix 50 ml of methanol, 37 ml of formaldehyde, and 12 ml of acetic acid.
2. 50% ethanol.
3. Pretreatment solution: 0.02% sodium thiosulfate ($\text{Na}_2\text{S}_2\text{O}_4$). To prepare, dissolve 20 mg in 100 ml.
4. Staining solution: 0.2% silver nitrate (AgNO_3), 0.03% formaldehyde. To prepare, dissolve 200 mg of silver nitrate in 100 ml of water and add 30 μl of formaldehyde.
5. Revealing solution: 6% sodium carbonate (Na_2CO_3), 0.02% formaldehyde, 0.0005% sodium thiosulfate. To prepare, dissolve 6 g of sodium carbonate in 90 ml of water, add 20 μl of formaldehyde and 2.5 ml of a 0.02% solution of sodium thiosulfate. Bring up to 100 ml with water.
6. Stop solution: 50% methanol and 12% acetic acid. To prepare mix 50 ml of methanol and 12 ml of acetic acid and bring up to 100 ml with water.
7. Gel image analysis: Scanned gel images can be analyzed using the Multi Gauge V3.0 software (Fujifilm, Minato, Japan).

3 Methods

3.1 Plant Growth and Senescence Induction

1. Sow around 50 Arabidopsis seeds on pots filled with soil mix watered to field capacity and vernalize at 4 °C for 3 days. Keep them on a tray and covered with a plastic film to maintain high humidity.
2. Transfer plants to a controlled growth chamber and grow under 9 h light at 21 °C and 15 h dark at 18 °C for 3 weeks (*see Note 4*).
3. To induce senescence transfer plants to long-day conditions: 16 h light at 21 °C and 8 h dark at 18 °C. Grow plants for 4 weeks under these conditions (*see Note 5*).

3.2 Cell Fractionation (Scheme of the Process Shown in Fig. 1)

1. Freeze 200 mg of rosette leaves (leaves are harvested regardless of their observed senescence degree) from different plants on liquid nitrogen.
2. Grind frozen samples using a mortar and pestle on ice with liquid nitrogen.
3. Transfer ground powder to 15 ml tubes placed on ice (*see Note 6*).
4. Add 4 ml of Fractionation buffer to the 15 ml tubes containing the powdered samples (scale up for larger sample amounts).
5. Vortex vigorously to ensure a good mixture.

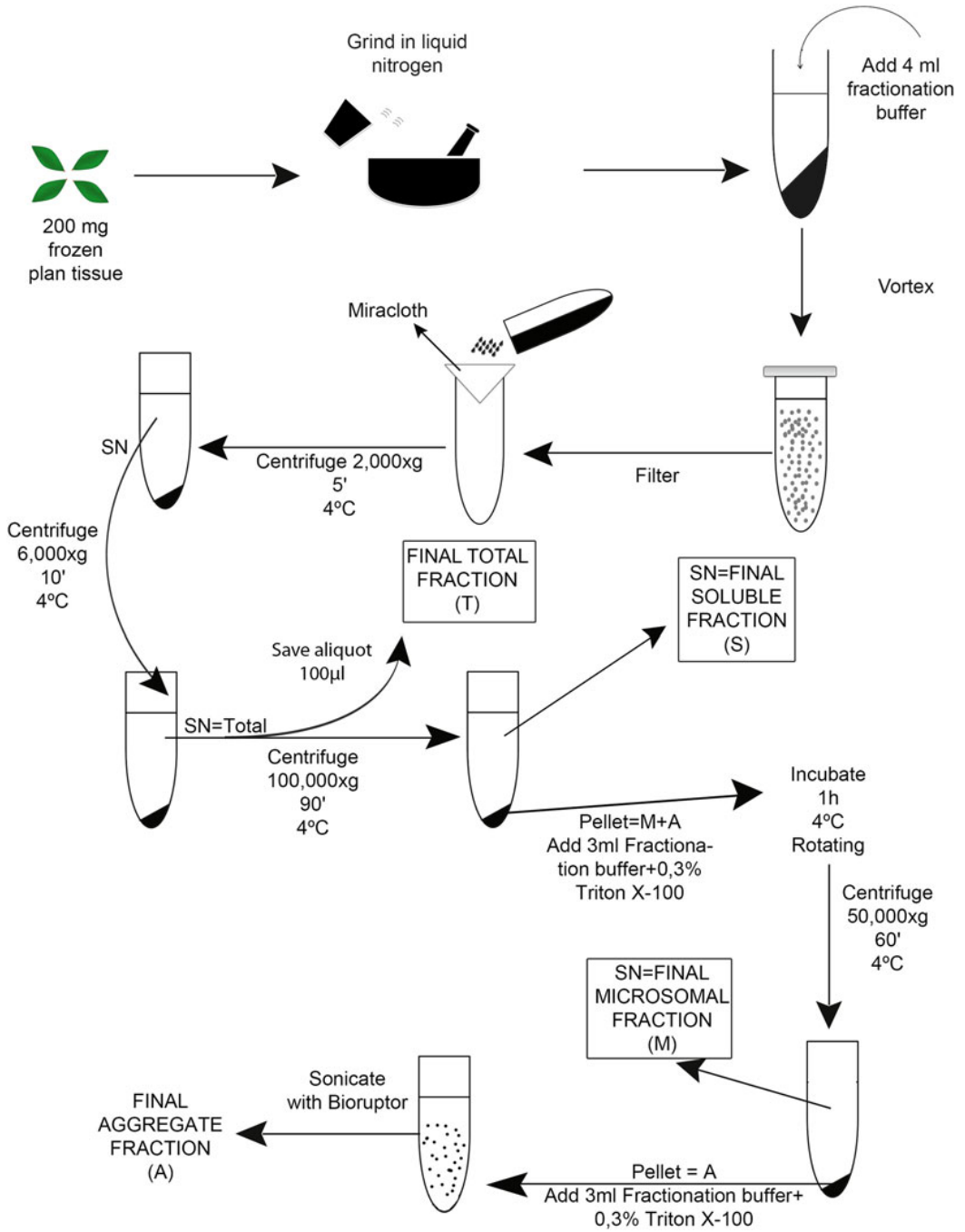


Fig. 1 Flow chart to obtain insoluble aggregates from plant tissue

6. Pass through a Miracloth filter to new falcon tubes in order to eliminate cell debris.
7. Centrifuge the suspensions at $2000 \times g$ for 5 min at 4 °C to remove large particles.
8. Collect the supernatants and subsequently centrifuge them at $6000 \times g$ for 10 min at 4 °C.
9. The resulting supernatants are the total (T) protein fractions. Transfer these supernatants to new falcon tubes (*see Note 7*).
10. Measure protein concentration of the different samples using the Protein Assay (Bio-Rad) following manufacturer's instructions.
11. Equal protein concentration among all samples, adjusting them at 3 ml (*see Note 8*).
12. Save an aliquot (200 μ l) of each sample on new 1.5 ml tubes labeled T and keep them on ice.
13. Transfer the supernatants to Beckman Coulter 4 ml ultracentrifuge tubes and centrifuge them at $100,000 \times g$ for 90 min at 4 °C (*see Note 9*) to separate the soluble fraction (S) (supernatant) from the fraction containing microsomal membranes and insoluble aggregates (M+A) (pellet).
14. Collect the soluble fractions and transfer them to new 15 ml tubes. Save an aliquot of 200 μ l of each soluble fraction and keep them on ice.

3.3 Aggregate Isolation

1. To separate microsomal proteins from insoluble protein aggregates in the pellet, add 3 ml of fractionation buffer supplemented with 0.3% Triton X-100. Resuspend the pellet by pipetting, transfer to 15 ml tubes, and incubate in a rotating shaker at 4 °C for 1 h (*see Note 10*).
2. Transfer the Triton X-100-treated M+A fractions back to 4 ml ultracentrifuge tubes, equilibrate them and centrifuge at $50,000 \times g$ for 60 min at 4 °C. The supernatant of this centrifugation step corresponds to the microsomal fraction (M), whereas the pellet contains the insoluble protein aggregates (A).
3. Collect the microsomal fractions and transfer them to fresh 15 ml tubes. Be careful not to disturb the pellet but ensure that no M fraction remains on the tube (*see Note 11*).
4. Add 3 ml of fractionation buffer supplemented with 0.3% Triton X-100 to the pellet, containing the insoluble protein aggregates and pipet up and down repeatedly to mix.
5. To solubilize the proteins, sonicate the samples using a Bioruptor® at 4 °C set on "High" with the following parameters: 3 cycles, 30 s "ON", 30 s "OFF" (*see Note 12*).
6. Add the corresponding amount of $5 \times$ SDS-loading buffer to every fraction collected (*see Note 13*). Boil them for 5 min and store at -20 °C.

3.4 Localization of Particular Proteins in the Aggregate Fraction

1. Run equal volumes of each fraction on SDS-PAGE gels (*see Note 14*).
2. Presence of a particular protein in one of the fractions can be analyzed by immunoblot (Fig. 2) using an antibody against the protein of interest.
3. Available control antibodies to show purity of the different fractions should be used in parallel (*see Note 15* and Fig. 2).
4. Coomassie staining of the membranes once the immunoblot is completed is highly recommended as an additional method to test purity of the fractions.

3.5 Relative Quantification of Aggregates

Use silver staining to compare the amount of proteins present in each fraction.

1. Run equal volumes of each fraction on SDS-PAGE gels.
2. Incubate the gels 1 h in the Fixing solution. Perform all steps at room temperature and using a rocking shaker.
3. Wash three times 20 s with 50% ethanol.
4. Incubate the gels 1 min in the Pre-treatment solution.
5. Wash three times 20 s with ultrapure water.
6. Incubate 20 min with the Staining solution in the dark (*see Note 16*).
7. Wash three times 20 s with ultrapure water.
8. Incubate with the Revealing solution until the bands become visible (*see Note 17*).

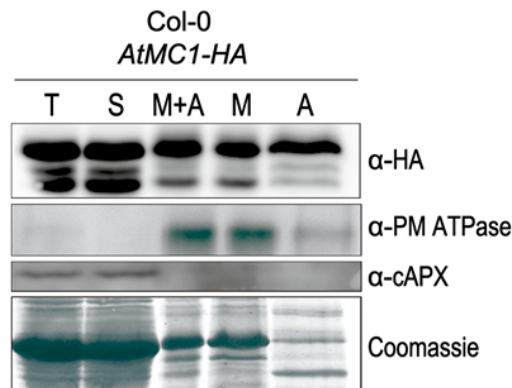


Fig. 2 Immunoblot of the protein fractions. Equal volumes of fractionated protein extracts of Arabidopsis Col-0 plants expressing the protein of interest (in this case, *AtMC1-HA*) were run on SDS-PAGE gels. After separation, the gels were either stained with Coomassie or analyzed by immunoblot using anti-HA antisera (α -HA), anti-cytosolic ascorbate peroxidase (α -cAPX) and anti plasma membrane H⁺ ATPase (α -PM ATPase). Reproduced with modifications from [7] with permission of Nature Publishing Group

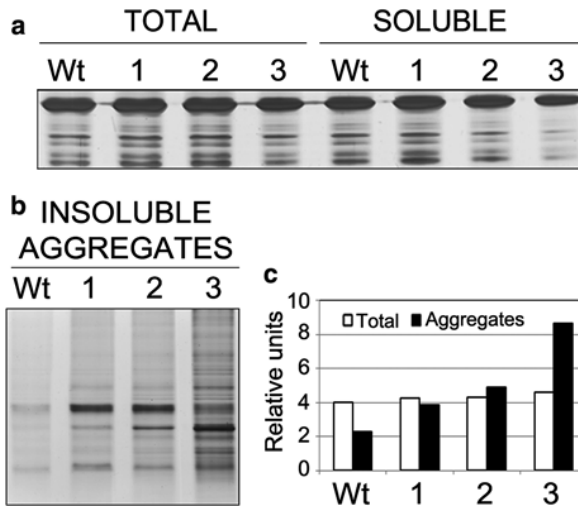


Fig. 3 Relative quantification of protein aggregates. Equal volumes of fractionated protein extracts of Arabidopsis wild-type (Wt) and mutant (1, 2, and 3) Col-0 plants were run on SDS-PAGE polyacrylamide gels and silver-stained. **(a)** Total and soluble fractions. **(b)** Insoluble protein aggregates. **(c)** Relative quantification of Total versus Aggregate fractions using the Multi Gauge V3.0 software. Silver stain images are reproduced with modifications from [7] with permission of Nature Publishing Group

9. Wash 5 s with water and add the Stop solution.
10. Gels can be stored at 4 °C in water for some weeks.
11. Since the intensity of the stain correlates with protein content, a representation of the quantity of proteins present in the aggregate fraction can be estimated by comparing the A and T fractions (Fig. 3a, b).
12. To calculate the intensity of the different lanes, analyze the scanned image of the gel scan using the image J software.
13. Analyze the bitmap (.bmp) images of the stained gels using an image analysis software to obtain numeric values for signal intensity and plot values on a graph (Fig. 3c).
14. Finally, divide the aggregate lane value by the total lane value and plot it.

4 Notes

1. Tris-HCl 1 M stock solution pH 8: weigh 121.14 g Tris base and transfer it to a 1 l bottle or glass beaker containing 900 ml water. Mix and adjust pH with HCl. Make up to 1 l with water. Ethylenediaminetetraacetic acid (EDTA) 1 M stock solution pH 8 is prepared dissolving 186.12 g EDTA in 1 l water.

preservation of the samples and to prevent damage to the instrument. Precooling the bath must be done at least 15 min before the sonication process. Water level on the bath must reach the red line on the tank. Use only distilled water to fill the tank (do not use deionized water).


13. It is sufficient to keep 200 μ l per fraction.
14. We normally run 40 μ l of each fraction per lane.
15. There are several antibodies that work well as soluble and microsomal fraction purity controls. In this case we used anti-cytosolic ascorbate peroxidase antisera (α -cAPX) as a soluble fraction marker and anti-plasma membrane ATPase antisera (α -PM ATPase) as microsomal fraction marker.
16. To keep the solution with the gels in the dark, wrap the incubation boxes with aluminum foil.
17. Usually takes very short. In less than 1 min bands start appearing. Stop once the desired intensity is achieved.

References

1. Tyedmers J, Mogk A, Bukau B (2013) Cellular strategies for controlling protein aggregation. *Nat Rev* 11:777–788
2. Shrestha A, Puente LG, Brunette S et al (2013) The role of Yca1 in proteostasis. Yca1 regulates the composition of the insoluble proteome. *J Proteomics* 81:24–30
3. Kim YE, Hipp MS, Bracher A et al (2013) Molecular chaperone functions in protein folding and proteostasis. *Annu Rev Biochem* 82:323–355
4. Lee U, Rioflorida I, Hong SW et al (2006) The Arabidopsis ChlpB/Hsp100 family of proteins: chaperones for stress and chloroplast development. *Plant J* 49:115–127
5. Howell HH (2013) Endoplasmic reticulum stress responses in plants. *Annu Rev Plant Biol* 64:477–499
6. Rajan VBV, D'Silva P (2009) Arabidopsis thaliana J-class heat shock proteins: cellular stress sensors. *Funct Integr Genomics* 9: 433–446
7. Coll NS, Smidler A, Puigvert M et al (2014) The plant metacaspase AtMC1 in pathogen-triggered programmed cell death and aging: functional linkage with autophagy. *Cell Death Differ* 21:1399–1408
8. Munch D, Rodriguez E, Bressendorff S et al (2014) Autophagy deficiency leads to accumulation of ubiquitinated proteins, ER stress, and cell death in Arabidopsis. *Autophagy* 10:1579–1587
9. Lee RE, Brunette S, Puente LG et al (2010) Metacaspase Yca1 is required for clearance of insoluble protein aggregates. *Proc Natl Acad Sci U S A* 107:13348–13353
10. Hill SM, Hao X, Liu B et al (2014) Life-span extension by a metacaspase in the yeast *Saccharomyces cerevisiae*. *Science* 344: 1389–1392

DRAFT 1

AtHIR2, a new regulator of AtMC1-mediated cell death in plants

Saúl Lema A.¹, Marc Valls^{1,2}, Núria Sánchez Coll¹, .

Centre for Research in Agricultural Genomics (CRAG), CSIC-IRTA-. Campus UAB-UB, 08193 Bellaterra, Catalonia, Spain. ²Department of Genetics, University of Barcelona.

Abstract

Metacaspases are a family of cysteine proteases. *Arabidopsis thaliana* contains 9 metacaspases (named AtMC1 to 9). We have previously shown that AtMC1 is a positive regulator of pathogen-triggered PCD and that negative regulation of AtMC1 by AtMC2 can prevent runaway cell death. In the present work, we set out to characterize AtHIR2, a putative AtMC1 interactor retrieved from our immunoaffinity purification screening under immune cell death conditions. Our results show that AtMC1 co-immunoprecipitates *in planta* with AtHIR2, and this interaction is not dependent of an intact catalytic site. Subcellular fractionation demonstrates that this interaction exclusively occurs in the microsomal fraction, indicating an active recruitment of AtMC1 to the plasma membrane.

Using *atmc1* and *athir2* mutants we also demonstrate genetically that both proteins are required for defense and HR triggered in *Arabidopsis* Col-0 by the avirulent bacteria *Pseudomonas syringae* pv. *tomato* (*Pto*) DC3000 (*AvrRpt2*.) Altogether these results strongly indicate that AtMC1 and AtHIR2 can be part of the same signaling pathway initiated by recognition of the *avrRpt2* effector by the NB-LRR RPS2 leading to HR and immunity. One of the early events triggered by effector recognition may be the formation of an immune complex at the membrane level, of which AtMC1 and AtHIR2 seem to constitute important components in signaling pathway as *in silico* analysis revealed interesting interactors that are involved in vesicle trafficking.

Introduction

To defeat pathogen attack plants have evolved a sophisticated signaling network that is activated by the initial perception of conserved molecules called

pathogen-associated molecular patterns (PAMPs) by means of pattern recognition receptors (PRRs). This initial perception is called pathogen-triggered immunity (PTI), which initiates a cascade of immune responses transduced via mitogen-activated protein kinases (MAPK) (Meng & Zhang, 2013) and WRKY transcription factors. When PTI response is not enough to counteract pathogen attack, plants initiate a second line of defense using intracellular receptors known as NB-LRR proteins. These proteins directly or indirectly recognize pathogen-delivered effectors, triggering the so-called effector triggered immunity (ETI). The majority of NB-LRR proteins can be divided into two subclasses: the coiled-coil (CC-NB-LRR) and Toll and interleukin-1 region (TIR) NB-LRR subclasses, depending on the nature of their N-terminal domain. In *Arabidopsis* the CC-NB-LRR proteins RPM1, and RPS2 have been well characterized (Boyes, Nam, & Dangl, 1998). RPM1 and RPS2 indirectly recognize *P. syringae* *avrRpm1* and *avrRpt2* effectors, respectively, through a common guard protein RIN4, which is a clearly different mechanism of recognition. RIN4 is phosphorylated by *avrRpm1* and this posttranscriptional modification is perceived by RPM1, whereas *avrRpt2* cleaves RIN4 and RPS2 recognizes the cleavage, initiating the machinery of defense in plants (Axtell & Staskawicz, 2003; Mackey et al., 2003; Mackey et al., 2002).

ETI involves an amplification of defense responses that often ends in a hypersensitive response (HR), a plant-specific programmed cell death (PCD) reaction that occurs locally at the site of attempted infection (Coll et al., 2011). In the last decades persistent effort has helped shedding some light into the molecular machinery regulating HR (Dickman & Fluhr, 2013; Kabbage et al., 2017). Although we are far from capturing the whole picture, the role of HR regulatory proteases has started to emerge (Balakireva & Zamyatin, 2018; Thomas & van der Hoorn, 2018). Among them, AtMC1 acts as a positive regulator of HR. (Coll et al., 2010). AtMC1 mediates positively the cell death response by the activation of RMP1 and RPP4, intracellular NB-LRR receptors (Coll et al., 2010) in this context *atmc1* mutant plants shows reduced immune response to HR mediated by RPM1 and RPP4 a CC- and TIR NB-LRR respectively, indicating the conjunction of response pathways (Coll et al., 2010). An important requirement for AtMC1 cell death function was the maintenance of catalytic integrity, essential for auto-processing, suggesting the negative regulation of AtMC1 by its own prodomain (Coll et al., 2010). AtMC1 was found to act in parallel to autophagy to control HR (Coll et al., 2014) and is negatively regulated by redox regulator AtLSD1 and the metacaspase AtMC2 (Coll et al., 2010).

To unravel further AtMC1 regulators, we used an unbiased approach consisting in immunoaffinity purification of AtMC1-containing complexes coupled to mass spectrometry under basal vs. immune cell death conditions (Figure 3) (Lema Asqui et al., 2017). The protease inhibitor AtSerp1 was retrieved as part of the AtMC1 complex under basal conditions. Functional characterization revealed that AtSerp1 physically interacted with AtMC1 via its catalytic domain in planta. Importantly, AtSerp1 blocked AtMC1 self-processing in vivo and inhibited AtMC1-mediated cell death (Lema Asqui et al., 2017).

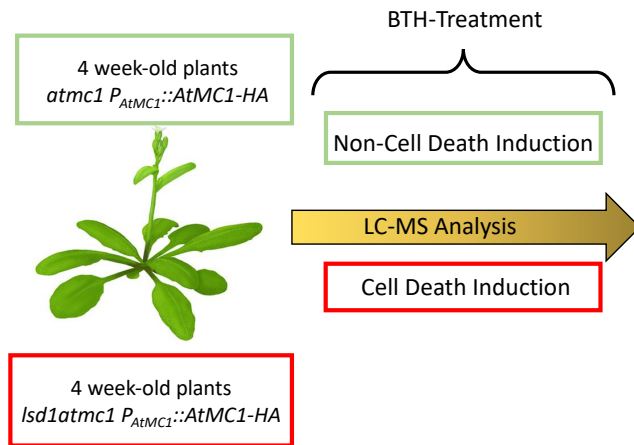


Figure 3. Schematic representation of LC/MS analysis.

Cells undergoing HR show transcriptional induction of a set of genes that were termed “hypersensitive induced reaction” (HIR) genes, which were first described in *Zea mays* (Nadimpalli et al., 2000). HIRs constitute a family of genes that encode plasma membrane-associated proteins present in different plant species, including tobacco (Karrer, Beachy, & Holt, 1998), maize (Nadimpalli et al., 2000), pepper (Jung & Hwang, 2007; Jung et al., 2008), wheat (G. Zhang et al., 2009), barley (Rostoks et al., 2003) and apple (Chen et al., 2017). HIR proteins are approximately 30 kDa in size and are proposed to be membrane associated via an N-terminal myristoylation site located in the SPFH domain, as the myristoyl group may acts as a lipid anchor to the plasma membrane (Figure 4) (Qi, Tsuda, Nguyen le, et al., 2011). In Arabidopsis the HIR family contains 4 members (AtHIR1-AtHIR4) exclusively found in plants (Di, Xu, Su, & Yuan, 2010). HIRs belong to the stomatin/prohibitin/flotillin/HflK/C (SPFH) domain-containing protein superfamily conserved in all species from

prokaryotes to eukaryotes, that contain according in silico predictions: SPFH domain, coiled coil structure that facilitates oligomerization, cholesterol recognition/interaction amino acid (CRAC/CARC) motif, and myristoylation and palmitoylation sites at the N-terminus of the SPFH domain necessary for anchoring to membranes (Daněk, Valentová, & Martinec, 2016). The SPFH domain also contributes to the formation of microdomains in different cell membranes, which constitute platforms for immune signaling processes (Browman, Hoegg, & Robbins, 2007).

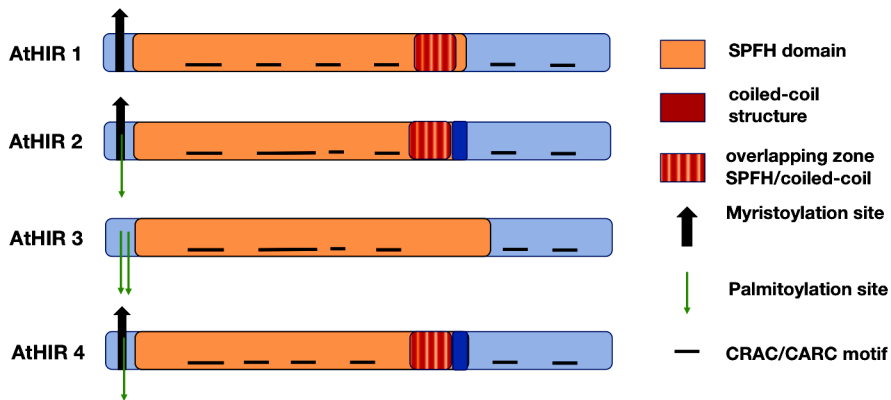


Figure 4. Schematic representation of HIR proteins. Adapted from Danek et. al., 2016.

HIR protein expression is generally increased during bacterial (F. Chen, Yuan, Li, & He, 2007; Jung & Hwang, 2007; Qi, Tsuda, Nguyen le, et al., 2011; L. Zhou et al., 2010) or fungal infection (J. P. Chen et al., 2012; Liu et al., 2013; Q. Zhou et al., 2012), but also is induced by elicitors as flg22 (Qi, Tsuda, Nguyen le, et al., 2011). Arabidopsis AtHIR1 and AtHIR2 have been shown to directly interact with RPS2 during transient expression in *N. Benthamiana* using biochemical and fluorescence approaches, however, although upon infection of *Pto* DC3000 (*avrRpt2*) only *athir2* mutant shows a clearly compromised resistance (Qi, Tsuda, Nguyen le, et al., 2011). Interestingly, AtHIR proteins are found only in the plasma membrane and not in the soluble fraction, furthermore, AtHIR1 and AtHIR2 could form homo-oligomers that are resistant to SDS, 2-mercaptoethanol, and heat (Qi, Tsuda, Nguyen le, et al., 2011). In particular, AtHIR2 has been shown to physically interact with RPS2 *in planta* (Qi, Tsuda, Nguyen le, et al., 2011) and FLS2 (Qi & Katagiri, 2012) forming a complex that activates immunity responses.

In the present work, we set out to characterize AtHIR2, a putative AtMC1 interactor retrieved from our immunoaffinity purification screening under immune cell death conditions. Our results show that AtMC1 co-immunoprecipitates *in planta* with AtHIR2, and this interaction is not dependent of an intact catalytic site. Subcellular fractionation demonstrates that this interaction exclusively occurs in the microsomal fraction, indicating an active recruitment of AtMC1 to the plasma membrane, where AtHIR2 is putatively anchored via its myristoylation site. Using *atmc1* and *athir2* mutants we also demonstrate genetically that both proteins are required for defense and HR triggered in *Arabidopsis* Col-0 by the avirulent bacteria *Pseudomonas syringae* pv. *tomato* (*Pto*) DC3000 (*AvrRpt2*.) Altogether these results strongly indicate that AtMC1 and AtHIR2 can be part of the same signaling pathway initiated by recognition of the *avrRpt2* effector by the NB-LRR RPS2 leading to HR and immunity. One of the early events triggered by effector recognition may be the formation of an immune complex at the membrane level, of which AtMC1 and AtHIR2 seem to constitute important components in signaling pathway as *in silico* analysis revealed interesting interactors that are involved in vesicle trafficking (Figure 5).

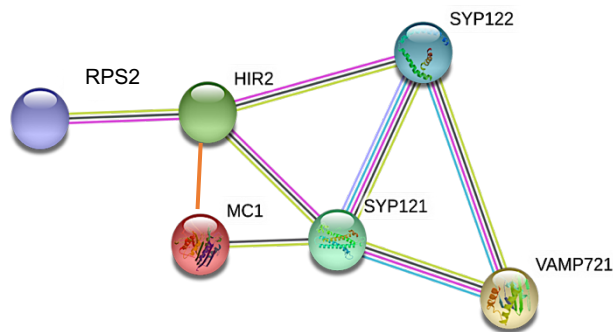


Figure 5. AtMC1-based network. AtMC1 interaction built *in silico* using a STRING, Search Tool for Retrieval of interacting Genes/Proteins, version 10. Edges represent the predicted functional links between proteins based on the following evidence, pink, experimental evidence; green, text mining; blue, co-occurrence; purple, homology; black, co-expression; orange, experimental determine in this work.

Material and Methods

Plant material and growth conditions

All experiments were performed using *Arabidopsis thaliana* (L.) Heynh. accession Col-0. Mutant *atmc1* and the transgenic *atmc1P_{AtMC1}::AtMC1-HA* and *lsd1atmc1P_{AtMC1}::AtMC1-HA* were previously described in Coll et al. (2010). Mutant *athir2* homozygous knockout line (At3g01290; SALK_124393, with an insertion in the 3 exon) was obtained from NASC stock center. *Arabidopsis* plants were grown under short-day conditions (9h light, 22°C/15 h dark, 20°C).

Nicotiana Benthamiana was grown under long-day conditions (16h light, 25°C/8h dark, 22 °C).

DNA constructs

For coimmunoprecipitation and microscopy fluorescence assays, *AtHIR2* full-length cDNA was directionally cloned into pENTR/D/TOPO Gateway vector (Invitrogen, USA) and recombined into the plant binary Gateway-compatible vector pGWB641 to obtain 35S::AtHIR2-YFP (Nakamura et al., 2010). The 35S::AtHIR2-CFP-HA version was obtained from Qi et al., 2012. The 35S::AtPIP2A-mcherry was obtained from Nahirñak et al., 2016, and the EST::AtMC1-Venus-HA construct was obtained from *AtMC1* directionally cloning into pENTR/D/TOPO Gateway vector (Invitrogen, USA) and recombined into the plant binary vector PMDC7 (Curtis & Grossniklaus, 2003). 35S::Serpin1-YFP version was described in (Lema Asqui et al., 2017).

Transient protein expression in *N. Benthamiana*

Transient *A. tumefaciens*-mediated transformation of *N. Benthamiana* leaves was performed as previously described (Lema et al., 2017; Coll et al., 2010). Briefly, whole *N. Benthamiana* leaves *ATMC1* were co-infiltrated with *A. tumefaciens* expressing different forms of *AtMC1* full length form, *AtMC1*-DN and *AtMC1*-CA previously described in Lema et al., 2017, alone or in combination with 35S::AtHIR2-YFP. *A. tumefaciens* containing the vector p19 was always co-infiltrated to minimize silencing (Voinnet, Rivas, Mestre, & Baulcombe, 2003).

Protein fractionation and co-immunoprecipitation assay

Cell fractionation to obtain soluble and microsomal protein fractions was performed according to Planas et al. (2016), with slight modifications. Essentially, 2g of frozen *N. benthamiana* leaves transiently expressing the desired constructs were ground using a mortar and pestle on fractionation buffer (2 ml/g tissue). No(Curtis & Grossniklaus, 2003) Nonidet P40 (Sigma-Aldrich, MERCK, Germany) was used instead of Triton x100. r co-immunoprecipitation, soluble and microsomal extracts were diluted to a final volume of 2 ml at a protein concentration of 2 mg/ml. Extracts were 2 mg/ml incubated with 50 μ l of magnetic beads conjugated to anti-GFP (MACS; Miltenyi Biotec, Germany), for 2h at 4°C under constant rotation. Bound proteins were eluted according to the manufacturer's instructions. Twenty-five μ g of total protein (input), and 20 μ l of the total eluate (50 μ l) were loaded onto an SDS-PAGE gel. Immunoblots were performed using a 1:5000 dilution of anti-GFP mouse monoclonal antibody (clone B-2; Santa Cruz Biotechnology, USA) or 1:5000 polyclonal anti-HA-HRP (clone 3F10; Roche, USA).

Chemical treatments

Dexamethasone (0.2 μ M) and Estradiol (10 μ M) were applied to *N. benthamiana* leaf surfaces 48 h after agro-infiltration using soaked cotton balls to induce expression of AtMC1 forms under the control of the dexamethasone promoter or estradiol promoter, respectively (Coll et al., 2010). Samples were collected 24 h later and stored at -80° C.

Bacterial growth and cell death analyses

Arabidopsis single cell death assay was done in 2-weeks old *Arabidopsis* plants by vacuum infiltration with 500,000 cfu/ml and incubated during 24 hours at room temperature. Leaves were then harvested and stained with trypan blue (Coll et al., 2014; Coll et al., 2010; Lema Asqui et al., 2017). Dip bacterial growth assay was performed following the protocol described by (Eitas, Nimchuk, & Dangl, 2008).

Results

AtHIR2 co-localizes and co-immunoprecipitates with AtMC1 in plasma membrane.

AtHIR2 was previously shown to localize at the plasma membrane (Qi, Tsuda, Nguyen, et al., 2011). To verify these data we co-expressed 35S::AtHIR2-YFP with a 35S::AtPIP2A-mCherry (Nahirnak et al., 2012; Nelson, Cai, & Nebenfuhr, 2007). As expected, AtHIR2 showed a clear co-localization with the membrane marker AtPIP2A (Figure 6).

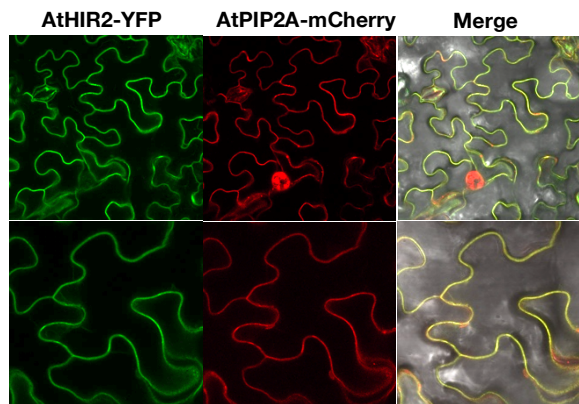


Figure 6. Co-localization of AtHIR2 and AtPIP2A proteins. Confocal Images of epidermal *N. Benthamiana* cell 48 h after *Agrobacterium* mediated transient expression. YFP, yellow fluorescent protein; mCherry, red fluorescent protein.

To determine whether AtHIR2 and AtMC1 co-localized, the fluorescently tagged versions of both proteins 35S::AtHIR2-CFP-HA and Est::AtMC1-HA-Venus, were transiently expressed in *N. benthamiana* independently or at the same time and their subcellular localization was evaluated using confocal laser scanning microscopy. As shown in figure 7 both proteins seemed to colocalize in the plasma membrane. AtMC1 was also visualized in the nucleus, which might be a consequence of venus cleavage.

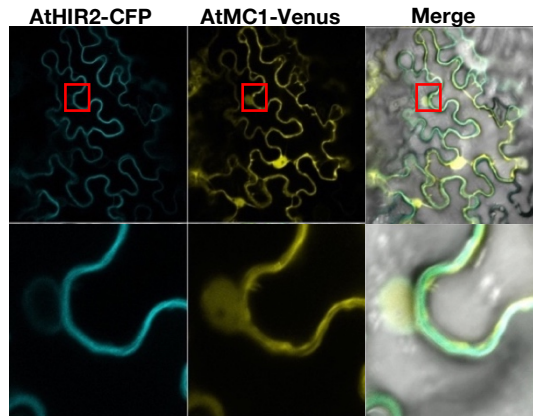


Figure 7. Co-localization of AtHIR2 and AtMC1 full length. Confocal Images of epidermal *N. benthamiana* cell 96 h after *Agrobacterium* mediated transient expression. CFP, cerulean fluorescent protein; Venus, green fluorescent protein.

To verify the putative plasma membrane co-localization of AtMC1 and AtHIR2 we subjected *N. benthamiana* leaves cells to osmotic shock as previously described (Nelson et al., 2007). Osmotic shock is known to detach the cytoplasm from the plasma membrane, helping to discriminate subcellular co-localization. We applied two different osmotic shocks: 1M NaCl for 5 min and 0,8 M Mannitol for 2 hours. After incubation, leaves were observed under the confocal microscope. The localization of AtHIR2 was not altered by either treatment, demonstrating an exclusive plasma membrane localization of the protein (Fig. 8). In contrast, osmotic shock treatments showed that AtMC1 has a bipartite localization in both the plasma membrane and at the cytoplasm. As a negative control, AtSerp1 was co-expressed with AtHIR2 under osmotic stress and AtSerp1 did exclusively express at the cytoplasm and did not co-localize with AtHIR2 (Fig. 9).

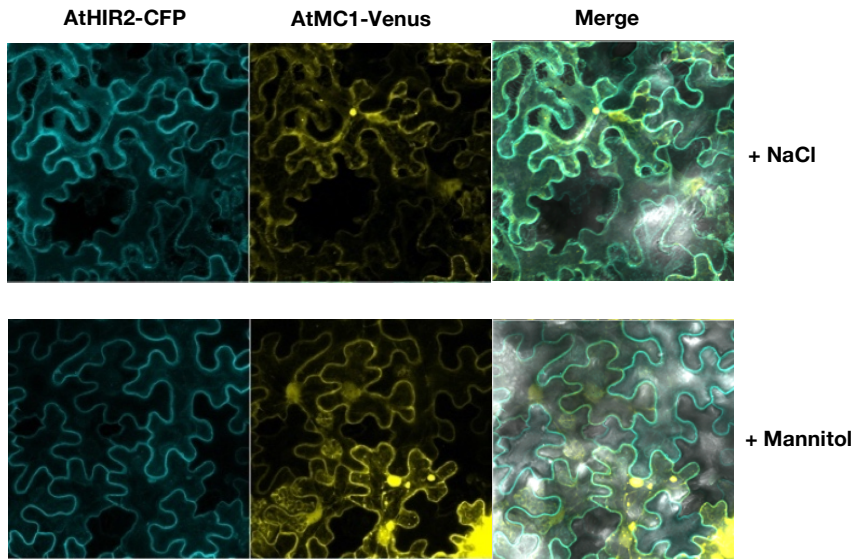


Figure 8. Co-localization of AtHIR2 and AtMC1 full length after osmotic stress treatment. Confocal Images of epidermal *N. Benthamiana* cells 96 h after Agrobacterium-mediated transient expression. CFP, cerulean fluorescent protein; Venus, green fluorescent protein.

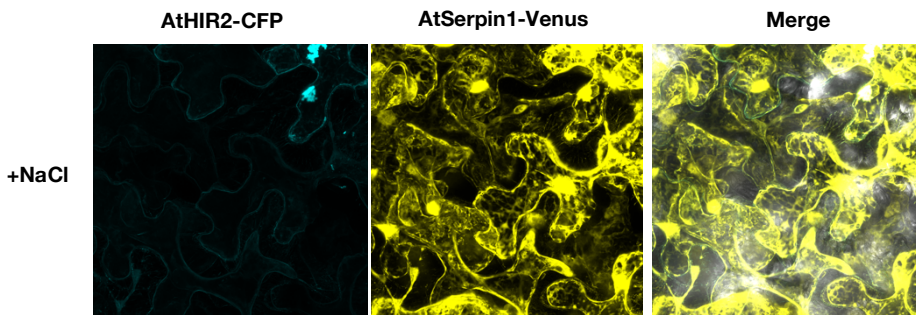


Figure 9. Co-localization of AtSerpin1 and AtMC1 full length after osmotic stress treatment. Confocal Images of epidermal *N. Benthamiana* cells 96 h after Agrobacterium-mediated transient expression. CFP, cerulean fluorescent protein; Venus, green fluorescent protein.

To further corroborate the immunoaffinity purification results that revealed AtHIR2 as part of AtMC1 complexes, we performed reverse co-immunoprecipitation experiments. For this we transiently expressed in *N. benthamiana* the different AtMC1 forms (Full-length, Δ N and CA) alone or in combination with 35S::AtHIR2-YFP. AtHIR2 was immunoprecipitated using magnetic beads coupled to GFP and co-immunoprecipitation of the different

AtMC1 forms was analyzed. Since AtHIR2 is a plasma membrane protein and AtMC1 has a dual plasma membrane/cytosol localization, the co-immunoprecipitation experiments were performed separately on soluble and microsomal protein fractions obtained from cell fractionation. Immunoblot of soluble and microsomal protein fractions (input) and the bound fractions confirmed AtMC1 and AtHIR2 co-immunoprecipitated. As expected, this co-immunoprecipitation only takes place in the microsomal fraction (Fig.10). The catalytic dead version of AtMC1 (AtMC1-CA) did not co-immunoprecipitate with AtHIR2 (Fig 10). This indicates that an intact AtMC1 catalytic site is not required for co-immunoprecipitation. To determine whether the AtMC1 N-terminal prodomain is required for the interaction with AtHIR2, we repeated the co-immunoprecipitation assays using a prodomain-less version of AtMC1 (AtMC1- Δ N-HA) (Coll et al., 2010; Lema Asqui et al., 2017). In this case results remain inconclusive, since AtMC1 Δ N co-immunoprecipitation with AtHIR2 seems unspecific (data not shown).

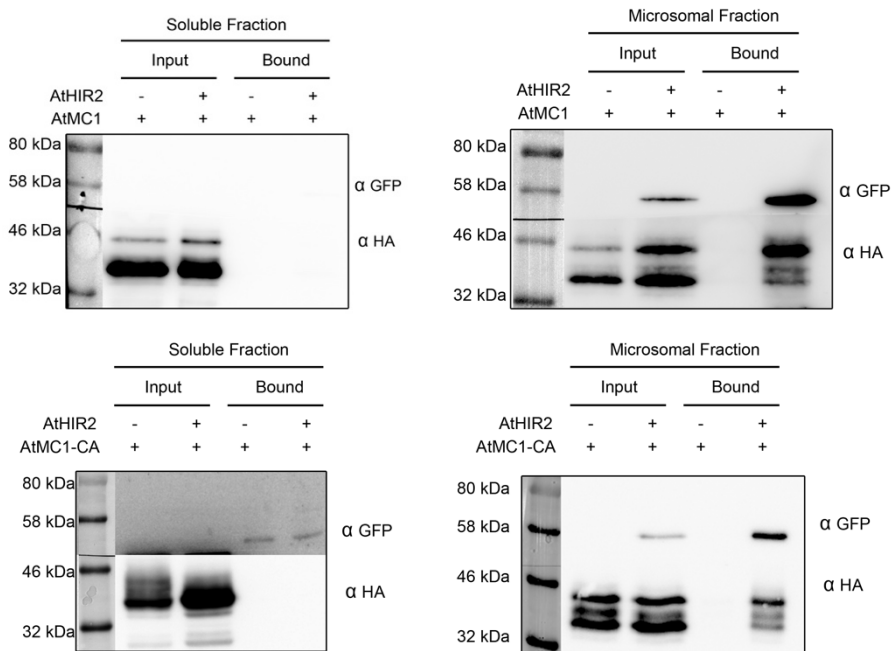


Figure 10. AtHIR2-AtMC1 co-immunoprecipitation occurs in microsomal fraction independently of mutation of the catalytic center. AtMC1 and AtMC1-CA (catalytic dead) HA tagged forms together with or without AtHIR2-YFP were transiently expressed in *N. Benthamiana* leaves. Soluble and microsomal fraction were extracted, incubated with magnetic beads coupled to green fluorescent protein (GFP), and after severe washes,

protein bounds to beads were eluted (bound). PDVF membrane was cut in two upper and lower panel and blotted against GFP or HA antibodies, respectively.

AtHIR2 and AtMC1 positively regulate HR triggered by *Pto* DC3000(*avrRpt2*).

AtHIR2 was previously shown to physically interact with RPS2 (Qi et al., 2011). RPS2 is a CC-NB-LRR that triggers ETI accompanied by an HR cell death response upon *avrRpt2* effector recognition (Hatsugai et al., 2017). It was previously shown that *athir2* mutants are hyper-susceptible to *Pto* DC3000 (*avrRpt2*), indicating that AtHIR2 is required for defense against this avirulent *Pto* strain. To address whether AtHIR2 and/or AtMC1 was required for RPS2-mediated HR we quantified HR cell death using a single cell death assay. We previously showed that AtMC1 was required for RPM1-mediated HR cell death (Coll et al., 2014; Coll et al., 2010; Lema Asqui et al., 2017). When *atmc1* mutants were infected with *Pto* DC3000(*avrRpm1*) HR cell death was induced to only half of the wild-type levels.

To quantify RPT2-mediated HR cell death we infected 2-week-old wild-type Col-0, *atmc1* and *athir2* plants with *Pto* DC3000 (*avrRpt2*). HR cell death levels were quantified according to (Asqui et al., 2017; Coll et al., 2010, 2014). As shown in Fig. 11, we observed partial suppression of RPS2-mediated HR in *atmc1*. HR levels in *atmc1* mutants are similar to those observed for RPM1-mediated HR (Coll et al., 2014; Coll et al., 2010; Lema Asqui et al., 2017) which shows a decreased levels of cell death in comparison to wild type. This indicates that AtMC1 mediates HR cell death in response to more than one CC-NB-LRR, but at differences that RPM1 mediated cell death appears at 12 hours, RPS2 shows a later cell death induction at 24 hours. Interestingly, *athir2* plants showed even lower cell death than *atmc1* mutants. This might suggest that AtHIR2 acts upstream of AtMC1 and/or regulates more signaling partners beyond AtMC1. We are currently generating *atmc1athir2* double mutant plants, which may potentially help us elucidate the positioning of AtMC1 and AtHIR2 in relation to each other in this RPT2-mediated signaling pathway.

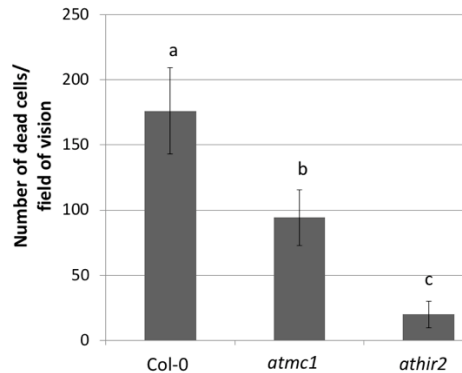


Figure 11. AtHIR2 and AtMC1 mediated cell death. Single cell death assay of specified *A. thaliana* lines. Dead cells were counted after staining with trypan blue under an optical microscope 24 after infection with 500,000 cfu/ml *Pto* DC3000 (*avrRpt2*). Values indicate the average of 20 samples per genotype. Letters indicate significant difference following post-ANOVA Tukey's honest significant test ($\alpha=0,005$). The experiment was repeated twice with similar results.

Measuring of bacterial growth in different *A. thaliana* lines upon *Pto* DC3000 *AvrRpt2* infection.

Our next goal was to determine whether the RPT2-mediated HR cell death suppression observed in *atmc1* and *athir2* mutants was coupled to alterations in bacterial growth suppression. For this, two-week old wild-type, *atmc1* and *athir2* Col-0 plants were dip-inoculated with a 500,000 cfu/ml bacterial suspension of *Pto* DC3000 (*avrRpt2*), and CFU were calculated at 0 and 3 days after inoculation. As shown in Fig. 12 absence of both AtMC1 or AtHIR2 results in increased susceptibility to *Pto* DC3000 (*avrRpt2*). This finding is extremely interesting: besides confirming previous results shown for AtHIR2 (Qi, Tsuda, Glazebrook, et al., 2011), it indicates that impartially on the recognition pathway mediated by NB-LRRs as previously described (Coll et al., 2010) for RPM1 and RPP4, where AtMC1 also regulates cell death response.

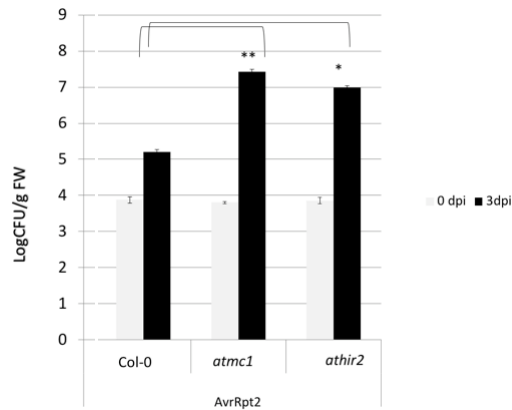


Figure 12. AtHIR2 and AtMC1 mutations compromised resistance to *Pto* DC3000 (*avrRpt2*). 2-week-old plants were vacuum-inoculated and bacterial growth was measured at 0 and 3 days post inoculation (dpi). Significant differences between Co-0 and mutants are indicated by asterisks for $\alpha=0,05$.

By the other hand, we infected above described lines with a virulent *Pto* DC3000 strain to elicit defense responses. We observed that after 3 days *athir2* mutant shows an increased susceptibility to *Pto* DC3000 empty vector at dose of 250000 cfu/ml, which suggests the involvement of AtHIR2 in basal immunity as previous was proposed by Qi et al., 2012 (Fig. 13). However, at difference of Qu results we could detect a slightly increased colonization of *Pto* DC3000 in *athir2* mutant this discrepancy between our results and Qi et al., 2011, may be due to the different *athir2* mutant lines used in this work and that T-DNA insertions are in touching different positions.

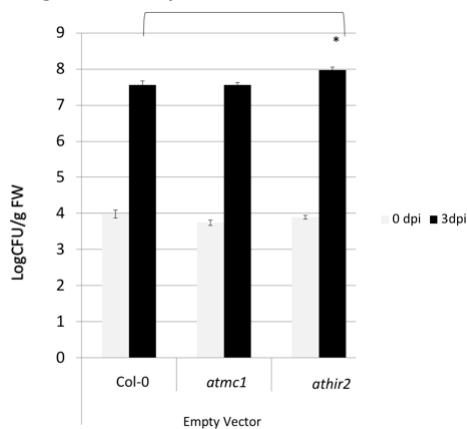


Figure 13. AtHIR2 mutations compromised resistance to *Pto* DC3000. 2-week-old plants were dip-inoculated and bacterial growth measured at 0 and 3 days post inoculation (dpi). Significant differences between Co-0 and mutants are indicated by asterisks for $\alpha=0.05$.

Discussion

AtMC1 might be recruited to the microsomal fraction by AtHIR2 in response to NB-LRR activation upon pathogen attack

For a long time, we have been speculating about the existence of a conserved function between animal inflammatory caspases (in particular caspase-1) and the plant metacaspase AtMC1 (Davis, Wen, & Ting, 2011). The main arguments were: i) presence of a prodomain containing cell death-related motifs, ii) positive regulation of immune PCD, iii) morphological similarity between plant HR and pyroptosis. However, whereas caspase-1 is recruited to supramolecular complexes upon pathogen challenged known as inflammasomes, no analogous AtMC1-containing complexes have been ever detected during pathogen-triggered PCD in plants, probably due the presence of architectural differences as was described in *Saccharomyces cerevisiae* (Wong et al., 2012) and *Trypanosoma brucei* (McLuskey et al., 2012), which may explain some of differences in the function: the crystal structure of Yeast Yca1 shows the existence of 2 two extra β -sheets, which precludes the active site avoiding the possibility of homodimerization.

Our data constitute the first *in vivo* indication in plants that AtMC1 is recruited by AtHIR2 to the plasma membrane upon pathogen challenge. This opens the possibility that indeed AtMC1-containing protein complexes are formed in response to a pathogen mediated PCD trigger. We also observed that the prodomain-less, putatively active form of AtMC1 (Coll et al., 2010) accumulates to higher levels in the soluble than in the microsomal fraction, independently of AtHIR2 co-expression. This finding indicates that AtMC1 activation may not be as important as its relocalization to the plasma membrane compartment where AtHIR2 is located. This is in fact in agreement with the idea that the prodomain is a negative regulator of AtMC1 (Coll et al., 2010) and acts as physical barrier for substrate access (McLuskey et al., 2012). These findings might be indicative of the existence of immune AtHIR2/AtMC1-containing supramolecular complexes located at the plasma membrane. However, their molecular interplay remains to be elucidated. For example, we still do not know which domains are

required for the interaction. Our data shows that an intact catalytic site in AtMC1 is not a pre-requisite for interaction with AtHIR2. This indicates that AtHIR2 might act as a positive regulator of AtMC1, but the interaction does not interrupt the AtMC1 self-cleavage of AtMC1. In addition, we were able to determine that AtHIR2 interacts only with the full-length form of AtMC1, which would suggest that AtHIR2 may act upstream of AtMC1 subsequent self-cleavage and activation.

AtMC1 and AtHIR2 positively regulate RPT2-mediated HR in response to *Pto* DC3000 (*avrRpt2*) infection

We previously demonstrated that AtMC1 is a positive regulator of HR in response to RPM1 activation via *Pto* DC3000 (*avrRpm1*) infection, and that this cell death activity is uncoupled from inhibition of pathogen growth (Coll et al., 2014; Coll et al., 2010; Lema Asqui et al., 2017). In contrast, AtMC1 regulates both defense and HR in response to the RPT2 activation triggered by *Pto* DC3000 (*avrRpt2*) infection. This fact may be due to the existence of common signaling machinery for flg22 and *avrRpt2* perception but having different uses (Hatsugai et al., 2017; Tsuda, Sato, Stoddard, Glazebrook, & Katagiri, 2009). Which is in agreement with the appearance of later cell death phenotype mediated by RPS2, whereas in our conditions the cell death phenotype was only possible to visualize after 24 hours.

Both *atmc1* and *athir2* mutants show reduced cell death levels in response to *Pto* DC3000 (*avrRpt2*) infection, being lower in *athir2* than in *atmc1* mutants. This could indicate that AtHIR2 acts upstream of AtMC1 or has more than one signaling partner beyond AtMC1 to cause HR cell death. Single cell death assays using the double *atmc1 athir2* mutant will help us genetically position these two regulators in the HR cell death pathway.

Our results also show that both AtMC1 and AtHIR2 are positive regulators of PTI. *atmc1* and *athir2* mutant plants show hyper-susceptibility to the virulent *Pto* DC3000 (EV) strain. In the case of AtHIR2, this corroborates previous findings suggesting a dual role of AtHIR2 in PTI and ETI (Qi & Katagiri, 2012; Qi, Tsuda, Glazebrook, & Katagiri, 2011; Qi, Tsuda, Nguyen le, et al., 2011).

There is still a lot of work to be done to acquire a complete picture of the functional interplay between AtMC1 and AtHIR2. However, our findings might put us to a path leading to a better understanding of the molecular events

regulating pathogen-triggered cell death. This is of major significance because until this moment a clear pathogen triggered cell death signaling cascade has not been described in plants, in contrast to the extensively studied immune cell death in animals (Davis et al., 2011). It is of special interest the observed recruitment of AtMC1 to the plasma membrane, as it is the site of initial complex assembly upon pathogen perception (Axtell & Staskawicz, 2003; Qi, Tsuda, Nguyen le, et al., 2011). This is particularly intriguing at a time where the strict definitional boundaries of PTI and ETI are becoming blurred (Thomma, Nürnberger, & Joosten, 2011). Besides this, it remains to be elucidated whether AtMC1 self-cleavage and activation of its protease activity is relevant for cell death signaling, how are AtMC1 and AtHIR2 recruited to the plasma membrane and whether there are other partners in the plasma membrane-associated cell death complex.

DISCUSSION

General discussion

A different mode of action to control and activate the hypersensitive response in plants via AtMC1.

Maintaining homeostasis inside the cell is a complex and energy-consuming process essentially for plant fitness. Due to their static nature, plants have developed the ability to rapidly and efficiently react to a changing environment. At the same time, plant sessility makes them an easy target for attack by multiple pathogens.

AtMC1 and the animal inflammatory caspase-1 seem to share some functional similarities (Coll et al., 2011), namely that they are both positive regulators of cell death induced upon immune receptor activation; and both are negatively regulated by an inactive member of their own family (caspase-11 in the case of caspase-1 and AtMC2 in the case of AtMC1) (Coll et al., 2011). Although, in animals the immune receptor activation results as consequence of homodimerization of inactive caspases forming inflammasomes structures. In plants, as metacaspases do not form oligomers due their own structure (McLuskey et al., 2012; Wong et al., 2012), the existence of structures similar to inflammasomes may not be possible. However, with the evidence presented in this work of coexistence of full length form and processed form, may render the formation of inflammasomes not necessary, as AtMC1 negative regulators upon pathogen infection can stop to control the AtMC1 production.

The necessity of plants to be prepared against potential pathogen attacks can be underscored by the stable expression over time of AtMC1 in different stages of development and in almost all tissues (Lam & Zhang, 2012). Mechanisms to prevent its activation under basal conditions must be in place to avoid unrestrained cell death propagation. Two negative regulators of AtMC1 function were identified earlier: AtMC2 and AtLSD1 (Coll et al., 2010).

Negative regulation as a fate-controller of AtMC1 determine its activation and degradation.

In this work, we have disclosed a novel negative regulator of AtMC1: the protease inhibitor AtSerpin1, which blocks AtMC1 autocatalytic activity *in planta* and prevent AtMC1-mediated cell death, to avoid spread to neighbored

cells. The Arabidopsis genome encodes 8 serpin genes (Fluhr, Lampl, & Roberts, 2012), among them, the most abundant and best characterized is AtSerpin1. The *in vitro* proteolytic activities of two type II metacaspases, AtMC4 and AtMC9, were shown to be inhibited by AtSerpin1 (Vercammen et al., 2004). In turn, AtMC9 was demonstrated to cleave AtSerpin1 *in vitro* at the predicted cleavage site (reactive center loop) in a dose-dependent manner (Vercammen et al., 2006). Our *in vivo* data indicate that AtMC1 might also be able to cleave AtSerpin1 through its reactive center loop, as the size of two fragments generated would be in agreement with the corresponding prediction, which reinforces the idea of AtSerpin1 as target substrates of metacaspases. In this work we demonstrated inhibition of AtMC1 by AtSerpin1 *in vivo*, using a transient expressed system. This inhibition was monitored as loss of self-processing of AtMC1 when co-expressed with AtSerpin1. Unfortunately, we have so far not been able to directly measure AtMC1 proteolytic activity, and thus we have not been able to precisely quantify the effect of AtSerpin1 on it.

We also observed that AtMC1-CA was partly degraded by the proteasome and coexpression with AtSerpin1 dramatically impaired AtMC1-CA proteasomal degradation. AtMC1-CA is more prone to aggregation than its wild-type counterpart (Coll et al., 2014). Since cells have evolved different surveillance mechanisms to detect and eliminate potentially toxic protein aggregates, it is not surprising that at least part of the AtMC1-CA pool is delivered to the proteasome for degradation. The fact that AtSerpin1 co-expression enhances AtMC1-CA proteasome-mediated degradation could indicate that AtSerpin1 might interact and/or induce a conformational change in AtMC1-CA facilitating its elimination via the proteasome. This mode of action is reminiscent of the mechanism in animals where Serpin1-Z is degraded by proteasome and autophagy via complex formation (Feng et al., 2017).

AtMC1 and AtSerpin1 colocalize and co-immunoprecipitate, indicating a possible interaction between the two proteins. The prodomain is not required for the interaction between AtMC1 and AtSerpin1, in contrast to the previously reported AtMC1-LSD1 co-immunoprecipitation (Coll et al., 2010). The interaction between AtMC1- Δ N and AtSerpin1 was weaker than with the full-length version of AtMC1, indicating a less stable interaction when the AtMC1 prodomain was missing. This might be explained by the fast cell death induction by AtMC1- Δ N, which makes it difficult to catch the exact moment of potential interaction.

An intact AtMC1 catalytic center was required for the co-immunoprecipitation. This was presumably not the case for AtMC9-AtSerp1 interaction, as a catalytic-dead version of AtMC9 was used as a bait for AtSerp1 identification in the yeast two-hybrid assay (Vercammen et al., 2006). The apparent discrepancy of the two observations might be explained by a weaker affinity between AtSerp1 and catalytic-dead metacaspase mutants but may also due the differences in the linker structure of type II metacaspases, as showed in caspases that p20 and p10 domains can be cleaved for activation, although is not clear if the case for metacaspases. In our experiment potentially, weak interactions are probably eliminated by the stringent washes of a co-immunoprecipitation.

A conserved inhibitor function over proteases.

Proteases are ubiquitous in all organisms and constitute as significant percentage of whole genome. They are quite important for a plethora of biological processes such as digestion, blood clotting, host defenses among others (Puente, Sanchez, Overall, & Lopez-Otin, 2003; Tripathi & Sowdhamini, 2006). Proteases activation is an irreversible event that must be tightly controlled to avoid a disorder in the homeostatic balance (Farady & Craik, 2010). AtSerp1 is an inhibitor of cell death proteases that covalently binds and modulates the activity of the cell death protease RD21 (Lampl, Alkan, Davydov, & Fluhr, 2013; Lampl et al., 2010). In this work was determined that AtSerp1 forms a non-canonical complex with AtMC1, detected under non-reducing conditions. This discrepancy between the mode of interaction between different metacaspases and AtSerp1 could be a result of the different mode of action of AtMC1 and 9, their localization (subcellular and tissular) and the processes in which they are involved, but also dependent difference of it structural configuration, and the fact that in type ii metacaspases the absence of prodomain facilitates the interaction.

Interestingly, the interplay between AtMC1 and AtSerp1 seem to involve the full-length rather than the cleaved versions of the proteins. Although AtMC1 may be able to cleave AtSerp1 at reactive center loop as previously was shown by Vercammen et al., 2016 for metacaspase 9, the size of the complex detected, as well as the co-immunoprecipitated fragments indicate a non-canonical mode of action. The fact that AtMC1

catalytic activity is required for the interaction with AtSerp1 could suggest the involvement of a third partner that needs to be cleaved in order for the inhibition to take place or undetectable modifications of AtMC1 and/or AtSerp1, or maybe that serpins undergo reversible and irreversible conformational changes regulating their activity can be a good explanation.

Overexpression of AtSerp1 or a mutation in the protease RD21 led to reduced cell death after infection with the necrotrophic fungi *Botrytis cinerea* and *Sclerotinia sclerotiorum* but enhanced cell death in response to the hemibiotrophic fungus *Colletotrichum higginsianum* (Lampl et al., 2013). In our conditions, infection with *Pto* DC3000 (*avrRpm1*), a hemibiotrophic bacterium that causes HR in *A. thaliana* Col-0 background via the RPM1 receptor, resulted in decreased cell death in plants overexpressing AtSerp1, comparable to *atmc1* mutants. Double *atmc1 atserpin1* mutants displayed an intermediate phenotype between wild-type and *atmc1* plants, which indicates that AtMC1 is negatively regulated by AtSerp1 and also that *atserpin1* may control other proteases involved in this cell death process beyond *atmc1*. Whether AtSerp1 inhibits AtMC1-regulated processes by directly interacting with AtMC1 or indirectly by modulating the activity of downstream proteases induced by AtMC1 remains an open question. Inhibition of AtMC1-mediated cell death by AtSerp1 is also demonstrated by the dramatic effect of AtSerp1 when transiently coexpressed with death-inducing forms of AtMC1 in *N. benthamiana* leaves. Discrepancy of results between *C. higginsianum* (Lampl et al., 2013) and *Pto* DC3000 (*avrRpm1*), may be explained by the fact that, despite both being hemibiotrophs, their lifestyle, time and mode of infection are radically different and thus it is difficult to compare cell death outcomes at a given time point.

Inhibition of different cell death proteases by AtSerp1 positions it as a conceivable guardian of cell homeostasis, preventing uncontrolled proteolysis of potentially dangerous proteins as AtMC1. The balance between the levels of AtSerp1 and the levels of potentially active death proteases might be a powerful modulator of cell fate. Under normal conditions, molecule-by-molecule inactivation may serve as an effective surveillance mechanism that prevents uncontrolled cell death.

It is also pointed out that AtMC1-activity requires many negative regulators to control 1) unrelated proteolysis as the case of AtMC2 and ATLS1, but also 2) to regulate his activity by AtMC1. All together our

results constitute a bigger contribution to understand cell death control in plants. But also, are of major evolutionary significance as they indicated a conserved function between metacaspases and caspases.

A step towards the elucidation of the HR cell death pathway ignited upon NB-LRR activation by pathogen recognition

In animals, the caspase-1-dependent immune cell death response is very well characterized (Davis et al., 2011). Activation of the caspase-1 depends on the assembly of complexes called inflammasomes and constitute the first line of immune response to cell stress, where upon immune receptor activation full-length versions of caspase-1 are recruited to be activated by releasing p20 and p10 subunit (Davis et al., 2011; Ogura, Sutterwala, & Flavell, 2006). In plants similar structures are absent, due to the marked difference in architecture of metacaspases (McLuskey et al., 2012; Wong et al., 2012). Although preliminary, our data may shed some light into the signaling cascade ignited upon immune receptor activation that leads to HR cell death, activating metacaspase 1.

In this work we confirmed the plasma membrane localization of AtHIR2 co-expressing together with a plasma membrane marker AtPIP2A, AtHIR2 showed a well-defined plasma membrane localization independently of cloning system that have been using, although we were not able to define a punctate localization as previously reported by (Choi et al., 2011; Lv et al., 2017), this not differ with the idea of microdomain formations and implication in stress responses (Ishikawa et al., 2015; Strehmel et al., 2017), as maybe due to low resolution conditions.

Our data raises several very interesting questions: for example, how is AtMC1 recruited to the membrane to form a complex with AtHIR2? Are AtMC1 and AtHIR2 part of a trafficking complex specifically involved in immune response? Interestingly, AtHIR2 was found to be associated with QaSNARE proteins AtSYP121 and AtSYP122, which might indicate that AtHIR2 is trafficked to the membrane via a particular vesicular transport regulated by these SYPs (Fujiwara et al., 2014). In the future we plan to perform experiments to test this hypothesis.

Our data shows that the lack of AtHIR2 results in increased susceptibility. In contrast, previous experiments performed by the Katagiri lab (Qi et al, 2011) did not show any difference in defense between wild-type and *athir2* mutant. This discrepancy might be the result of experimental differences, for instance, we used young 2-week-old plants, whereas Qi et al, 2011 used 4 weeks. The observed increased susceptibility to *Pto* DC3000 (EV) could indicate that AtHIR2 can be involved in a pathogen recognition complex during PTI response.

Another interesting observation was that mutation of either AtHIR2 or AtMC1 compromised the RPS2-mediated HR triggered by *avrRpt2* effector recognition. To the already existed evidence of AtMC1 HR triggered compromised in the case of RPM1 and RPP4, TIR and CC NB-LRR, respectively (Coll et al.,2010). Our data suggest that the lack of *atmc1* result in an evident decreased of cell death levels. The discrepancy in pathogen growth between RPM1 and RPS2 mediated pathways, may explain by the differences in the timing of HR signaling, also because AvrRpt2- HR and AvrRpm1-HR use different signaling machineries. One clear difference between AvrRpt2-HR and AvrRpm1-HR is that AvrRpm1- HR is much faster than AvrRpt2-HR when the effectors are delivered from *Pseudomonas syringae*.

All together these results can be summarized in our working model (Fig, 14) in which we suggest that the control of AtMC1 by negative regulators seems imperative under basal conditions. Pathogen challenge may disrupt this negative regulation of AtMC1 to allow its recruitment to the membrane to AtHIR2-containing complexes and perhaps activation of its protease activity. We hope that with this work we have contributed to a better understanding about the tight and complex regulation of AtMC1-mediated HR.

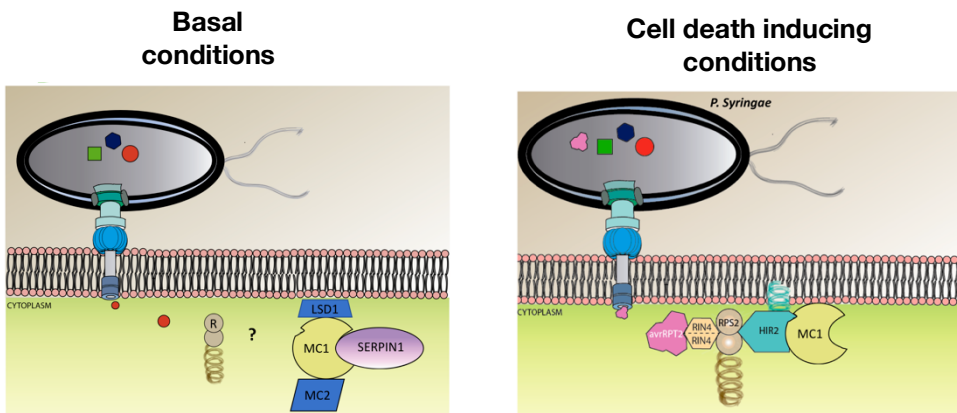


Figure 14. Metacaspase AtMC1 dual-model. Left panel AtMC1 is inhibited by negative regulators under basal conditions. Right panel positively regulates HR cell death mediated by RPS2 recognition of the invading pathogen.

CONCLUSIONS

Conclusions

1. AtSerp1 is negative regulator of AtMC1 mediating cell death and blocking self-processing *in planta*
2. AtSerp1-AtMC1 interaction requires an intact catalytic site.
3. AtSerp1 controls the degradation of AtMC1 in a non-canonical manner, improving the degradation of AtMC1 catalytic dead form through proteasome pathway.
4. AtSerp1 inhibits AtMC1-mediated cell death, but also may control other proteases beyond AtMC1.
5. AtSerp1 shows a conserved inhibitor function in other kingdoms and biological processes.
6. AtHIR2 is partner interactor of AtMC1-mediated cell death regulator.
7. AtHIR2 and AtMC1 co-immunoprecipitates and co-localizes in the plasma membrane and microsomal fraction, respectively.
8. AtMC1 mediates cell death via *avrRpt2* recognition.
9. AtMC1 and AtHIR2 seem to be a part of a trafficking complex specifically involved in immune response.

SUMMARY

Summary in English

The hypersensitive response (HR) is a paradigmatic type of programmed cell death, that occurs in response to pathogen recognition at the site of attempted invasion. Notwithstanding more than a century of research on HR, many are the aspects that are still unknown about how it is so tightly regulated and how it can be contained spatially to a few cells. The hypersensitive response in the *Arabidopsis thaliana* is controlled by type I metacaspase AtMC1 which is a positive regulator of pathogen-triggered PCD and autophagy, and that negative regulation of AtMC1 by AtLSD1 or AtMC2 can prevent runaway cell death. However, it remains unclear how the cell death signaling is activated after pathogen attack and whether additional HR negative regulators exist to control the AtMC1 activity.

In our lab was set upping an unbiased approach to identify new AtMC1 regulators based in an immunoaffinity purification of AtMC1-containing complexes coupled to mass spectrometry. The use of this approach has allowed us to identify new regulators of AtMC1 activity, in basal versus cell death inducing conditions.

In the context of the second objective we were able to revealed that in basal conditions AtSerp1 acts *in vivo* as an inhibitor of AtMC1-mediated cell death and autocatalytic processing in plants, emerging as a new inhibitor of cell death proteases in plants. Indicating a conserved function of a protease inhibitor on cell death regulators across different kingdoms.

The third part of this work continued with the characterization of AtHIR2 as positive regulator under cell death inducing conditions. We set out to characterize AtHIR2, a putative AtMC1 interactor retrieved from our immunoaffinity purification screening. Our results show that AtMC1 co-immunoprecipitates *in planta* with AtHIR2, and this interaction is not dependent of an intact catalytic site. Subcellular fractionation demonstrates that this interaction exclusively occurs in the microsomal fraction, indicating an active recruitment of AtMC1 to the plasma membrane.

Taken together all these results, we expected to contribute into elucidation of the regulation of Hypersensitive Response and the complex machinery that allows to cells make fate vital decisions to defense against pathogens. Our

results will contribute on future approaches to developed new strategies in the fight against plant pathogens diseases in crops.

Resumen en español

La respuesta hipersensible (RH) es un tipo paradigmático de muerte celular programada, que ocurre en respuesta al reconocimiento de patógenos en el sitio del intento de invasión. A pesar de más de un siglo de investigación sobre RH, muchos son los aspectos que aún se desconocen acerca de cómo está tan fuertemente regulada y cómo puede ser contenida espacialmente a solo unas pocas células. La respuesta hipersensible en *Arabidopsis thaliana* está controlada por la metacaspasa tipo I (AtMC1), que es un regulador positivo de la muerte celular programada desencadenada por patógenos y la autofagia, donde la regulación negativa de AtMC1 por AtLSD1 o AtMC2 puede prevenir la muerte celular incontrolada. Sin embargo, aún no está claro cómo se activa la señalización de muerte celular después de un ataque de patógenos y si existen reguladores negativos de RH adicionales para controlar la actividad del AtMC1.

En nuestro laboratorio se estableció un enfoque imparcial para identificar nuevos reguladores AtMC1 basados en una purificación de inmunoafinidad de complejos que contienen AtMC1 acoplados a la espectrometría de masas. El uso de este enfoque nos ha permitido identificar nuevos reguladores de la actividad de AtMC1, en condiciones basales versus condiciones de inducción de muerte celular.

En el contexto del segundo objetivo pudimos revelar que en condiciones basales AtSerp1 actúa *in vivo* como un inhibidor de la muerte celular mediada por AtMC1 y del procesamiento auto-catalítico en plantas, emergiendo como un nuevo inhibidor de proteasas de muerte celular en plantas. Indicando una función conservada de un inhibidor de proteasa en reguladores de muerte celular a través de diferentes reinos.

La tercera parte de este trabajo continuó con la caracterización de AtHIR2 como regulador positivo bajo condiciones inducidas de muerte celular. Nos propusimos caracterizar AtHIR2, un interactor putativo de AtMC1 recuperado de nuestro análisis de purificación de inmunoafinidad. Nuestros resultados muestran que AtMC1 co-inmunoprecipita en planta con AtHIR2, y esta interacción no depende de un sitio catalítico intacto. El fraccionamiento sub celular demuestra que esta interacción ocurre exclusivamente en la fracción

microsomal, lo que indica un reclutamiento activo de AtMC1 a la membrana plasmática.

Tomados en conjunto todos estos resultados, esperamos contribuir en la elucidación de la regulación de la Respuesta Hipersensible y la compleja maquinaria que permite a las células tomar decisiones vitales para la defensa contra los patógenos. Nuestros resultados contribuirán a futuros enfoques para desarrollar nuevas estrategias en la lucha contra las enfermedades de los patógenos de las plantas en los cultivos.

BIBLIOGRAPHY

Bibliography

- Ausubel, F. M. (2005). Are innate immune signaling pathways in plants and animals conserved? *Nat Immunol*, 6(10), 973-979. doi:10.1038/ni1253
- Axtell, M. J., & Staskawicz, B. J. (2003). Initiation of RPS2-Specified Disease Resistance in Arabidopsis Is Coupled to the AvrRpt2-Directed Elimination of RIN4. *Cell*, 112(3), 369-377. doi:10.1016/s0092-8674(03)00036-9
- Balakireva, A. V., & Zamyatnin, A. A. (2018). Indispensable Role of Proteases in Plant Innate Immunity. *Int J Mol Sci*, 19(2), 629. doi:10.3390/ijms19020629
- Bendahmane, A., Kanyuka, K., & Baulcombe, D. C. (1999). The Rx gene from potato controls separate virus resistance and cell death responses. *Plant Cell*, 11(5), 781-792. doi:10.1105/tpc.11.5.781
- Bent, A. F., Kunkel, B. N., Dahlbeck, D., Brown, K. L., Schmidt, R., Giraudat, J., . . . Staskawicz, B. J. (1994). RPS2 of Arabidopsis thaliana: a leucine-rich repeat class of plant disease resistance genes. *Science*, 265(5180), 1856-1860. doi:10.1126/science.8091210
- Bisgrove, S. R., Simonich, M. T., Smith, N. M., Sattler, A., & Innes, R. W. (1994). A disease resistance gene in Arabidopsis with specificity for two different pathogen avirulence genes. *Plant Cell*, 6(7), 927-933. doi:10.1105/tpc.6.7.927
- Block, A., Li, G., Fu, Z. Q., & Alfano, J. R. (2008). Phytopathogen type III effector weaponry and their plant targets. *Curr Opin Plant Biol*, 11(4), 396-403. doi:10.1016/j.pbi.2008.06.007
- Bollhoner, B., Zhang, B., Stael, S., Denance, N., Overmyer, K., Goffner, D., . . . Tuominen, H. (2013). Post mortem function of AtMC9 in xylem vessel elements. *New Phytol*, 200(2), 498-510. doi:10.1111/nph.12387
- Boyes, D. C., Nam, J., & Dangl, J. L. (1998). The Arabidopsis thaliana RPM1 disease resistance gene product is a peripheral plasma membrane protein that is degraded coincident with the hypersensitive response. *Proceedings of the National Academy of Sciences*, 95(26), 15849-15854. doi:10.1073/pnas.95.26.15849
- Browman, D. T., Hoegg, M. B., & Robbins, S. M. (2007). The SPFH domain-containing proteins: more than lipid raft markers. *Trends Cell Biol*, 17(8), 394-402. doi:10.1016/j.tcb.2007.06.005

- Burkinshaw, B. J., & Strynadka, N. C. (2014). Assembly and structure of the T3SS. *Biochim Biophys Acta*, 1843(8), 1649-1663. doi:10.1016/j.bbamcr.2014.01.035
- Carmona-Gutierrez, D., Frohlich, K. U., Kroemer, G., & Madeo, F. (2010). Metacaspases are caspases. Doubt no more. *Cell Death Differ*, 17(3), 377-378. doi:10.1038/cdd.2009.198
- Chen, F., Yuan, Y., Li, Q., & He, Z. (2007). Proteomic analysis of rice plasma membrane reveals proteins involved in early defense response to bacterial blight. *PROTEOMICS*, 7(9), 1529-1539. doi:10.1002/pmic.200500765
- Chen, J. P., Yu, X. M., Zhao, W. Q., Li, X., Meng, T., Liu, F., . . . Liu, D. Q. (2012). Temporal and tissue-specific expression of wheat TaHIR2 gene and resistant role of recombinant protein during interactions between wheat and leaf rust pathogen. *Physiological and Molecular Plant Pathology*, 79, 64-70. doi:10.1016/j.pmpp.2012.05.001
- Chichkova, N. V., Kim, S. H., Titova, E. S., Kalkum, M., Morozov, V. S., Rubtsov, Y. P., . . . Vartapetian, A. B. (2004). A plant caspase-like protease activated during the hypersensitive response. *Plant Cell*, 16(1), 157-171. doi:10.1105/tpc.017889
- Chinchilla, D., Bauer, Z., Regenass, M., Boller, T., & Felix, G. (2006). The Arabidopsis receptor kinase FLS2 binds flg22 and determines the specificity of flagellin perception. *Plant Cell*, 18(2), 465-476. doi:10.1105/tpc.105.036574
- Choi, C. J., & Berges, J. A. (2013). New types of metacaspases in phytoplankton reveal diverse origins of cell death proteases. *Cell Death Dis*, 4, e490. doi:10.1038/cddis.2013.21
- Coburn, B., Sekirov, I., & Finlay, B. B. (2007). Type III secretion systems and disease. *Clin Microbiol Rev*, 20(4), 535-549. doi:10.1128/CMR.00013-07
- Coll, N. S., Epple, P., & Dangl, J. L. (2011). Programmed cell death in the plant immune system. *Cell Death Differ*, 18(8), 1247-1256. doi:10.1038/cdd.2011.37
- Coll, N. S., Smidler, A., Puigvert, M., Popa, C., Valls, M., & Dangl, J. L. (2014). The plant metacaspase AtMC1 in pathogen-triggered programmed cell death and aging: functional linkage with autophagy. *Cell Death Differ*, 21(9), 1399-1408. doi:10.1038/cdd.2014.50
- Coll, N. S., Vercammen, D., Smidler, A., Clover, C., Van Breusegem, F., Dangl, J. L., & Epple, P. (2010). Arabidopsis type I metacaspases control cell death. *Science*, 330(6009), 1393-1397. doi:10.1126/science.1194980

- Cui, H., Tsuda, K., & Parker, J. E. (2015). Effector-triggered immunity: from pathogen perception to robust defense. *Annu Rev Plant Biol*, 66(1), 487-511. doi:10.1146/annurev-arplant-050213-040012
- Curtis, M. D., & Grossniklaus, U. (2003). A gateway cloning vector set for high-throughput functional analysis of genes in planta. *Plant Physiol*, 133(2), 462-469. doi:10.1104/pp.103.027979
- Daněš, M., Valentová, O., & Martinec, J. (2016). Flotillins, Erlins, and HIRs: From Animal Base Camp to Plant New Horizons. *Critical Reviews in Plant Sciences*, 35(4), 191-214. doi:10.1080/07352689.2016.1249690
- Daneva, A., Gao, Z., Van Durme, M., & Nowack, M. K. (2016). Functions and Regulation of Programmed Cell Death in Plant Development. *Annu Rev Cell Dev Biol*, 32(1), 441-468. doi:10.1146/annurev-cellbio-111315-124915
- Dangl, J. L., & Jones, J. D. (2001). Plant pathogens and integrated defence responses to infection. *Nature*, 411(6839), 826-833. doi:10.1038/35081161
- Dangl, J. L., Ritter, C., Gibbon, M. J., Mur, L. A., Wood, J. R., Goss, S., . . . Vivian, A. (1992). Functional homologs of the Arabidopsis RPM1 disease resistance gene in bean and pea. *Plant Cell*, 4(11), 1359-1369. doi:10.1105/tpc.4.11.1359
- Davis, B. K., Wen, H., & Ting, J. P. (2011). The inflammasome NLRs in immunity, inflammation, and associated diseases. *Annu Rev Immunol*, 29, 707-735. doi:10.1146/annurev-immunol-031210-101405
- de Torres, M., Mansfield, J. W., Grabov, N., Brown, I. R., Ammouneh, H., Tsiamis, G., . . . Boch, J. (2006). Pseudomonas syringae effector AvrPtoB suppresses basal defence in Arabidopsis. *Plant J*, 47(3), 368-382. doi:10.1111/j.1365-313X.2006.02798.x
- DeYoung, B. J., & Innes, R. W. (2006). Plant NBS-LRR proteins in pathogen sensing and host defense. *Nat Immunol*, 7(12), 1243-1249. doi:10.1038/ni1410
- Di, C., Xu, W., Su, Z., & Yuan, J. S. (2010). Comparative genome analysis of PHB gene family reveals deep evolutionary origins and diverse gene function. *BMC bioinformatics*, 11 Suppl 6, S22. doi:10.1186/1471-2105-11-S6-S22
- Dickman, M. B., & Fluhr, R. (2013). Centrality of host cell death in plant-microbe interactions. *Annu Rev Phytopathol*, 51(1), 543-570. doi:10.1146/annurev-phyto-081211-173027

- Dietrich, R. A., Delaney, T. P., Uknes, S. J., Ward, E. R., Ryals, J. A., & Dangl, J. L. (1994). Arabidopsis mutants simulating disease resistance response. *Cell*, *77*(4), 565-577.
- Dodds, P. N., & Rathjen, J. P. (2010). Plant immunity: towards an integrated view of plant-pathogen interactions. *Nat Rev Genet*, *11*(8), 539-548. doi:10.1038/nrg2812
- Dodson, G., & Wlodawer, A. (1998). Catalytic triads and their relatives. *Trends in biochemical sciences*, *23*(9), 347-352.
- Durrant, W. E., & Dong, X. (2004). Systemic acquired resistance. *Annu Rev Phytopathol*, *42*(1), 185-209. doi:10.1146/annurev.phyto.42.040803.140421
- Eitas, T. K., Nimchuk, Z. L., & Dangl, J. L. (2008). Arabidopsis TAO1 is a TIR-NB-LRR protein that contributes to disease resistance induced by the *Pseudomonas syringae* effector AvrB. *Proc Natl Acad Sci U S A*, *105*(17), 6475-6480. doi:10.1073/pnas.0802157105
- Elmore, J. M., Lin, Z. J., & Coaker, G. (2011). Plant NB-LRR signaling: upstreams and downstreams. *Curr Opin Plant Biol*, *14*(4), 365-371. doi:10.1016/j.pbi.2011.03.011
- Farady, C. J., & Craik, C. S. (2010). Mechanisms of macromolecular protease inhibitors. *ChemBiochem*, *11*(17), 2341-2346. doi:10.1002/cbic.201000442
- Feng, L., Zhang, J., Zhu, N., Ding, Q., Zhang, X., Yu, J., . . . Shen, Y. (2017). Ubiquitin ligase SYVN1/HRD1 facilitates degradation of the SERPINA1 Z variant/alpha-1-antitrypsin Z variant via SQSTM1/p62-dependent selective autophagy. *Autophagy*, *13*(4), 686-702. doi:10.1080/15548627.2017.1280207
- Flor, H. H. (1971). Current Status of the Gene-For-Gene Concept. *Annual review of phytopathology*, *9*(1), 275-296. doi:10.1146/annurev.py.09.090171.001423
- Fluhr, R., Lampl, N., & Roberts, T. H. (2012). Serpin protease inhibitors in plant biology. *Physiol Plant*, *145*(1), 95-102. doi:10.1111/j.1399-3054.2011.01540.x
- Fujiwara, M., Uemura, T., Ebine, K., Nishimori, Y., Ueda, T., Nakano, A., . . . Fukao, Y. (2014). Interactomics of Qa-SNARE in Arabidopsis thaliana. *Plant Cell Physiol*, *55*(4), 781-789. doi:10.1093/pcp/pcu038
- Gomez-Gomez, L., & Boller, T. (2000). FLS2: an LRR receptor-like kinase involved in the perception of the bacterial elicitor flagellin in Arabidopsis. *Mol Cell*, *5*(6), 1003-1011. doi:10.1016/S1097-2765(00)80265-8

- Grant, M. R., Godiard, L., Straube, E., Ashfield, T., Lewald, J., Sattler, A., . . . Dangl, J. L. (1995). Structure of the Arabidopsis RPM1 gene enabling dual specificity disease resistance. *Science*, *269*(5225), 843-846. doi:10.1126/science.7638602
- Hatsugai, N., Igarashi, D., Mase, K., Lu, Y., Tsuda, Y., Chakravarthy, S., . . . Katagiri, F. (2017). A plant effector-triggered immunity signaling sector is inhibited by pattern-triggered immunity. *EMBO J*, *36*(18), 2758-2769. doi:10.15252/embj.201796529
- Hatsugai, N., Kuroyanagi, M., Nishimura, M., & Hara-Nishimura, I. (2006). A cellular suicide strategy of plants: vacuole-mediated cell death. *Apoptosis*, *11*(6), 905-911. doi:10.1007/s10495-006-6601-1
- Hiraiwa, N., Nishimura, M., & Hara-Nishimura, I. (1999). Vacuolar processing enzyme is self-catalytically activated by sequential removal of the C-terminal and N-terminal propeptides. *FEBS letters*, *447*(2-3), 213-216. doi:10.1016/S0014-5793(99)00286-0
- Hofius, D., Tsitsigiannis, D. I., Jones, J. D., & Mundy, J. (2007). Inducible cell death in plant immunity. *Semin Cancer Biol*, *17*(2), 166-187. doi:10.1016/j.semcancer.2006.12.001
- Ingle, R. A., Carstens, M., & Denby, K. J. (2006). PAMP recognition and the plant-pathogen arms race. *BioEssays*, *28*(9), 880-889. doi:10.1002/bies.20457
- Jones, J. D., & Dangl, J. L. (2006). The plant immune system. *Nature*, *444*(7117), 323-329. doi:10.1038/nature05286
- Jung, H. W., & Hwang, B. K. (2007). The leucine-rich repeat (LRR) protein, CaLRR1, interacts with the hypersensitive induced reaction (HIR) protein, CaHIR1, and suppresses cell death induced by the CaHIR1 protein. *Mol Plant Pathol*, *8*(4), 503-514. doi:10.1111/j.1364-3703.2007.00410.x
- Jung, H. W., Lim, C. W., Lee, S. C., Choi, H. W., Hwang, C. H., & Hwang, B. K. (2008). Distinct roles of the pepper hypersensitive induced reaction protein gene CaHIR1 in disease and osmotic stress, as determined by comparative transcriptome and proteome analyses. *Planta*, *227*(2), 409-425. doi:10.1007/s00425-007-0628-6
- Kabbage, M., Kessens, R., Bartholomay, L. C., & Williams, B. (2017). The Life and Death of a Plant Cell. *Annu Rev Plant Biol*, *68*, 375-404. doi:10.1146/annurev-arplant-043015-111655
- Karrer, E. E., Beachy, R. N., & Holt, C. A. (1998). Cloning of tobacco genes that elicit the hypersensitive response. *Plant molecular biology*, *36*(5), 681-690.

- Katagiri, F., Thilmony, R., & He, S. Y. (2002). The *Arabidopsis thaliana*-*Pseudomonas syringae* interaction. *Arabidopsis Book*, 1, e0039. doi:10.1199/tab.0039
- Klemencic, M., & Funk, C. (2017). Type III metacaspases: calcium-dependent activity proposes new function for the p10 domain. *New Phytol.* doi:10.1111/nph.14660
- Kunkel, B. N., Bent, A. F., Dahlbeck, D., Innes, R. W., & Staskawicz, B. J. (1993). RPS2, an *Arabidopsis* disease resistance locus specifying recognition of *Pseudomonas syringae* strains expressing the avirulence gene *avrRpt2*. *Plant Cell*, 5(8), 865-875. doi:10.1105/tpc.5.8.865
- Kunze, G., Zipfel, C., Robatzek, S., Niehaus, K., Boller, T., & Felix, G. (2004). The N terminus of bacterial elongation factor Tu elicits innate immunity in *Arabidopsis* plants. *Plant Cell*, 16(12), 3496-3507. doi:10.1105/tpc.104.026765
- Kuroyanagi, M., Yamada, K., Hatsugai, N., Kondo, M., Nishimura, M., & Hara-Nishimura, I. (2005). Vacuolar processing enzyme is essential for mycotoxin-induced cell death in *Arabidopsis thaliana*. *J Biol Chem*, 280(38), 32914-32920. doi:10.1074/jbc.M504476200
- Lacomme, C., & Roby, D. (1999). Identification of new early markers of the hypersensitive response in *Arabidopsis thaliana*(1). *FEBS Lett*, 459(2), 149-153. doi:10.1016/S0014-5793(99)01233-8
- Lam, E., & Zhang, Y. (2012). Regulating the reapers: activating metacaspases for programmed cell death. *Trends Plant Sci*, 17(8), 487-494. doi:10.1016/j.tplants.2012.05.003
- LampI, N., Alkan, N., Davydov, O., & Fluhr, R. (2013). Set-point control of RD21 protease activity by AtSerpin1 controls cell death in *Arabidopsis*. *Plant J*, 74(3), 498-510. doi:10.1111/tpj.12141
- LampI, N., Budai-Hadrian, O., Davydov, O., Joss, T. V., Harrop, S. J., Curmi, P. M., . . . Fluhr, R. (2010). *Arabidopsis* AtSerpin1, crystal structure and in vivo interaction with its target protease RESPONSIVE TO DESICCATION-21 (RD21). *J Biol Chem*, 285(18), 13550-13560. doi:10.1074/jbc.M109.095075
- Lema Asqui, S., Vercammen, D., Serrano, I., Valls, M., Rivas, S., Van Breusegem, F., . . . Coll, N. S. (2017). AtSERPIN1 is an inhibitor of the metacaspase AtMC1-mediated cell death and autocatalytic processing in planta. *New Phytol.* doi:10.1111/nph.14446
- Li, Y., Chen, L., Mu, J., & Zuo, J. (2013). LESION SIMULATING DISEASE1 interacts with catalases to regulate hypersensitive cell death in

- Arabidopsis. *Plant Physiol*, 163(2), 1059-1070. doi:10.1104/pp.113.225805
- Liu, F., Yu, X., Zhao, W., Chen, J., Goyer, C., Yang, W., & Liu, D. (2013). Effects of the leaf rust pathogen on expression of TaHIR4 at the gene and protein levels in wheat. *Journal of Plant Interactions*, 8(4), 304-311. doi:10.1080/17429145.2013.823247
- Lockshin, R. A., & Williams, C. M. (1964). Programmed cell death—II. Endocrine potentiation of the breakdown of the intersegmental muscles of silkworms. *Journal of Insect Physiology*, 10(4), 643-649. doi:10.1016/0022-1910(64)90034-4
- Lockshin, R. A., & Williams, C. M. (1965). Programmed Cell Death--I. Cytology of Degeneration in the Intersegmental Muscles of the Pernyi Silkworm. *J Insect Physiol*, 11(2), 123-133. doi:10.1016/0022-1910(65)90099-5
- Lorang, J., Kidarsa, T., Bradford, C. S., Gilbert, B., Curtis, M., Tzeng, S. C., . . . Wolpert, T. J. (2012). Tricking the guard: exploiting plant defense for disease susceptibility. *Science*, 338(6107), 659-662. doi:10.1126/science.1226743
- Mackey, D., Belkadir, Y., Alonso, J. M., Ecker, J. R., & Dangl, J. L. (2003). Arabidopsis RIN4 is a target of the type III virulence effector AvrRpt2 and modulates RPS2-mediated resistance. *Cell*, 112(3), 379-389.
- Mackey, D., Holt, B. F., Wiig, A., & Dangl, J. L. (2002). RIN4 interacts with *Pseudomonas syringae* type III effector molecules and is required for RPM1-mediated resistance in Arabidopsis. *Cell*, 108(6), 743-754.
- McDowell, J. M., & Dangl, J. L. (2000). Signal transduction in the plant immune response. *Trends Biochem Sci*, 25(2), 79-82. doi:10.1016/s0968-0004(99)01532-7
- McLuskey, K., Rudolf, J., Proto, W. R., Isaacs, N. W., Coombs, G. H., Moss, C. X., & Mottram, J. C. (2012). Crystal structure of a *Trypanosoma brucei* metacaspase. *Proc Natl Acad Sci U S A*, 109(19), 7469-7474. doi:10.1073/pnas.1200885109
- Meng, X., & Zhang, S. (2013). MAPK cascades in plant disease resistance signaling. *Annu Rev Phytopathol*, 51(1), 245-266. doi:10.1146/annurev-phyto-082712-102314
- Minina, E. A., Coll, N. S., Tuominen, H., & Bozhkov, P. V. (2017). Metacaspases versus caspases in development and cell fate regulation. *Cell Death Differ*, 24(8), 1314-1325. doi:10.1038/cdd.2017.18
- Morel, J. B., & Dangl, J. L. (1997). The hypersensitive response and the induction of cell death in plants. *Cell Death Differ*, 4(8), 671-683. doi:10.1038/sj.cdd.4400309

- Mur, L. A., Kenton, P., Lloyd, A. J., Ougham, H., & Prats, E. (2008). The hypersensitive response; the centenary is upon us but how much do we know? *J Exp Bot*, 59(3), 501-520. doi:10.1093/jxb/erm239
- Nadimpalli, R., Yalpani, N., Johal, G. S., & Simmons, C. R. (2000). Prohibitins, stomatins, and plant disease response genes compose a protein superfamily that controls cell proliferation, ion channel regulation, and death. *J Biol Chem*, 275(38), 29579-29586. doi:10.1074/jbc.M002339200
- Nahirnak, V., Almasia, N. I., Fernandez, P. V., Hopp, H. E., Estevez, J. M., Carrari, F., & Vazquez-Rovere, C. (2012). Potato snakin-1 gene silencing affects cell division, primary metabolism, and cell wall composition. *Plant Physiol*, 158(1), 252-263. doi:10.1104/pp.111.186544
- Nelson, B. K., Cai, X., & Nebenfuhr, A. (2007). A multicolored set of in vivo organelle markers for co-localization studies in Arabidopsis and other plants. *Plant J*, 51(6), 1126-1136. doi:10.1111/j.1365-313X.2007.03212.x
- Newman, M. A., Sundelin, T., Nielsen, J. T., & Erbs, G. (2013). MAMP (microbe-associated molecular pattern) triggered immunity in plants. *Front Plant Sci*, 4, 139. doi:10.3389/fpls.2013.00139
- Nimchuk, Z., Eulgem, T., Holt, B. F., 3rd, & Dangl, J. L. (2003). Recognition and response in the plant immune system. *Annu Rev Genet*, 37(1), 579-609. doi:10.1146/annurev.genet.37.110801.142628
- Ogura, Y., Sutterwala, F. S., & Flavell, R. A. (2006). The inflammasome: first line of the immune response to cell stress. *Cell*, 126(4), 659-662. doi:10.1016/j.cell.2006.08.002
- Puente, X. S., Sanchez, L. M., Overall, C. M., & Lopez-Otin, C. (2003). Human and mouse proteases: a comparative genomic approach. *Nat Rev Genet*, 4(7), 544-558. doi:10.1038/nrg1111
- Qi, Y., & Katagiri, F. (2012). Membrane microdomain may be a platform for immune signaling. *Plant Signal Behav*, 7(4), 454-456. doi:10.4161/psb.19398
- Qi, Y., Tsuda, K., Glazebrook, J., & Katagiri, F. (2011). Physical association of pattern-triggered immunity (PTI) and effector-triggered immunity (ETI) immune receptors in Arabidopsis. *Mol Plant Pathol*, 12(7), 702-708. doi:10.1111/j.1364-3703.2010.00704.x
- Qi, Y., Tsuda, K., Nguyen le, V., Wang, X., Lin, J., Murphy, A. S., . . . Katagiri, F. (2011). Physical association of Arabidopsis hypersensitive induced

- reaction proteins (HIRs) with the immune receptor RPS2. *J Biol Chem*, 286(36), 31297-31307. doi:10.1074/jbc.M110.211615
- Rasmussen, M. W., Roux, M., Petersen, M., & Mundy, J. (2012). MAP Kinase Cascades in Arabidopsis Innate Immunity. *Front Plant Sci*, 3, 169. doi:10.3389/fpls.2012.00169
- Reape, T. J., Molony, E. M., & McCabe, P. F. (2008). Programmed cell death in plants: distinguishing between different modes. *J Exp Bot*, 59(3), 435-444. doi:10.1093/jxb/erm258
- Rostoks, N., Schmierer, D., Kudrna, D., & Kleinhofs, A. (2003). Barley putative hypersensitive induced reaction genes: genetic mapping, sequence analyses and differential expression in disease lesion mimic mutants. *Theor Appl Genet*, 107(6), 1094-1101. doi:10.1007/s00122-003-1351-8
- Silva, A., Almeida, B., Sampaio-Marques, B., Reis, M. I., Ohlmeier, S., Rodrigues, F., . . . Ludovico, P. (2011). Glyceraldehyde-3-phosphate dehydrogenase (GAPDH) is a specific substrate of yeast metacaspase. *Biochim Biophys Acta*, 1813(12), 2044-2049. doi:10.1016/j.bbamcr.2011.09.010
- Smertenko, A., & Franklin-Tong, V. E. (2011). Organisation and regulation of the cytoskeleton in plant programmed cell death. *Cell Death Differ*, 18(8), 1263-1270. doi:10.1038/cdd.2011.39
- Stackman, E. C. (1915). Relation between puccinia graminis and plants highly resistant to its attack. *Journal of Agricultural Research*, IV(3).
- Sundstrom, J. F., Vaculova, A., Smertenko, A. P., Savenkov, E. I., Golovko, A., Minina, E., . . . Bozhkov, P. V. (2009). Tudor staphylococcal nuclease is an evolutionarily conserved component of the programmed cell death degradome. *Nat Cell Biol*, 11(11), 1347-1354. doi:10.1038/ncb1979
- Thomas, E. L., & van der Hoorn, R. A. L. (2018). Ten Prominent Host Proteases in Plant-Pathogen Interactions. *Int J Mol Sci*, 19(2), 639. doi:10.3390/ijms19020639
- Thomma, B. P., Nürnberger, T., & Joosten, M. H. (2011). Of PAMPs and effectors: the blurred PTI-ETI dichotomy. *The Plant Cell*, 23(1), 4-15. doi:10.1105/tpc.110.082602
- Tripathi, L. P., & Sowdhamini, R. (2006). Cross genome comparisons of serine proteases in Arabidopsis and rice. *BMC genomics*, 7, 200. doi:10.1186/1471-2164-7-200
- Tsiatsiani, L., Breusegem, F., Gallois, P., Zavalov, A., Lam, E., & Bozhkov, P. (2011). Metacaspases. *Cell Death and Differentiation*, 18(8). doi:10.1038/cdd.2011.66

- Tsuda, K., Sato, M., Stoddard, T., Glazebrook, J., & Katagiri, F. (2009). Network properties of robust immunity in plants. *PLoS Genet*, 5(12), e1000772. doi:10.1371/journal.pgen.1000772
- Uren, A. G., O'Rourke, K., Aravind, L. A., Pisabarro, M. T., Seshagiri, S., Koonin, E. V., & Dixit, V. M. (2000). Identification of paracaspases and metacaspases: two ancient families of caspase-like proteins, one of which plays a key role in MALT lymphoma. *Molecular Cell*, 6(4), 961-967.
- Vercammen, D., Belenghi, B., van de Cotte, B., Beunens, T., Gavigan, J. A., De Rycke, R., . . . Van Breusegem, F. (2006). Serpin1 of *Arabidopsis thaliana* is a suicide inhibitor for metacaspase 9. *J Mol Biol*, 364(4), 625-636. doi:10.1016/j.jmb.2006.09.010
- Vercammen, D., van de Cotte, B., De Jaeger, G., Eeckhout, D., Casteels, P., Vandepoele, K., . . . Van Breusegem, F. (2004). Type II metacaspases Atmc4 and Atmc9 of *Arabidopsis thaliana* cleave substrates after arginine and lysine. *J Biol Chem*, 279(44), 45329-45336. doi:10.1074/jbc.M406329200
- Verma, S., Dixit, R., & Pandey, K. C. (2016). Cysteine Proteases: Modes of Activation and Future Prospects as Pharmacological Targets. *Front Pharmacol*, 7, 107. doi:10.3389/fphar.2016.00107
- Watanabe, N., & Lam, E. (2005). Two *Arabidopsis* metacaspases AtMCP1b and AtMCP2b are arginine/lysine-specific cysteine proteases and activate apoptosis-like cell death in yeast. *J Biol Chem*, 280(15), 14691-14699. doi:10.1074/jbc.M413527200
- Williams, B., & Dickman, M. (2008). Plant programmed cell death: can't live with it; can't live without it. *Mol Plant Pathol*, 9(4), 531-544. doi:10.1111/j.1364-3703.2008.00473.x
- Wong, A. H., Yan, C., & Shi, Y. (2012). Crystal structure of the yeast metacaspase Yca1. *J Biol Chem*, 287(35), 29251-29259. doi:10.1074/jbc.M112.381806
- Xiang, T., Zong, N., Zou, Y., Wu, Y., Zhang, J., Xing, W., . . . Zhou, J. M. (2008). *Pseudomonas syringae* effector AvrPto blocks innate immunity by targeting receptor kinases. *Curr Biol*, 18(1), 74-80. doi:10.1016/j.cub.2007.12.020
- Zhang, G., Dong, Y.-L., Zhang, Y., Li, Y.-M., Wang, X.-J., Han, Q.-M., . . . Kang, Z.-S. (2009). Cloning and Characterization of a Novel Hypersensitive-induced Reaction Gene from Wheat Infected by Stripe Rust Pathogen. *Journal of Phytopathology*, 157(11-12), 722-728. doi:10.1111/j.1439-0434.2009.01556.x

- Zhang, Y., & Lam, E. (2011). Sheathing the swords of death: post-translational modulation of plant metacaspases. *Plant Signal Behav*, 6(12), 2051-2056. doi:10.4161/psb.6.12.18247
- Zhou, L., Cheung, M. Y., Li, M. W., Fu, Y., Sun, Z., Sun, S. M., & Lam, H. M. (2010). Rice hypersensitive induced reaction protein 1 (OsHIR1) associates with plasma membrane and triggers hypersensitive cell death. *BMC Plant Biol*, 10(1), 290. doi:10.1186/1471-2229-10-290
- Zhou, Q., Gao, H., Wang, M., Xu, Y., Guo, Y. Z., Wan, Y. Z., & Zhao, Z. Y. (2012). Characterization of defense-related genes in the 'Qinguan' apple in response to *Marssonina coronaria*. *South African Journal of Botany*, 80, 36-43. doi:10.1016/j.sajb.2012.01.005
- Zipfel, C. (2014). Plant pattern-recognition receptors. *Trends Immunol*, 35(7), 345-351. doi:10.1016/j.it.2014.05.004
- Zipfel, C., Kunze, G., Chinchilla, D., Caniard, A., Jones, J. D., Boller, T., & Felix, G. (2006). Perception of the bacterial PAMP EF-Tu by the receptor EFR restricts *Agrobacterium*-mediated transformation. *Cell*, 125(4), 749-760. doi:10.1016/j.cell.2006.03.037

ANEXS

Type III Secretion–Dependent and –Independent Phenotypes Caused by *Ralstonia solanacearum* in *Arabidopsis* Roots

Haibin Lu,¹ Saul Lema A,¹ Marc Planas-Marquès,¹ Alejandro Alonso-Díaz,¹ Marc Valls,^{1,2,†} and Núria S. Coll^{1,†}

¹Centre for Research in Agricultural Genomics (CSIC-IRTA-UAB-UB), Bellaterra, Catalonia, Spain; and ²Genetics Department, Universitat de Barcelona, Catalonia, Spain

Accepted 17 August 2017.

The causal agent of bacterial wilt, *Ralstonia solanacearum*, is a soilborne pathogen that invades plants through their roots, traversing many tissue layers until it reaches the xylem, where it multiplies and causes plant collapse. The effects of *R. solanacearum* infection are devastating, and no effective approach to fight the disease is so far available. The early steps of infection, essential for colonization, as well as the early plant defense responses remain mostly unknown. Here, we have set up a simple, in vitro *Arabidopsis thaliana*–*R. solanacearum* pathosystem that has allowed us to identify three clear root phenotypes specifically associated to the early stages of infection: root-growth inhibition, root-hair formation, and root-tip cell death. Using this method, we have been able to differentiate, on *Arabidopsis* plants, the phenotypes caused by mutants in the key bacterial virulence regulators *hrpB* and *hrpG*, which remained indistinguishable using the classical soil-drench inoculation pathogenicity assays. In addition, we have revealed the previously unknown involvement of auxins in the root rearrangements caused by *R. solanacearum* infection. Our system provides an easy-to-use, high-throughput tool to study *R. solanacearum* aggressiveness. Furthermore, the observed phenotypes may allow the identification of bacterial virulence determinants and could even be used to screen for novel forms of early plant resistance to bacterial wilt.

The soilborne phytopathogen *Ralstonia solanacearum* is the causal agent of bacterial wilt, one of the most destructive bacterial crop diseases worldwide (Hayward 1991; Mansfield et al. 2012). Also referred to as the *R. solanacearum* species complex because of its wide phylogenetic diversity, this bacterium can cause disease on more than 200 plant species, including many important economic crops (Genin and Denny

2012). *R. solanacearum* accesses the plant through the root and traverses many root layers until it reaches the xylem, where it profusely multiplies. From there, it spreads through the aerial part and causes wilting of the stem and leaves (Genin 2010).

Wilting symptoms caused by *R. solanacearum* are largely dependent on the presence of a functional type III secretion system (T3SS) (Boucher et al. 1985). The T3SS is a needle-like structure present in many pathogenic bacteria that allows secretion of virulence proteins—called effectors—into the host cells (Galán and Collmer 1999; Hueck 1998). In plant-associated bacteria, the genes responsible for the regulation and assembly of the T3SS are known as *hypersensitive response and pathogenicity (hrp)* genes (Lindgren et al. 1986). Transcription of the *hrp* genes and its related effectors is activated by HrpB, the downstream regulator of a well-described regulatory cascade induced by contact with the plant cell wall (Brito et al. 2002). The cascade includes the membrane receptor PrhA, the signal transducer PrhI, and the transcriptional regulators PrhJ and HrpG (Brito et al. 2002). HrpG is downstream of PrhJ and directly controls HrpB expression (and thus, expression of the T3SS genes), but it also activates a number of HrpB-independent virulence determinants, such as genes for ethylene synthesis (Valls et al. 2006).

Since the establishment of the *R. solanacearum* pathosystem almost two decades ago, leaf wilting has been typically used as the major readout to study the *Arabidopsis thaliana*–*R. solanacearum* interactions (Deslandes et al. 1998). Soil drenching with a bacterial suspension, followed by leaf symptom evaluation over a time course, constitutes a solid measure to quantify the degree of resistance or susceptibility of the plant toward the pathogen. The disadvantages of this system are the uncontrolled influence of soil microbiota and its high variability due to infection stochasticity, as shown in potato (Cruz et al. 2014). In addition, leaf wilting is the last step of *R. solanacearum* infection and does not provide information about early steps of colonization. Furthermore, soil opacity hinders direct observation of any morphological changes associated to bacterial invasion of plant tissues.

The establishment of gnotobiotic assays in which *R. solanacearum* is inoculated on plants grown axenically has opened the door to studying the early steps of infection. *R. solanacearum* in vitro inoculation assays have been successfully established for tomato (Vasse et al. 1995), petunia (Zolobowska and Van Gijsegem 2006), and the model plants *Medicago truncatula* (Vaillau et al. 2007) and *Arabidopsis thaliana* (Digonnet et al. 2012). These studies have shed light on some common, as well as species-specific, root phenomena associated with *R. solanacearum* infection. Reduced primary root elongation after infection is a common feature observed in all species analyzed. Other common root phenotypes that appeared after

Haibin Lu, Saul A. Lema, and Marc Planas-Marquès contributed equally to this work.

Current address for Haibin Lu: State Key Laboratory of Crop Stress Biology for Arid Areas and College of Agronomy, Northwest A&F University, No.3 Taicheng Road, Yangling, Shaanxi 712100, China.

†Corresponding authors: Marc Valls; E-mail: marcvals@ub.edu and Núria S. Coll; E-mail: nuria.sanchez-coll@cragenomica.es

*The e-Xtra logo stands for “electronic extra” and indicates that five supplementary figures and one supplementary table are published online.

infection were swelling of the root tip (in tomato, petunia, and *M. truncatula*), inhibition of lateral root growth (in petunia and *Arabidopsis*), and cell death (in *M. truncatula* and *Arabidopsis*). In petunia, *R. solanacearum* infection resulted as well in the formation of root lateral structures (Zolobowska and Van Gijsegem 2006). These structures resembled prematurely terminated lateral roots, were present both in resistant and susceptible lines, and were efficient colonization sites.

In vitro pathosystems have helped define the different stages of *R. solanacearum* infection. The bacterium was found to gain access into the tomato root through wound sites or natural openings such as emerging lateral roots (Saile et al. 1997; Vasse et al. 1995). In *M. truncatula* and *Arabidopsis*, the bacteria can also enter intact roots through the root apex (Digonnet et al. 2012; Vaillau et al. 2007). In petunia, it was shown that penetration occurs equally in resistant or susceptible plants (Zolobowska and Van Gijsegem 2006). The second stage of infection involves invasion of the root cortical area. In this stage, *R. solanacearum* quickly transverse the root cylinder centripetally via intercellular spaces, directed to the vasculature (Digonnet et al. 2012; Vasse et al. 1995). Massive cortical cell degeneration can be observed during this phase. The fact that cells not directly in contact with the bacteria also die led to a proposal that certain cell-wall fragments degraded by *R. solanacearum* may act as signals to induce plant programmed cell death (Digonnet et al. 2012). During the third stage of infection, *R. solanacearum* enters into the vascular cylinder and colonizes the xylem. In *Arabidopsis*, it was shown that vascular invasion is promoted by collapse of two xylem pericycle cells (Digonnet et al. 2012). Once inside the xylem, bacteria start proliferating and moving between adjacent vessels by degrading the cell walls but remain confined in the xylem. In the last stage of infection, disease

symptoms become apparent at the whole organism level, as the stem and leaves start wilting.

All these studies have significantly broadened our understanding of the root invasion process. However, the molecular mechanisms that control these phenotypes and their timing remain vastly unexplored. In addition, no clear correlation has been established between any of the observed phenotypes and the host's resistance or susceptibility to *R. solanacearum*. Here, we have set up a simple in vitro pathosystem to determine the impact of *R. solanacearum* on *Arabidopsis* root morphology at the first stages of infection.

RESULTS

In vitro infection with *R. solanacearum* causes a triple phenotype on *Arabidopsis* roots.

To analyze the impact of *R. solanacearum* infection on *Arabidopsis* root morphology, we established a simple in vitro inoculation assay. Sterile seeds were sown on Murashige Skoog (MS) media plates and were grown vertically for 7 days so that plant roots developed at the surface of the medium and could be easily inoculated and visualized. Plantlets were then inoculated 1 cm above the root tip with 5 μ l of a solution containing *R. solanacearum*. Infection with the wild-type GMI1000 strain caused root-growth arrest (Fig. 1A). To determine whether this effect depended on the inoculation point, we inoculated at the top, middle, and tip of the root. *R. solanacearum* causes root-growth inhibition regardless of the infection point (Supplementary Fig. S1). Hence, all experiments were performed inoculating 1 cm above the root tip. Interestingly, along with root-growth inhibition, we observed two additional root phenotypes caused by *R. solanacearum* infection, i.e., production of root hairs at the root-tip maturation zone (Fig. 1B) and cell death at

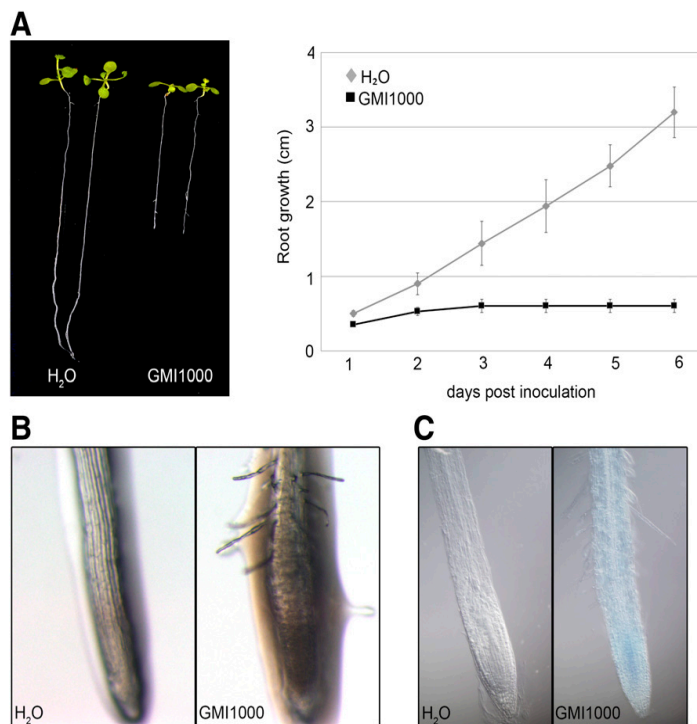


Fig. 1. Root phenotypes caused by *Ralstonia solanacearum* GMI1000 in vitro infection. Six-day-old Col-0 seedlings were inoculated with 5 μ l of a GMI1000 solution or with water as a control. **A**, GMI1000 inhibition of root growth. The left panel shows stereoscope images of the plantlets under white light at 6 days postinoculation (dpi), and the right panel presents root length data at different times after infection. **B**, Root-hair formation on the root tip caused by GMI1000 infection. Root-tip pictures obtained, as before, at 6 dpi. **C**, Observation of cell death at root tips visualized by Evans blue staining. Representative Nomarski microscope pictures of stained roots obtained 6 dpi; 10 to 15 plants were used in three independent experiments.

the root tip. Cell death was visualized as either Evans blue (Fig. 1C) or propidium iodide staining (Supplementary Fig. S2), both of which are commonly used as cell-death markers as they are excluded from living cells by the plasma membrane (Curtis and Hays 2007; Gaff and Okong'O-gola 1971).

***R. solanacearum* hrp mutants are altered in their capacity to cause the triple-root phenotype.**

With these three phenotypes in hand, we set out to identify their causative bacterial genetic determinants. For this, we analyzed the triple-root phenotypes on plants inoculated with *R. solanacearum* GMI1000 carrying mutations on the master regulators of virulence HrpG and HrpB. Bacteria bearing a disrupted *hrpG* lost the ability to inhibit root growth but not those bearing disrupted *hrpB* versions (*hrpB* and *hrpB*Ω) (Fig. 2A).

Inoculation with the $\Delta hrpG$, in which the whole open reading frame had been deleted, and its complemented strain, $\Delta hrpG$ (*hrpG*), confirmed the requirement of HrpG but not HrpB to induce the phenotypes. Similarly, bacterial strains disrupted in the membrane receptor *prhA*, the signal transducer *prhI*, and, to a lesser extent, the transcriptional regulator *prhJ* were all strongly affected in their capacity to inhibit root growth (Fig. 3). This is logical, since all these mutants show decreased *hrpG* transcription (Brito et al. 2002). Since *hrp* mutants are all nonpathogenic (Boucher et al. 1985), the key role of HrpG in root inhibition compared with HrpB could be due to the fact that HrpG controls a larger number of bacterial virulence activities that have been proposed to be required for xylem colonization (Valls et al. 2006; Vasse et al. 2000). To check if root phenotypes correlated with bacterial colonization, 4-week-old

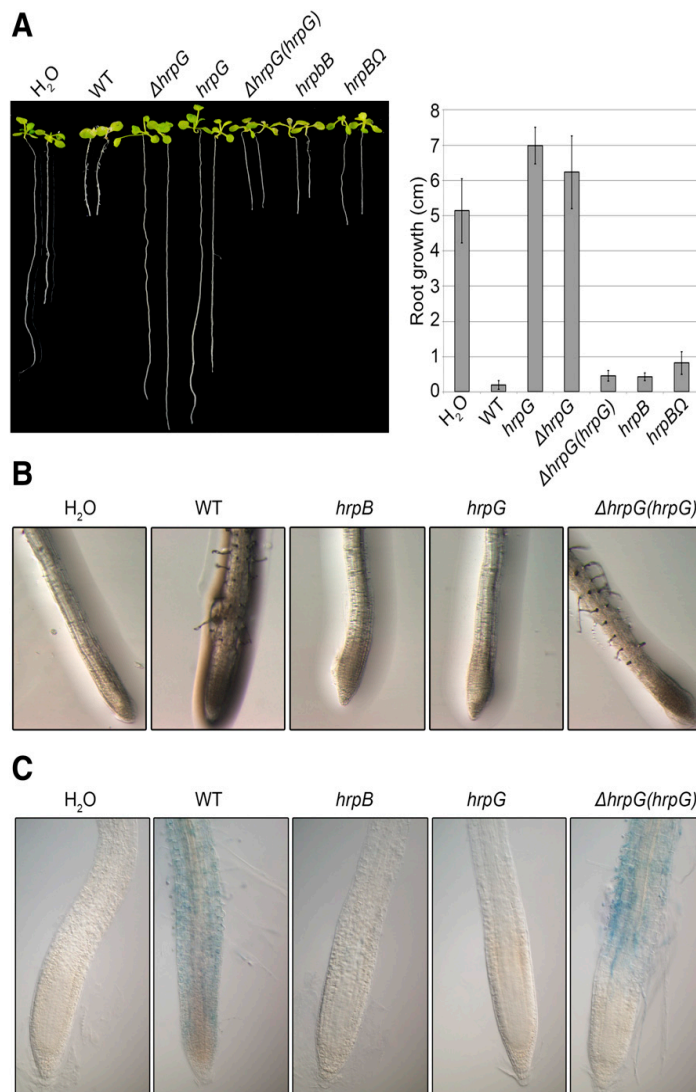


Fig. 2. HrpG is required for all the phenotypes caused by GMI1000, while HrpB is only essential for cell death and root-hair formation. Six-day-old Col-0 seedlings were inoculated with water (control) or with the following strains: GMI1000 wild type (WT), $\Delta hrpG$ (whole gene deletion), *hrpG* (Tn5 transposon insertion), $\Delta hrpG$ (*hrpG*), *hrpB* (Tn5 transposon insertion), and *hrpB*Ω (Ω cassette insertion). **A**, Mutations on HrpG but not on HrpB abolish growth inhibition. Left panel presents a picture taken at 9 days postinoculation (dpi), and the right panel presents root growth measurements at 9 dpi. **B**, Both *hrpG* and *hrpB* mutations abolish root-hair formation. Pictures were taken at 6 dpi. **C**, Neither the *hrpG* nor *hrpB* mutant cause root-tip cell death. Pictures of infected seedlings at 6 dpi stained with Evans blue. Each experiment was repeated at least three times, using five to ten plants.

Arabidopsis Col-0 plants were inoculated with the wild-type *R. solanacearum* GMI1000 or its *hrpB* and *hrpG* deletion mutant counterparts. Bacterial loads were measured in aerial tissues of inoculated *Arabidopsis* plants 14 days after inoculation as colony-forming units (CFU) per gram of tissue. Supplementary Fig. S3 shows that the capacity to colonize *Arabidopsis* plants of *hrpB* is significantly higher than of *hrpG* mutants. Thus, although *hrp* mutants had been already described to multiply in planta (Hanemian et al. 2013), HrpG seems to be more essential than HrpB for the bacterium to colonize the plant xylem and reach the aerial tissues.

Finally, we also observed that mutations in the *hrpB* and *hrpG* regulators abolished root-hair formation and cell death caused by *R. solanacearum* on roots (Fig. 2B and C). In summary, we proved that root-hair production and cell-death induction are T3SS-dependent phenotypes. In contrast, root-growth

inhibition, for which HrpG is required, does not depend on a functional T3SS.

R. solanacearum strains unable to cause the triple-root phenotype are nonvirulent on *Arabidopsis*.

Our next goal was to determine whether the ability to cause the triple phenotype in *Arabidopsis* roots was conserved across different *R. solanacearum* strains and if there was a correlation to aggressiveness. For this, we inoculated in vitro-grown *Arabidopsis* Col-0 roots with *R. solanacearum* strains belonging to different phylotypes: our reference strain GMI1000 and strain Rd15 (phylotype I); CIP301 and CFBP2957 (phylotype IIA); NCPPB3987, UY031, and UW551 (phylotype IIB); and CMR15 (phylotype III). Interestingly, infection with phylotype IIA strains CIP301 and CFBP2957 resulted in root-growth inhibition (Fig. 4A), root-hair production (Fig. 4B) and cell death at the root tip (Fig. 4C), similar to what we observed with phylotype I and III strains. In contrast, phylotype IIB strains NCPPB3987, UY031, and UW551 did not cause growth inhibition nor root-hair production or cell death on infected roots. Thus, different *R. solanacearum* strains vary in their ability to cause the triple-root phenotype. To determine whether these phenotypes correlated with pathogenicity, we performed root infection assays on *Arabidopsis* plants grown on soil and recorded the appearance of wilting symptoms over time (Fig. 4D). Infection of wild-type Col-0 plants with the strains that were unable to cause the triple-root phenotype (NCPPB3987, UY031, and UW551) did not result in wilting, which indicates a direct correlation between absence of root phenotypes in vitro and absence of symptoms in plants grown in soil. On the contrary, from all *R. solanacearum* strains causing the triple-root phenotype, only GMI1000, Rd15, and CMR15 resulted in plant wilting. As seen before for the *hrpG* and *hrpB* mutants, symptom scoring has limitations in evaluating slight *R. solanacearum* pathogenicity differences. Thus, we inoculated *Arabidopsis* plants with all studied bacterial strains and measured bacterial numbers in the aerial part 14 days postinoculation (dpi). The results, shown in Figure 4E, indicated that the two phylotype IIA strains (CIP301 and CFBP2957) that showed the triple phenotype but were not causing disease colonized the aerial part of the plants to higher numbers than the strains not causing the root responses. These results show that *Arabidopsis* root phenotypes partially correlate with the capacity of *R. solanacearum* to colonize *Arabidopsis* Col-0 plants; the strains that are not able to produce the triple-root phenotype are nonvirulent.

R. solanacearum-triggered root-hair formation is mediated by plant auxins.

To ascertain whether any of the phenotypes triggered by *R. solanacearum* infection were mediated by known plant defense regulators, we tested how different *Arabidopsis* mutants responded to the pathogen (Supplementary Fig. S4). Our results showed that reactive oxygen species (ROS) produced by the membrane NADPH oxidases AtRbohD and AtRbohF were not required for root-growth inhibition, root-hair production, or cell death in response to infection. Plants that were insensitive to jasmonic acid (*jai3-1*) or that could not synthesize it (*dde2*) or its conjugated form (*jar1-1*) showed root-growth inhibition, root-hair production, and cell death similar to the wild type. Similarly, the *sid2* mutant, defective in salicylic acid biosynthesis, and the ethylene insensitive mutant *ein2* responded with the same root morphologies as wild-type to *R. solanacearum* infection. On the contrary, the auxin insensitive mutants *tir1* and *tir1/afb2* showed growth inhibition (Fig. 5A) and root-tip cell death (Fig. 5B) but were not able to produce root hairs in response to infection (Fig. 5C). This result indicates that root-hair production triggered by *R. solanacearum* infection requires auxin signaling. To monitor potential changes in auxin levels

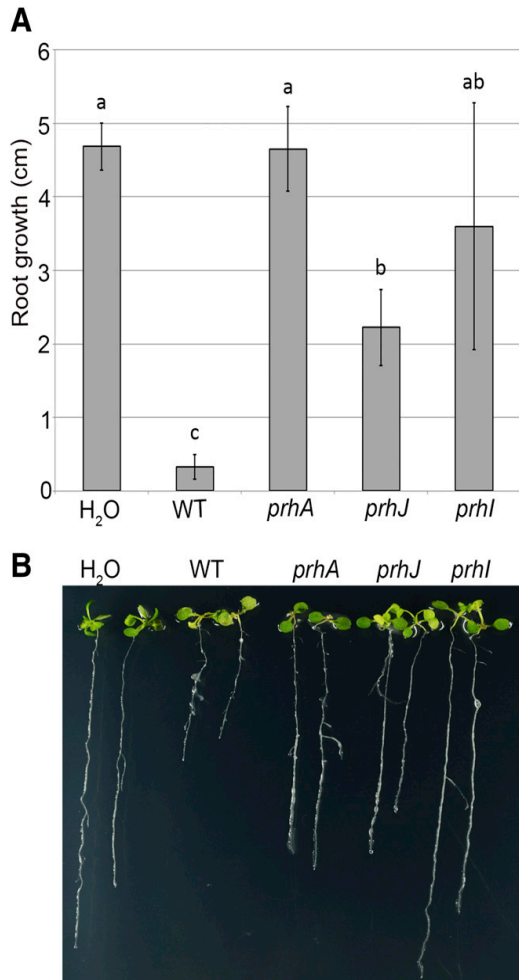


Fig. 3. Detection of plant signals is essential for GMI1000 to cause root-growth inhibition. Six-day-old Col-0 seedlings were inoculated with GMI1000 (WT), its derivative strains disrupted for components of the *hrp* signaling cascade or treated with water. **A**, Root growth was measured at 9 days postinoculation (dpi) and **B**, pictures were taken at 9 dpi. Letters above bars indicate statistical significance; bars not sharing letters represent significant mean differences by one-way analysis of variance ($P < 0.05$, $\alpha = 0.05$) with post hoc Scheffé ($\alpha = 0.05$). Five to seven plants were used in three independent experiments.

during infection, we analyzed expression of the auxin signaling reporter *DR5rev::GFP* in roots of infected versus control plants. As shown in Figure 5D, *R. solanacearum* inoculation induced a strong vascular green fluorescent protein (GFP) signal 48 h postinfection, suggesting that infection may result in increased auxin signaling levels in the vascular cylinder.

R. solanacearum encodes a HrpG-regulated ethylene-forming enzyme (*efe*) gene (Valls et al. 2006). To assess whether bacterial ethylene-mediated root-growth inhibition, we infected wild-type *Arabidopsis* with *R. solanacearum* GMI1000 wild-type strain or with the *efe* mutant. Supplementary Figure S5 shows that infection with the mutant resulted in root-growth inhibition, indicating that ethylene produced by the bacteria is not responsible for this phenotype. Bacterial ethylene was also not required for the root-hair formation phenotype, because infection with the *efe* mutant did not affect root-hair formation

as expected if HrpB, which does not activate the *efe* operon, controls this phenotype (Fig. 2B).

Absence of the triple-root phenotype in *Arabidopsis* might reveal new sources of resistance to strain GMI1000.

Next, we wanted to determine the degree of conservation of the correlation between absence of the triple phenotype and resistance to *R. solanacearum*. For this, besides Col-0, we selected the accessions C24, Cvi-0, Ler-1, Bl-1, and Rrs-7 from among the 20 proposed as representatives of the maximum variability of *Arabidopsis* (Delker et al. 2010). In addition, we included Nd-1, known to be resistant to *R. solanacearum* (Deslandes et al. 1998), and Tou-A1-74, which does not show the triple phenotype (discussed below). Despite the differences in root length among accessions, the majority displayed the triple-root phenotype after inoculation with *R. solanacearum*

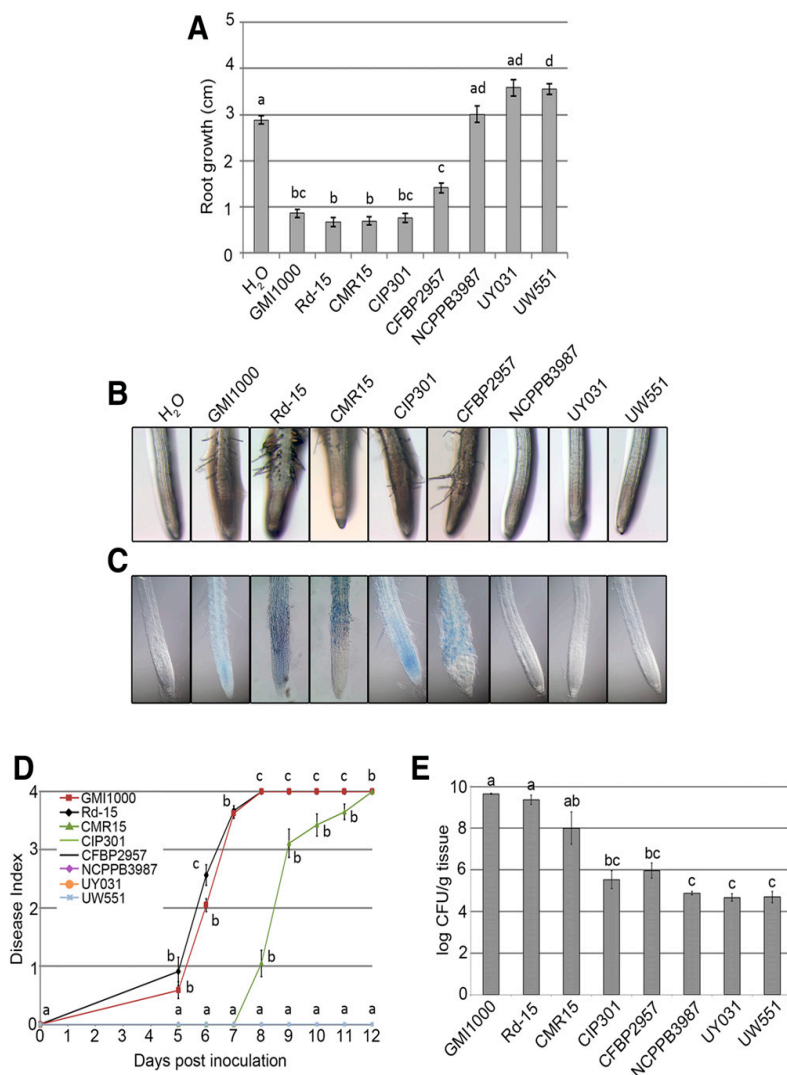


Fig. 4. The ability to cause root-growth inhibition, root-hair formation, and cell death varies across different *Ralstonia solanacearum* strains. Six-day-old Col-0 seedlings were inoculated with the indicated *R. solanacearum* wild-type strains or water. **A**, Root growth at 6 days postinoculation (dpi). **B**, Pathogenicity assay. **C**, Bacterial multiplication in planta measured 14 days after inoculation. **D**, Root-hair formation at 6 dpi. **E**, Roots from infected seedlings, at 6 dpi, stained with Evans blue. For all graphs, letters indicate statistical significance; values not sharing letters represent significant mean differences by one-way analysis of variance ($P < 0.05$, $\alpha = 0.05$) with post hoc Scheffé ($\alpha = 0.05$). In **B**, the statistical test was applied separately for each timepoint. Each experiment was repeated at least three times using ten to 15 plants.

(Fig. 6A, B, C). Only *Rrs-7* and *Tou-A1-74* did not show any of the three phenotypes in response to infection. To determine whether the presence or absence of the triple phenotype correlated to susceptibility to *R. solanacearum* GMI1000, we performed a pathogenicity assay using these accessions (Fig. 6D). Interestingly, *Rrs-7* but not *Tou-A1-74* was resistant to *R. solanacearum*, indicating that absence of the root phenotypes could be used to identify some sources of resistance to the pathogen. Resistance to *R. solanacearum* was not found in random accessions showing

the triple-root phenotype, which, however, did not correlate with susceptibility, since the resistant accessions Nd-1 (Deslandes et al. 1998) and BI-1 reacted with root-growth inhibition, root-hair production, and cell death after infection (Fig. 6D).

DISCUSSION

Plant host root phenotypes appear as early symptoms of colonization by *R. solanacearum*.

The use of in vitro pathosystems to study the interactions between the vascular pathogen *R. solanacearum* and some of its plant hosts has emerged as a very powerful technique to understand the early stages of infection (Digonnet et al. 2012; Turner et al. 2009; Vaillau et al. 2007; Vasse et al. 1995, 2000; Zolobowska and Van Gijsegem 2006). In this work, we have used in vitro-grown *Arabidopsis* as the model host to deepen our knowledge on the first steps of *R. solanacearum* root invasion. In vitro infection has several advantages: i) it reveals easily screenable root phenotypes associated with the infection that would remain hidden when using the soil-drench inoculation; ii) it facilitates microscopy studies to determine the penetration point and the infection itinerary through the root cell layers; and iii) it is a useful tool to study the genetic determinants controlling both *R. solanacearum* virulence and host defense.

A very detailed microscopic analysis of the gnotobiotic *Arabidopsis*-*R. solanacearum* interaction has been recently published (Digonnet et al. 2012). This study revealed the path followed by *R. solanacearum* through *Arabidopsis* roots, highlighting the sites of bacterial multiplication and the specific cell-wall barriers degraded by the bacterium. Moving forward this knowledge, our data defines a set of root phenotypes associated to infection that can be correlated to bacterial aggressiveness and plant resistance and are genetically amenable, both from the bacterial and the plant side.

In our system, infection of intact roots with a droplet of *R. solanacearum* resulted in root-growth inhibition, root-hair production, and cell death. Root-growth inhibition or delayed elongation has been previously observed as a result of *R. solanacearum* infection, when using gnotobiotic systems (Digonnet et al. 2012; Turner et al. 2009; Vaillau et al. 2007; Vasse et al. 1995; Zolobowska and Van Gijsegem 2006). One could hypothesize that root-growth inhibition is the direct cause of the massive cell death observed after infection in the root cortex of *Arabidopsis* (Digonnet et al. 2012; this work) or other species (Turner et al. 2009; Vasse et al. 1995). However, this does not seem to be the case, since a *hrpB* mutant strain causes root-growth inhibition in the absence of cell death. Considering this, root-growth inhibition would rather reflect xylem colonization, which takes place both for wild-type *R. solanacearum* GMI1000 and the *hrpB* mutant. In agreement with this interpretation, the *hrpG* mutant, which has an extremely reduced capacity to invade the xylem (Vasse et al. 1995, 2000), does not cause root-growth inhibition after infection. This further highlights the proposed role of HrpG as a central regulator controlling still-unknown activities essential for the bacterium to reach and multiply in the plant xylem (Valls et al. 2006; Vasse et al. 2000). These activities are likely encoded in genes regulated by HrpG independently of HrpB, as the latter is able to colonize the xylem. Among the 184 genes specifically regulated by HrpG, an obvious candidate responsible for the root-growth inhibition is the gene controlling bacterial production of the phytohormone ethylene. However, we found the bacterial mutant defective in this gene still inhibited root growth, indicating that xylem colonization and subsequent root inhibition is controlled by other, still-undefined HrpG-regulated genes.

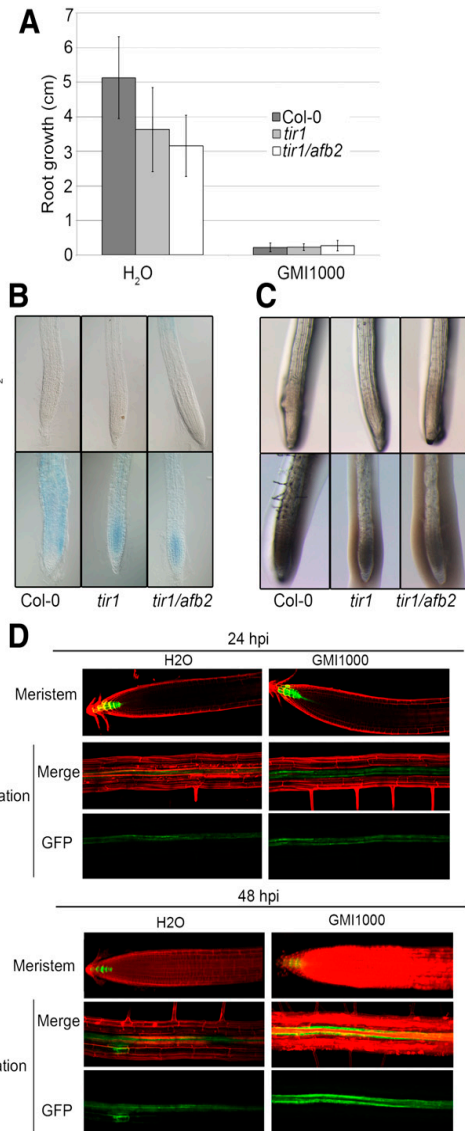


Fig. 5. Auxin signaling is required for *Ralstonia solanacearum*-triggered root-hair formation in *Arabidopsis* but not for root-growth inhibition and cell death. Six-day-old Col-0, *tir1*, and *tir1/afb2* seedlings were inoculated with *R. solanacearum* GMI1000 or water and, at 6 days postinoculation, **A**, root growth was measured **B**, root-hair formation was evaluated, and **C**, roots from infected seedlings were stained with Evans blue. **D**, Expression of the auxin signaling marker DR5 was analyzed under the confocal microscope in roots of transgenic Col-0 *DR5rev::GFP* plants infected with *R. solanacearum* GMI1000 or water at 24 and 48 h after inoculation. Representative pictures of both the meristem area and maturation zone are shown. Six to ten plants were used in three different experimental replicates.

Auxin signaling alterations caused by *R. solanacearum* infection likely trigger root structure rearrangements, resulting in root-hair formation.

Our plant mutant analysis showed that neither of the defense regulators salicylic acid, jasmonic acid, ethylene, or NADPH-produced ROS were required for any of the root phenotypes observed after *R. solanacearum* GMI1000 infection. On the contrary, we showed that auxin signaling was clearly required for infection-triggered root-hair formation. This is not surprising, since auxin is one of the main orchestrators of root-hair formation (Grierson et al. 2014; Lee and Cho 2013) and can promote this process (Pitts et al. 1998). Root hairs are outgrowths of epidermal cells that contribute to nutrient and water absorption (Grierson et al. 2014), but they also participate in plant-microbe interactions. For instance, root hairs are the entry point of both mutualistic rhizobacteria (Rodríguez-Navarro et al. 2007) and pathogenic bacteria such as *Plasmodiophora brassicaeae*, the causal agent of clubroot disease (Kageyama

and Asano 2009). Interestingly, auxin signaling was proposed to promote cell-wall remodeling to allow root-hair growth (Breakspear et al. 2014) and it has been shown to be a key component of both pathogenic and mutualistic root-hair infections (Jahn et al. 2013; Laplaze et al. 2015).

During *R. solanacearum*-*Arabidopsis* interactions, auxin signaling may have additional important roles beyond its involvement in root-hair formation. *R. solanacearum* inoculation resulted in an induction of *DR5rev::GFP* expression in the root vascular cylinder at early stages of infection, indicative of increased auxin signaling levels. Furthermore, plant infection results in increased expression of several auxin-related genes (Zuluaga et al. 2015). On a hypothetical scenario, *R. solanacearum* could directly and specifically (e.g., via a T3SS effector) manipulate one or more of the host auxin signaling pathways to its own benefit. There are many examples of effector-mediated manipulation of the host auxin pathway (Kazan and Lyons 2014). In most cases the pathogen uses its type III effector

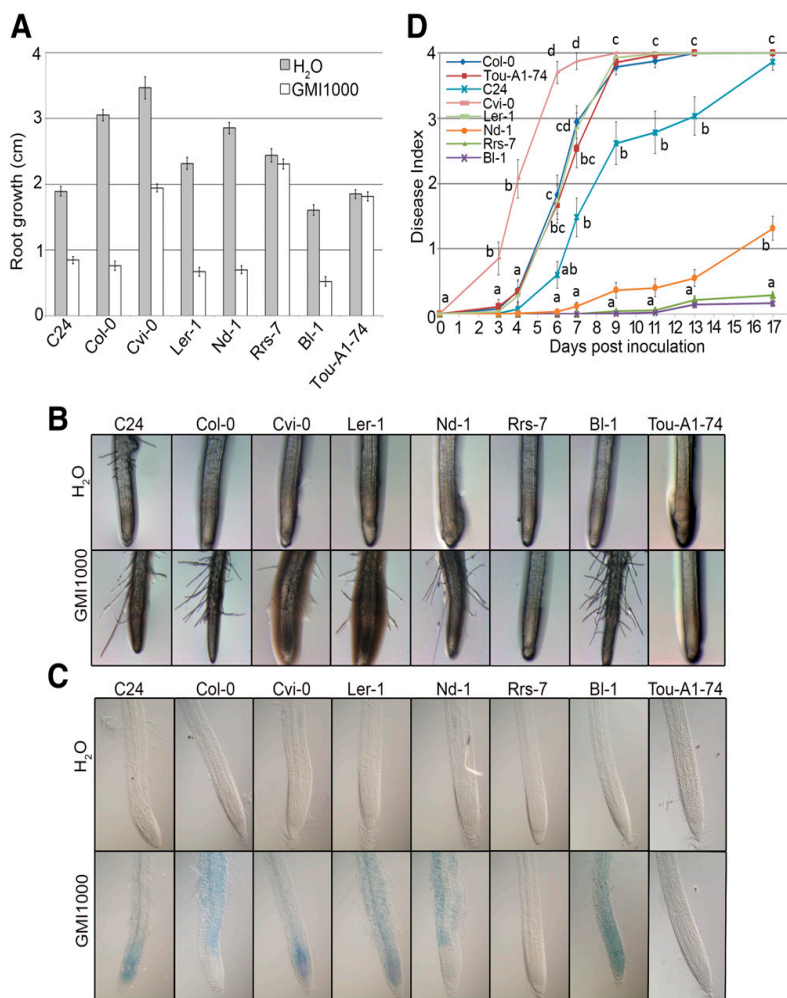


Fig. 6. The absence of the triple phenotype caused by *Ralstonia solanacearum* in *Arabidopsis* is indicative of resistance. Six-day-old *Arabidopsis* seedlings from ecotypes C24, Col-0, Cvi-0, Ler-1, Nd-1, Rrs-7, BI-1, and Tou-A1-74 were inoculated with *R. solanacearum* GMI1000 or water and, at 6 days postinoculation, **A**, root growth was measured, **B**, root hair was visualized, and **C**, cell death was observed after Evans blue staining. **D**, Five-week old plants grown in Jiffy pots were inoculated with GMI1000. The disease index measured symptoms on a 1 to 4 scale (0 = no wilting, 1 = 25% wilted leaves, 2 = 50%, 3 = 75%, and 4 = death). Letters indicate statistical significance; values not sharing letters represent significant mean differences by one-way analysis of variance ($P < 0.05$, $\alpha = 0.05$) with post hoc Scheffé ($\alpha = 0.05$). The statistical test was applied separately for each timepoint. Seven to 13 plants were used in each of three experiments.

arsenal to specifically increase auxin levels in the host by targeting auxin biosynthesis, signaling, or transport. Elevated auxin levels are beneficial for many pathogens, toward which auxin promotes susceptibility. This is the case of *Pseudomonas syringae*, *Xanthomonas oryzae*, and *Magnaporthe oryzae*, among others. In rice, elevated susceptibility has been linked to auxin-induced loosening of the protective cell wall, which would facilitate pathogen colonization. Other pathogens increase the host susceptibility by secreting auxin into the host, which, in turn, induces auxin production inside the host's cells and promotes susceptibility (Fu et al. 2011). Our data points toward a potential link to increased auxin levels as a result of invasion, although further work needs to be done to determine whether this is directly correlated with an increase in susceptibility. In this context, it also remains to be clarified whether auxin-mediated root-hair formation during infection facilitates *R. solanacearum* invasion or whether it is a mere consequence of elevated auxin levels in certain root cells. Also, it is not known whether root hairs may constitute favorite entry points for the bacteria.

Absence of the triple-root phenotype to screen for *R. solanacearum* virulence factors or resistance in *Arabidopsis*.

When analyzing different *R. solanacearum* strains, the absence of the root phenotypes is directly linked to the inability of the bacterium to cause symptoms. Thus, strains not capable of inducing the triple-root phenotype show low pathogenicity on *Arabidopsis*, as is the case for NCPPB3987, UY031, and UW551. Presence of the phenotype is not always correlated with increased aggressiveness of a particular strain. CIP301 and CFBP2957 are not pathogenic on *Arabidopsis* Col-0 plants, despite causing the triple-root phenotype. Gene-for-gene interactions may mask these root phenotypic features and block *R. solanacearum* before it starts causing wilt. This may indicate that the Col-0 accession possesses resistance proteins that recognize effectors secreted by the two phylotype IIA strains or that phylotype IIA strains lack one or several virulence factors required to establish disease on *Arabidopsis* or repress some plant defenses. Similarly, the *hrpG* mutant, which has an extremely reduced capacity to invade the xylem, does not cause root inhibition (discussed above).

Our data show that the lack of the triple-root phenotype can be linked to resistance to *R. solanacearum*. This is the case of *Arabidopsis* accession Rrs-7, which appears completely resistant to *R. solanacearum* GMI1000 and does not display any of the described root phenotypes. Resistance to *R. solanacearum* is very rare among *Arabidopsis* accessions. The clear enrichment of resistant accessions among those lacking the capacity to cause the triple phenotype indicates that the root phenotypes described here can be used to screen plant varieties in search for resistance. The fact that other resistant accessions present the phenotypes may indicate that they possess alternative forms of resistance or that other factors, including gene-for-gene interactions, override the observed phenotypes. This could be the case of the resistant accession Nd-1, which is able to detect *R. solanacearum* GMI1000 infection through recognition of the effector PopP2 by the resistance protein RRS1-R (Deslandes et al. 2003). This system could, thus, be used to differentiate ecotypes with resistances due to a gene-for-gene recognition (Nd-1 resistance associated to the presence of the triple response) compared with other resistance mechanisms (Rrs-7 resistance associated with absence of the triple-root response). Along this line, *Arabidopsis* BI-1, which also does not wilt but shows clear infection, indicated by the appearance of the root phenotypes, may also recognize *R. solanacearum* through an alternative effector-resistance protein pair and stop invasion.

Taken together, our results on both the bacterial and the plant side favor the notion that absence of the root phenotypes is indicative of ineffective colonization that may reflect novel forms of resistance. Thus, the absence of the root phenotypes described here could help in the search for plant varieties with higher resistance to devastating bacterial wilt disease.

MATERIALS AND METHODS

Biological material.

Arabidopsis thaliana ecotypes BI-1, C24, Col-0, Cvi-0, Ler-1, Nd-1, Rrs-7 (Clark and Schweikert 2007; Delker et al. 2010), Tou-A1-74 (Horton et al. 2012), and the Col-0 mutants *sid2-2*, *dde2-2*, and *ein2-1* (Tsuda et al. 2009), *tir1-1* (Dharmasiri et al. 2005), *tir1-1/afb2-3* (Parry et al. 2009), *jar1-1* (Staswick and Tiryaki 2004), *jai3-1* (Chini et al. 2007), and *atrbohD* and *atrbohF* (Torres et al. 2002) were used. The Col-0 transgenic line *DR5rev::GFP* (Friml et al. 2003) was used to monitor auxin signaling.

All *R. solanacearum* strains used are described in Supplementary Table S1. Bacteria were grown at 28°C in solid or liquid rich B medium (1% Bacto peptone, 0.1% yeast extract, and 0.1% casamino acids, all from Becton, Dickinson and Co. [Franklin Lakes, NJ, U.S.A.]), adding the appropriate antibiotics as described by Monteiro et al. (2012).

In vitro inoculation assay.

Seeds were sterilized, with a solution containing 30% bleach and 0.02% Triton-X 100, for 10 min, were washed five times with Milli-Q water, and were sown (20 seeds per plate) on MS plates containing vitamins (Duchefa Biochemie B.V., Haarlem, The Netherlands) and 0.8% agar (Becton, Dickinson and Co.). Sown plates were stratified at 4°C in the dark for 2 days. Then, plates were transferred to chambers and were grown for 6 to 7 days under constant conditions of 21 to 22°C, 60% humidity, and a 16-h light and 8-h dark photoperiod.

For inoculation, *R. solanacearum* was collected, by centrifugation (1,300 × g, 5 min), from overnight liquid cultures, was resuspended with water, and was adjusted to a final optical density at 600 nm (OD₆₀₀) of 0.01. Six- to 7-day-old *Arabidopsis* seedlings, grown on plates as detailed above, were inoculated with 5 µl of the bacterial solution, which was applied 1 cm above the root tip, as described previously (Digonnet et al. 2012). Plates with the infected seedlings were sealed with micropore tape (3M Deutschland GmbH, Neuss, Germany) and were transferred to a controlled growth chamber at 25°C, 60% humidity, and a 12-h light and 12-h dark photoperiod. Root length of infected seedlings was recorded over time. For root-hair evaluation, pictures were taken 6 dpi with an Olympus DP71 stereomicroscope (Olympus, Center Valley, PA, U.S.A.) at 11.5x. To analyze cell death, roots from seedlings grown on plates were collected 6 dpi and were immediately stained by carefully submerging them into a solution containing 0.05% (wt/vol) of Evans blue (Sigma-Aldrich, Buchs, Switzerland) for 30 min at room temperature. Roots were then washed twice with distilled water and were photographed under a 20x lens with a Nomarski Axiophot DP70 microscope (Zeiss, Oberkochen, Germany). For propidium iodide staining, roots of infected seedlings were soaked into a 1-µg/ml staining solution (Sigma-Aldrich) and were immediately photographed with a 20x magnification on an Olympus FV1000 (Olympus) or a Leica SP5 (Wetzlar, Germany) confocal microscope.

Pathogenicity assays.

R. solanacearum pathogenicity tests were carried out using the soil-drench method (Monteiro et al. 2012). Briefly, *Arabidopsis*

was grown for 4 to 5 weeks on Jiffy pots (Jiffy Group, Lorain, OH, U.S.A.) in a controlled chamber at 22°C, 60% humidity, and an 8-h light and 16-h dark photoperiod. Jiffys were cut at one-third from the bottom and were immediately submerged for 30 min into a solution of overnight-grown *R. solanacearum* adjusted to OD₆₀₀ = 0.1 with distilled water (35 ml of bacterial solution per plant). Then, inoculated plants were transferred to trays containing a thin layer of soil drenched with the same *R. solanacearum* solution and were kept in a chamber at 28°C, 60% humidity, and 12 h of light and 12 h of dark. Plant wilting symptoms were recorded every day and were expressed according to a disease index scale (0 = no wilting, 1 = 25% wilted leaves, 2 = 50%, 3 = 75%, and 4 = death). At least 30 plants were used in each assay, performed in at least three replicate experiments.

R. solanacearum vessel colonization was tested in *Arabidopsis* plants inoculated with a lower inoculum (OD₆₀₀ = 0.01). To quantify bacterial colonization, the plant aerial parts were cut 14 days after inoculation and were homogenized. Dilutions of the homogenate plant material were plated on rich B medium supplemented with the appropriate antibiotics and the bacterial content was measured as CFU per gram of fresh plant tissue. At least 20 plants were inoculated per *R. solanacearum* strain and the experiment was repeated three times.

ACKNOWLEDGMENTS

We are grateful to M. Estelle (University of California San Diego) for the *tir1* and *tir1/afb2* seeds; to K. Tsuda (Max Planck Institute for Plant Breeding Research) for the *sid2*, *ein2*, and *dde2* seeds; to R. Solano (Spanish National Center for Biotechnology) for the *jai3-1* and *jar1-1* seeds; and to M. Quint (Leibniz institute of Plant Biochemistry) for *Arabidopsis* accessions Bl-1, C24, Cvi-0, Ler-1, Nd-1, and RRS-7. We thank M. A. Moreno-Risueño for helpful comments and critically reading the manuscript. We also thank S. Poussier, I. Robène, E. Wicker, S. Genin, C. P. Cheng, P. Hanson, and P. Prior for providing *R. solanacearum* strains and for their advice in the choice of relevant ones. This work was funded by Ministry of Economy and Competitiveness (MINECO) projects AGL2013-46898-R and AGL2016-78002-R to N. S. Coll and M. Valls and RyC 2014-1658 to N. S. Coll and EU-Marie Curie Actions (PCDMC-321738 and PIIIF-331392) and BP_B 00030 from the Catalan Government to N. S. Coll. We also want to acknowledge the support of the COST Action SUSTAIN (FA1208), the “Severo Ochoa Programme for Centres of Excellence in R&D” 2016-2019 (SEV-2015-0533) from the MINECO, and by the Centres de Recerca de Catalunya programme and the government of Catalonia.

LITERATURE CITED

Boucher, C. A., Barberis, P. A., Trigalet, A. P., and Demery, D. A. 1985. Transposon mutagenesis of *Pseudomonas solanacearum*: Isolation of Tn5-induced avirulent mutants. *J. Gen. Microbiol.* 131:2449-2457.

Breakspear, A., Liu, C., Roy, S., Stacey, N., Rogers, C., Trick, M., Morieri, G., Mysore, K. S., Wen, J., Oldroyd, G. E. D., Downie, J. A., and Murray, J. D. 2014. The root hair “infectome” of *Medicago truncatula* uncovers changes in cell cycle genes and reveals a requirement for auxin signaling in rhizobial infection. *Plant Cell* 26:4680-4701.

Brito, B., Aldon, D., Barberis, P., Boucher, C., and Genin, S. 2002. A signal transfer system through three compartments transduces the plant cell contact-dependent signal controlling *R. solanacearum hrp* genes. *Mol. Plant-Microbe Interact.* 15:109-119.

Clark, R. M., and Schweikert, G. 2007. Common sequence polymorphisms shaping genetic diversity in *Arabidopsis thaliana*. *Science* 317:338-342.

Cruz, A. P., Ferreira, V., Pianzola, M. J., Siri, M. I., Coll, N. S., and Valls, M. 2014. A novel, sensitive method to evaluate potato germplasm for bacterial wilt resistance using a luminescent *Ralstonia solanacearum* reporter strain. *Mol. Plant-Microbe Interact.* 27:277-285.

Curtis, M. J., and Hays, J. B. 2007. Tolerance of dividing cells to replication stress in UVB-irradiated *Arabidopsis* roots: Requirements for DNA translesion polymerases eta and zeta. *DNA Repair (Amst.)* 6:1341-1358.

Chini, A., Fonseca, S., Fernandez, G., Adie, B., Chico, J. M., Lorenzo, O. 2007. The JAZ family of repressors is the missing link in jasmonate signalling. *Nature* 448:666-671.

Delker, C., Poschl, Y., Raschke, A., Ullrich, K., Ettingshausen, S., Hauptmann, V., Grosse, I., and Quint, M. 2010. Natural variation of transcriptional auxin response networks in *Arabidopsis thaliana*. *Plant Cell* 22:2184-2200.

Deslandes, L., Olivier, J., Peeters, N., Feng, D. X., Khounloham, M., Boucher, C., Somssich, I., Genin, S., and Marco, Y. 2003. Physical interaction between RRS1-R, a protein conferring resistance to bacterial wilt, and PopP2, a type III effector targeted to the plant nucleus. *Proc. Natl. Acad. Sci. U.S.A.* 100:8024-8029.

Deslandes, L., Pileur, F., Liaubet, L., Camut, S., Can, C., Williams, K., Holub, E., Beynon, J., Arlat, M., and Marco, Y. 1998. Genetic characterization of RRS1, a recessive locus in *Arabidopsis thaliana* that confers resistance to the bacterial soilborne pathogen *Ralstonia solanacearum*. *Mol. Plant-Microbe Interact.* 11:659-667.

Dharmasiri, N., Dharmasiri, S., and Estelle, M. 2005. The F-box protein TIR1 is an auxin receptor. *Nature* 435:441-445.

Digonnet, C., Martinez, Y., Denance, N., Chasseray, M., Dabos, P., Ranocha, P., Marco, Y., Jauneau, A., and Goffner, D. 2012. Deciphering the route of *Ralstonia solanacearum* colonization in *Arabidopsis thaliana* roots during a compatible interaction: Focus at the plant cell wall. *Planta* 236:1419-1431.

Friml, J., Vieten, A., Sauer, M., Weijers, D., Schwarz, H., Hamann, T., Offringa, R., and Jurgens, G. 2003. Efflux-dependent auxin gradients establish the apical-basal axis of *Arabidopsis*. *Nature* 426:147-153.

Fu, J., Liu, H., Li, Y., Yu, H., Li, X., Xiao, J., and Wang, S. 2011. Manipulating broad-spectrum disease resistance by suppressing pathogen-induced auxin accumulation in rice. *Plant Physiol.* 155:589-602.

Gaff, D. F., and Okong’ O-gola, O. 1971. The use of non-permeating pigments for testing the survival of cells. *J. Exp. Bot.* 22:756-758.

Galán, J. E., and Collmer, A. 1999. Type III secretion machines: Bacterial devices for protein delivery into host cells. *Science* 284:1322-1328.

Genin, S. 2010. Molecular traits controlling host range and adaptation to plants in *Ralstonia solanacearum*. *New Phytol.* 187:920-928.

Genin, S., and Denny, T. P. 2012. Pathogenomics of the *Ralstonia solanacearum* species complex. *Annu. Rev. Phytopathol.* 50:67-89.

Grierson, C., Nielsen, E., Ketelaarc, T., and Schiefelbein, J. 2014. Root hairs. *Arabidopsis Book* 12:e0172.

Hayward, A. C. 1991. Biology and epidemiology of bacterial wilt caused by *Pseudomonas solanacearum*. *Annu. Rev. Phytopathol.* 29:65-87.

Hanemian, M., Zhou, B., Deslandes, L., Marco, Y., and Trémousaygue, D. 2013. *Hrp* mutant bacteria as biocontrol agents: Toward a sustainable approach in the fight against plant pathogenic bacteria. *Plant Signal. Behav.* 8:e25678.

Horton, M. W., Hancock, A. M., Huang, Y. S., Toomajian, C., Atwell, S., Auton, A., Mulyati, N. W., Platt, A., Sperone, F. G., Vilhjálmsson, B. J., Nordborg, M., Borevitz, J. O., and Bergelson, J. 2012. Genome-wide patterns of genetic variation in worldwide *Arabidopsis thaliana* accessions from the RegMap panel. *Nat. Genet.* 44:212-216.

Hueck, C. J. 1998. Type III protein secretion systems in bacterial pathogens of animals and plants. *Microbiol. Mol. Biol. Rev.* 62:379-433.

Jahn, L., Mucha, S., Bergmann, S., Horn, C., Staswick, P., Steffens, B., Siemens, J., and Ludwig-Müller, J. 2013. The clubroot pathogen (*Plasmodiophora brassicae*) influences auxin signaling to regulate auxin homeostasis in *Arabidopsis*. *Plants* 2:726-749.

Ageyama, K., and Asano, T. 2009. Life cycle of *Plasmodiophora brassicae*. *J. Plant Growth Regul.* 28:203-211.

Kazan, K., and Lyons, R. 2014. Intervention of phytohormone pathways by pathogen effectors. *Plant Cell* 26:2285-2309.

Laplaze, L., Lucas, M., and Champion, A. 2015. Rhizobial root hair infection requires auxin signaling. *Trends Plant Sci.* 20:332-334.

Lee, R. D., and Cho, H. T. 2013. Auxin, the organizer of the hormonal/ environmental signals for root hair growth. *Front. Plant Sci.* 4:448.

Lindgren, P. B., Peet, R. C., and Panopoulos, N. J. 1986. Gene cluster of *Pseudomonas syringae* pv. *phaseolicola* controls pathogenicity of bean plants and hypersensitivity of nonhost plants. *J. Bacteriol.* 168:512-522.

Mansfield, J., Genin, S., Magori, S., Citovsky, V., Sriariyanum, M., Ronald, P. 2012. Top 10 plant pathogenic bacteria in molecular plant pathology. *Mol. Plant Pathol.* 13:614-629.

Monteiro, F., Sole, M., van Dijk, I., and Valls, M. 2012. A chromosomal insertion toolbox for promoter probing, mutant complementation, and pathogenicity studies in *Ralstonia solanacearum*. *Mol. Plant-Microbe Interact.* 25:557-568.

Parry, G., Calderon-Villalobos, L. I., Prigge, M., Peret, B., Dharmasiri, S., Itoh, H., Lechner, E., Gray, W. M., Bennett, M., and Estelle, M. 2009. Complex regulation of the TIR1/AFB family of auxin receptors. *Proc. Natl. Acad. Sci. U.S.A.* 106:22540-22545.

- Pitts, R. J., Cernac, A., and Estelle, M. 1998. Auxin and ethylene promote root hair elongation in *Arabidopsis*. *Plant J.* 16:553-560.
- Rodríguez-Navarro, D. N., Dardanelli, M. S., and Ruiz-Sainz, J. E. 2007. Attachment of bacteria to the roots of higher plants. *FEMS Microbiol. Lett.* 272:127-136.
- Saile, E., McGarvey, J. A., Schell, M. A., and Denny, T. P. 1997. Role of extracellular polysaccharide and endoglucanase in root invasion and colonization of tomato plants by *Ralstonia solanacearum*. *Phytopathology* 87:1264-1271.
- Staswick, P. E., and Tiryaki, I. 2004. The oxylipin signal jasmonic acid is activated by an enzyme that conjugates it to isoleucine in *Arabidopsis*. *Plant Cell* 16:2117-2127.
- Torres, M. A., Dangl, J. L., and Jones, J. D. 2002. *Arabidopsis* gp91phox homologues *AtrbohD* and *AtrbohF* are required for accumulation of reactive oxygen intermediates in the plant defense response. *Proc. Natl. Acad. Sci. U.S.A.* 99:517-522.
- Tsuda, K., Sato, M., Stoddard, T., Glazebrook, J., and Katagiri, F. 2009. Network properties of robust immunity in plants. *PLoS Genet.* 5:e1000772.
- Turner, M., Jauneau, A., Genin, S., Tavella, M. J., Vailleau, F., Gentzmittel, L., and Jardinaud, M. F. 2009. Dissection of bacterial wilt on *Medicago truncatula* revealed two type III secretion system effectors acting on root infection process and disease development. *Plant Physiol.* 150:1713-1722.
- Vailleau, F., Sartorel, E., Jardinaud, M. F., Chardon, F., Genin, S., Huguet, T., Gentzmittel, L., and Petitprez, M. 2007. Characterization of the interaction between the bacterial wilt pathogen *Ralstonia solanacearum* and the model legume plant *Medicago truncatula*. *Mol. Plant-Microbe Interact.* 20:159-167.
- Valls, M., Genin, S., and Boucher, C. 2006. Integrated regulation of the type III secretion system and other virulence determinants in *Ralstonia solanacearum*. *PLoS Pathog.* 2:e82.
- Vasse, J., Frey, P., and Trigalet, A. 1995. Microscopic studies of intercellular infection and protoxylem invasion of tomato roots by *Pseudomonas solanacearum*. *Mol. Plant Microbe Interact.* 8:241-251.
- Vasse, J., Genin, S., Frey, P., Boucher, C., and Brito, B. 2000. The *hrpB* and *hrpG* regulatory genes of *Ralstonia solanacearum* are required for different stages of the tomato root infection process. *Mol. Plant-Microbe Interact.* 13:259-267.
- Zolobowska, L., and Van Gijsegem, F. 2006. Induction of lateral root structure formation on petunia roots: A novel effect of GMI1000 *Ralstonia solanacearum* infection impaired in Hrp mutants. *Mol. Plant-Microbe Interact.* 19:597-606.
- Zuluaga, A. P., Sole, M., Lu, H., Gongora-Castillo, E., Vaillancourt, B., Coll, N., Buell, C. R., and Valls, M. 2015. Transcriptome responses to *Ralstonia solanacearum* infection in the roots of the wild potato *Solanum commersonii*. *BMC Genomics* 16:246.

